NATIONAL MEDICAL RESEARCH CENTRE OF PSYCHIATRY AND NEUROLOGY NAMED AFTER V. M. BEKHTEREV

As a manuscript

STULOV
ILYA KONSTANTINOVICH

MAGNETIC RESONANCE MORPHOMETRY OF THE BRAIN WITH ASSESSMENT OF HIPPOCAMPAL FORMATION SUBFIELDS IN THE DIFFERENTIAL DIAGNOSIS OF MILD COGNITIVE IMPAIRMENT OF DIFFERENT GENESIS

Scientific speciality 3.1.25. Diagnostic radiology

DISSERTATION
for the degree of
Candidate of Medical Sciences
Translated from Russian

Scientific Supervisors:
Doctor of Medical Sciences, Professor
Ananyeva Natalia Isaevna
Candidate of Medical Sciences, Associate Professor
Zalutskaya Natalia Mikhailovna

St Petersburg
2024

CONTENTS

INTRODUCTION

Relevance of the research topic

Cognitive impairment are a global medical and socio-economic problem with a high prevalence in the population and a rapidly increasing incidence due to the increasing size and longevity of the population. Worldwide, approximately 55 million people have dementia and this number is projected to increase to 78 million by 2030 (Gauthier S. et al., 2021). However, up to 75% of people with dementia worldwide are undiagnosed.

The etiological factors of cognitive impairment can be neurodegenerative and cerebrovascular diseases, toxic and metabolic encephalopathies, traumas, neuroinfections and others. The most common cause of cognitive impairment in the elderly is Alzheimer's disease (AD) and cerebrovascular diseases, as well as their combination. Depending on the severity of cognitive impairment it is customary to distinguish dementia and pre-dementia cognitive impairment (subjective, mild and moderate) (Koberskaya N. N. et al., 2022).

Currently, the study of neurodegenerative and cerebrovascular diseases at the pre-dementia stage, is particularly relevant due to the continuous improvement of modern therapy and the search for new drugs (Emelin A. Yu., 2020; Grishina D. A., Lokshina A. B., 2021; Zakharov V. V. et al., 2022).

Mild cognitive impairment (MCI) is a syndrome characterised by a decline in intellectual functions beyond the natural age-related norm, but not reaching the stage of dementia (Petersen R. C. et al., 2018; Levin O. S., Chimagomedova A. Sh., 2022). The prevalence of MCI syndrome in elderly individuals increases with age: so in the age group of 60-64 years it is 6.7%, and in the group of 80-84 years - 25.2% (Petersen R. C. et al., 2018). The risk of dementia development among patients with MCI is up to 10-15% per year (Behrman S. et al., 2017).

According to the Alzheimer's Association, AD accounts for approximately 60-80% of dementia cases (Alzheimer's Association, 2018). Researchers consider the amnestic type of mild cognitive impairment (aMCI) as a prodromal stage of AD and

characterize it mainly by episodic memory impairment (De Simone M.S. et al., 2019; Lokshina A. B. et al., 2021; Koberskaya N. N. et al., 2022). Extracellular deposition of β-amyloid (Aβ) in the form of senile plaques and intracellular accumulation of neurofibrillary tangles (NFT) in various parts of the brain cause neurodegeneration in AD. This leads to damage and death of neurons and is accompanied by atrophic changes (Rao Y. L. et al., 2022).

Vascular cognitive impairment (VCI) rank second in the prevalence of cognitive decline after AD and have several pathogenetic variants. The subcortical variant of VCI is the most common and is associated with cerebral small vessel disease (CSVD) (Bogolepova A. N. et al., 2021). In foreign literature, researchers have coined the term "subcortical vascular mild cognitive impairment" (svMCI) to diagnose cognitive impairment at the pre-dementia stage, which is considered a prodromal stage of subcortical vascular dementia (Qiu Y. et al., 2021).

One of the key structures most susceptible to neurodegenerative process in AD is the hippocampal formation (HF) (Zhao K. et al., 2020; Park H. Y. et al., 2022). A peculiarity of the HF is the presence of several anatomically and functionally different subfields: the hippocampus proper or ammon horn (CA1-4), dentate gyrus, and subicular complex. Some authors also refer the entorhinal cortex to the HF because of its close location and the presence of important functional connections with the hippocampus (van Staalduinen E. K., 2022).

Recent studies show that atrophic changes in the HF in AD occur unevenly, with predominant lesions in certain subfields at the earliest stages of the disease and affecting other subfields as the disease progresses (Zeng Q. et al., 2021). However, most studies treat the HF as a single structure, without dividing it into subfields. Accordingly, identifying atrophic changes in specific HF subfields may improve the diagnosis of AD at early stages.

It is important to note that few studies in the available literature have described atrophic changes of the HF in VCI on the background of CSVD. Nevertheless, some studies have revealed selective vulnerability of certain HF subfields to ischaemic and

hypoxic damage at pre-demanding stages of VCI, including in svMCI (Li X. et al., 2016; Wong F. C. C. et al., 2021; Gulyaeva N. V., 2021).

Thus, it is urgent to study the features of atrophic changes of HF subfields in MCI of different genesis, which will improve differential diagnosis in this category of patients, prescribe timely treatment and modify risk factors.

Level of development of the topic

Recently, there has been a rapid development of neuroscience associated with revolutionary advances in medicine and technology, including neuroimaging. One of the most informative and promising methods of studying the structure and function of the brain is magnetic resonance imaging (MRI) (Trufanov A. G. et al., 2018; Levashkina I. M., Serebryakova S. V., 2016; T. N. Trofimova, A. D. Khalikov, M. D. Semyonova, 2017; Ananyeva N. I. et al., 2019: 9; Pozdnyakov A. V. et al., 2020; Kamyshanskaya I.G., et al., 2021).

Voxel-based morphometry (VBM), based on high contrast images between grey and white matter of the brain and cerebrospinal fluid, is a modern MRI technique allowing lifetime quantitative assessment of brain structures. Quantitative data on the thickness of different cortical regions and the volume of brain structures are of topical importance, both in understanding variants of age-related norms and for clarifying pathological changes in the brain, especially in the early stages of the disease (Neznanov N. G. et al., 2018; Ananyeva N. I. et al., 2022).

World literature extensively discusses the interest of limbic system structures, including the HF, in AD and a number of other neurodegenerative and psychiatric diseases (Ananyeva N. I. et al., 2019: 10, 12; Cherenkova S. E. et al., 2020; Yakhno N. N. et al., 2020; Zeng Q. et al., 2021; Sun Y. et al., 2023). However, a number of studies have provided evidence of HF sensitivity to ischaemic changes as well, as determined in patients with subcortical vascular dementia (Du A. T. et al., 2002; Van de Pol L. et al., 2011; Kim G. H. et al., 2015) and svMCI (Li X. et al., 2016; Wong F. C. C. et al., 2021).

The study of neurodegenerative and cerebrovascular diseases at the pre-dementia stage is a particularly urgent task at present. Nevertheless, studies devoted to the

evaluation of HF in the diagnosis of MCI are few and contradictory. Most of the works consider the HF as a single structure, or they conducted the studies at advanced stages of the disease (Gridin V. N. et al., 2017; Yakhno N. N. et al. 2019).

With significant advances in high-resolution MRI data acquisition techniques and specific computerised analysis methods, new opportunities to study specific HF subfields have emerged. However, to date, the specific vulnerability of HF subfields to neurodegenerative and vascular processes remains poorly understood. The correlations between atrophic changes of HF subfields and neuropsychological examination parameters have not been determined.

Thus, to date, in the available literature there are single publications devoted to MR-morphometry of HF subfields in MCI, which are sometimes contradictory. There is no relevant data on specific changes of HF subfields in the differential diagnosis of MCI of different genesis.

Purpose of the study

To develop magnetic resonance semiotics of structural changes in the brain, including hippocampal formation subfields, to improve the differential diagnosis of mild cognitive impairment of various genesis.

Research objectives

1. Optimise the protocol of structural MRI of the brain in the examination of patients with MCI of different genesis.
2. To study regional changes in the subfields of the hippocampal formation in patients with MCI in comparison with physiological age aging using MR morphometry.
3. To clarify MR-semiotics of atrophic changes of hippocampal formation subfields in aMCI and svMCI.
4. To make comparisons between neuroimaging and neuropsychological data in patients with MCI of different genesis
5. To develop a model of differential diagnostics of MCI of different genesis using MR-morphometry data and the method of binary logistic regression.

Scientific novelty of the study

For the first time, volumetric analysis of HF subfields was performed using MR brain morphometry with the use of FreeSurfer 6.0 software in patients with MCI of different genesis and in physiological aging.

We have developed an MRI protocol to improve the diagnosis of pathological brain changes in patients with MCI.

Regional differences of atrophic changes in aMCI of neurodegenerative and vascular genesis have been established. Localisations of statistically significant structural changes of the brain in aMCI and svMCI, including HF subfields, were determined. It is shown that atrophic changes in aMCI of different genesis occur unevenly, with a predominant decrease in the volumes of certain HF subfields.

For the first time, we evaluated the relationship between the volumes of HF subfields and neuropsychological examination indicators in patients with MCI of different genesis. These studies showed the influence of atrophic changes in certain subfields of the HF on the decrease in verbal associative and visual memory.

A model of differential diagnosis based on the method of binary logistic regression using MR-morphometry data has been proposed, which makes it possible to distinguish patients with aMCI from patients with svMCI with high sensitivity and specificity.

Theoretical and practical significance of the work

The results of this work contribute to the solution of a number of currently relevant clinical problems. In particular, the obtained fundamental knowledge about the nature of damage to certain brain structures in patients with MCI of different genesis and the relationship of these changes with disorders of various types of memory, allowed to improve the accuracy of early differential diagnosis of neurodegenerative and vascular processes.

It identified new neuroimaging biomarkers in AD and VCI at the early stage, consisting of certain patterns of atrophic changes in the HF subfields, which makes it possible to apply these results in the diagnosis and treatment control in the future.

It has clarified the interrelationships of focal brain damage in patients with MCI syndrome and in physiological aging with atrophic changes in the HF subfields and cognitive impairment. These data demonstrate the synergistic interaction of neurodegenerative and vascular processes in the development of cognitive impairment.

We can use the results of the study in clinical practice by radiologists, neurologists, psychiatrists, neuropsychologists, which will improve diagnosis and optimise therapy of patients at early stages of the disease.

Research methodology and methods

The research methodology is based on the results of clinical and neurological, neuropsychological and neuroimaging diagnostics of mild cognitive impaitment of various genesis described in the domestic and foreign literature.

The object of the study was patients with amnestic mild cognitive impairment and subcortical vascular mild cognitive impairment, as well as conditionally healthy individuals matched for age, sex, and education.

The subject of the study is post-processing processing of MR data using FreeSurfer 6.0 software with subsequent analysis of quantitative changes in the cortex, white matter, and various brain structures, including the HF and its subfields.

The study is a cross-sectional case-control study carried out according to the principles of evidence-based medicine and clinical diagnostic methods of research and scientific data processing. The methods of data collection, processing and analysis that meet the requirements for research work were used in the work.

We conducted the study in four stages according to the following scheme:

1. stage: analysing data from domestic and foreign literature devoted to the research topic

2. stage:

– obtaining written informed consent from all participants

– performance of clinical-neurological, neuropsychological and laboratory examinations

– MRI of the brain using standard sequences (T1-, T2-weighted images (WI), FLAIR, T2* and DWI) supplemented by targeted examination of the mediobasal regions of the temporal lobes for visual assessment of brain changes.

– performance of brain MRI using a T1 gradient echo pulse sequence with isotropic voxel and 1mm thickness (3D MPRAGE) for morphometry.

3. stage: post-processing using specialised software FreeSurfer 6.0. with additional segmentation of HF subfields

4. stage:

– statistical processing of the obtained data

– development of a model of differential diagnostics of MCI of different genesis

The points put forward for defence

1. MRI with subsequent post-processing data processing using FreeSurfer 6.0 software allows an objective quantitative assessment of changes in various cortical regions and brain structures, including hippocampal formation subfields, in patients with the syndrome of mild cognitive impairment of various genesis.

2. Patients with mild cognitive impairment have characteristic patterns of atrophic changes in the hippocampal formation corresponding to the etiology of the process, the determination of which allows to increase the accuracy of differential diagnosis and distinguish the detected changes from physiological aging.

3. The subfields of the hippocampal formation are responsible for the formation of different types of memory, which is proved by the results of neuropsychological testing and the specificity of atrophic changes.

4. Application of machine learning algorithms to analyse MR-morphometry data allows to detect biomarkers of neuronal damage and use them to develop models of differential diagnostics of mild cognitive impairment of different genesis.

Main scientific results

The results of the conducted study showed that there are certain regularities of atrophic changes in the HF subfields in MCI of neurodegenerative and vascular genesis, presented in the articles (Stulov I.K. et al., 2022: 244; Stulov I.K.. et al., 2023: 242). In

these articles, the concept and design of the study, analysis of the results belong to Stulov I.K., co-authors - clinical examination and neuropsychological testing of patients, as well as a review of literature sources. Based on the data obtained by MR-morphometry and binary logistic regression, a model of differential diagnostics of aMCI from svMCI was developed, which is described in the article (Stulov I. K. et al., 2023: 239). The general formulation of the problem, the choice of solution methods, and the processing of the results, in the construction of the differential diagnosis model, belong to Stulov I. K., the counseling in the mathematical analysis belongs to Vuks A. Ya., the other co-authors - preparation of the manuscript and review of literature sources. Correlations between the severity of cognitive impairment and focal changes in the brain have been revealed, as well as correlations between impairment of various types of memory and atrophic changes in the HF subfields described in (Stulov I.K. et al., 2023: 241; Stulov I.K. et al., 2023: 243). In these papers, the concept and design of the study, literature review and analysis of the results belong to Stulov I. K.; the clinical examination and neuropsychological testing of the patients, analysis of the results, and preparation of the manuscript belong to the co-authors.

Conformity of the thesis with the scientific speciality

The aim, objectives and content of the thesis correspond to the passport of the speciality 3.1.25. - "Radiology".

Measure of confidence and validity of results

The reliability and validity of the results of the study are assessed by a sufficient and representative sample (n=90), comprehensive clinical, neurological and neuropsychological examination, application of modern methods of medical neuroimaging, post-processing of the obtained data using modern software (FreeSurfer 6.0) and correct application of modern mathematical and statistical methods of data processing.

The main results of the work were reported and discussed at: scientific and park conferences (Interdisciplinary approach to comorbidity of psychiatric disorders on the way to integrative treatment 2021, Polenov readings 2022, Topical issues of pharmacotherapy and psychotherapy of psychiatric disorders 2022), international

congresses (Nevsky Radiological Forum 2019, 2022, 2023), All-Russian scientific and practical conference with international participation (School of V. M. Bekhterev: from origins to modernity 2017), conferences with international participation (Brain diseases: innovative approaches to diagnosis and treatment 2022, Davidenkov Readings 2017), All-Russian congresses with international participation (Neuropsychiatry in transdisciplinary space: from fundamental research to clinical practice 2023, Davidenkov Readings 2023).

Approbation of the dissertation work was carried out at the interdepartmental meeting of the National Medical Research Centre for psychiatry and neurology named after V. M. Bekhterev (from 02.11.2023, protocol №).

Publications on the subject of the thesis

13 printed works have been published on the subject of the thesis research, including 2 publications in the editions recommended by the Higher Attestation Commission of the Ministry of Science and Higher Education of the Russian Federation, including 1 article in the journal indexed in the international database Scopus. A patent for the computer database "Magnetic resonance morphometry of the brain with assessment of hippocampal formation in mild cognitive disorders of different genesis" was obtained (certificate of state registration of the database No. 2023621026 dated 29.03.2023). Methodological recommendations "Detection of neuroimaging biomarkers at the early stage of Alzheimer's disease" were published.

Putting the results of the work into practice

The results of the work have been implemented in the practice of the magnetic resonance tomography room of the X-ray department, as well as the neuroimaging research department of the National Medical Research Centre for psychiatry and neurology named after V. M. Bekhterev.

Author's personal contribution

The topic and plan of the thesis, its main ideas and content were developed together with the scientific supervisors on the basis of many years of focused research.

Patient selection clinical criteria were developed jointly with a psychiatrist and a neuropsychologist.

The author independently formulated and justified the relevance of the thesis topic, goal, objectives and stages of the scientific research. The author personally created an electronic database of patients.

The dissertant personally performed MRI of the brain in 90 patients, with subsequent post-processing of images using FreeSurfer 6.0 software. The author's personal contribution to the study of literature, collection, synthesis, analysis of the obtained data and writing of the thesis is 100%.

Scope and structure of the thesis

The dissertation has 151 pages of typewritten text, consists of an introduction, literature review, chapter with the characteristics of the examined patients and methods of research, chapter with the results of the study, discussion, conclusion, conclusions, practical recommendations and a list of literature, including 62 domestic and 244 foreign sources. The work is illustrated with 30 tables and 21 figures

CHAPTER 1. CURRENT STATE OF THE ART OF NEUROIMAGING DIAGNOSTICS OF MILD COGNITIVE IMPAIRMENT (LITERATURE REVIEW)

1.1. Mild cognitive impairment. Definition. Classification

Currently, the term "mild cognitive impairment" is widely used in the world to describe cognitive impairment beyond the age norm, but not reaching the stage of dementia. In the Russian-language literature, the term "mild cognitive impairment syndrome" is most often used (V. V. Zakharov, N. N. Yakhno, 2004; A. Lokshina. B., 2020; Levin O. S., Chimagomedova A. Sh., 2022; Koberskaya N. N. et al., 2022).

The prevalence of MCI syndrome varies widely around the world and ranges from 3% to 42% according to different studies (Ward A. et al., 2012; Sachdev P. S. et al., 2015). This wide range is probably due to the use of different criteria for the diagnosis of MCI and the study population. In a meta-analysis by the American Academy of Neurology, the prevalence of MCI in the elderly and seniors was 6.7% at ages 60-64 years and 25.2% at ages 80-84 years (Petersen R. C. et al., 2018).

Most studies report that the rate of progression from MCI to dementia is 20-40% of cases per year, with an additional 20% or so returning to normal, which may be due to different etiologies of cognitive impairment (Koepsell T. D., Monsell S. E., 2012; Roberts R., Knopman D. S., 2013).

In our country, the incidence of MCI syndrome and the features of its progression are not sufficiently studied. Nevertheless, cerebrovascular pathology is considered to be of the greatest importance in the development of MCI syndrome (Litvinenko I. V. et al., 2019; Lokshina A. B. et al., 2021).

MCI are a heterogeneous group of conditions arising from various neurological, somatic and psychiatric diseases. The main causes of MCI in older age are various neurodegenerative diseases (primarily AD), cerebrovascular diseases, dysmetabolic disorders and their combinations (Bogolepova A. N. et al., 2021). Neuroinfections, autoimmune diseases, craniocerebral traumas, liquorodynamic disorders, etc. can also be the causes of MCI.

In 1999, R. C. Petersen et al. first proposed criteria for MCI based on clinical and neuropsychological data (Petersen R. C. et al., 1999). At that time, the authors considered MCI as an intermediate stage between normal aging and clinically probable AD. However, since memory decline was considered a prerequisite, and impairment of other cognitive functions and social adaptation were not assessed, these criteria were criticised by other researchers.

In 2004, the criteria were modified to distinguish four main clinical variants of MCI: amnestic monofunctional, amnestic polyfunctional, non-amnestic polyfunctional and non-amnestic monofunctional (Petersen R. C., 2004). The monofunctional and polyfunctional amnestic types of MCI are characterised by memory impairment and are predominantly transformed into dementia in AD. The polyfunctional non-amnestic type is characterised by impairment of several cognitive functions with relative preservation of memory, which is usually found in cerebrovascular lesions, dementia with Lewy bodies, Parkinson's disease, and others. The monofunctional non-amnestic type is characterised by impairment of one cognitive function (except memory), which is more commonly found in cortico-basal degeneration, posterior cortical atrophy, etc.

In our country, O.S. Levin proposed a comprehensive etiological classification of MCI with regard to the neuropsychological profile according to which four types of disorders are distinguished (Levin O. S., 2010; Levin O. S., 2012; Vasenina E. E. et al., 2018):

1. Amnestic type with a characteristic defect of episodic memory associated with memory impairment (defect of reproduction, mediated memory and recognition). This type of MCI is predominantly transformed into AD.

2. The dysregulatory type of MCI is characterised by a predominant impairment of regulatory functions and is associated with dysfunction of the frontal lobes. In this type of MCI, dysfunction of the frontal lobes may be due to primary pathological changes in the frontal cortex or secondary to changes in deep structures (subcortical-frontal syndrome), which leads to disruption of functional connections between subcortical structures and the prefrontal cortex. Patients have difficulties in

performing tasks related to planning, complex step-by-step action, and thinking. This type of MCI is most typical for dyscirculatory encephalopathy.

3. A combination of hippocampal amnestic syndrome with impairment of regulatory or other cognitive functions characterises mixed type of AD. This type can progress both to dementia in AD and to dementia with Levi's corpuscles, vascular dementia, etc.

4. Monofunctional type of MCI is a variant of MCI in which there is a disproportionately severe decline in one of the other cognitive domains (more often visual-spatial or speech), while memory often remains intact. This type of MCI most often leads to the development of dementia with Levi's corpuscles in the case of visual-spatial impairment, and to primary progressive aphasia in severe speech impairment.

Thus, MCI syndrome is characterised by etiopathogenetic and clinical heterogeneity, and in most cases represents a prodromal stage of AD and vascular dementia.

1.1.1. Alzheimer's disease

Alzheimer's disease is a neurodegenerative disease characterised by gradual onset in old age or old age, steady progression of memory and higher brain function disorders leading to dementia with the formation of a characteristic complex of neuropathological, neuroimaging and biochemical features. AD is responsible for up to 60-80% of all dementia cases (Alzheimer's Association, 2018).

AD was first described by the German psychiatrist Alois Alzheimer, who in 1907 published the case history of Augusta D. and typical pathomorphological features of AD (Alzheimer A., 1907).

There are hereditary (familial) and sporadic forms of AD. According to the International Classification of Diseases, Tenth Revision (ICD-10), depending on the onset of symptoms, early-onset (before the age of 65) and late-onset (after the age of 65) forms of AD are distinguished.

Risk factors for the development of AD can be divided into modifiable and non-modifiable (Dubois B. et al., 2016). The strongest risk factor for the development of AD is the elderly and old age. It is noted that in the group of people over 65 years of age, the number of patients doubles every five years (Kukull W. A. et al., 2002). In addition to age, non-modifiable risk factors include a family history of AD (especially in the early form), and carriage of genetic polymorphisms, the most studied of which is the presence of APOE 4 allele, as well as more than 20 others (CLU, ABCA7, SORL1, TREM2, etc.) (Lambert J. C. et al., 2013; Giri M., Zhang M., Lü Y., 2016; Guan M. et al., 2023).

The main risk factor for AD with early onset is family history. Hereditary forms have autosomal dominant transmission and account for up to 5-10% of the total number of patients with AD. Mutations found in genes encoding the proteins presenilin-1 (PS1, chromosome 14), presenilin-2 (PS2, chromosome 1) and amyloid precursor protein (APP, chromosome 21) (Tang Y. P., Gershon E. S., 2003; Tanzi R. E., 2012).

According to statistics, 40-50% of AD with early onset and up to 80% of AD with late onset are associated with carriage of an allele of the apolipoprotein E (APOE4) gene (Fan L. et al., 2020). The presence of one or two copies of APOE4 alleles increases the risk of developing AD up to 3 and 12 times, respectively (Malashenkova I. K., 2018; Ryu J. C. et al., 2019).

Numerous modifiable risk factors have been studied: low education level, hypodynamia, arterial hypertension, diabetes mellitus, obesity, smoking, alcohol, head injuries, epilepsy, depression, environmental pollution, and others. (Deckers K. et al., 2015; Li X. et. al., 2015; Morris M. C. et al., 2015; Edwards III G. A. et al., 2017, 2019; Vetreno R. P., Crews F. T., 2018).

One of the most popular hypotheses of AD development is the "amyloid cascade hypothesis" (Hardy J., Allsop D., 1991). According to this hypothesis, the key link for triggering the cascade of neurodegenerative process is the disruption of amyloid precursor protein (APP) metabolism. APP is a type 1 transmembrane protein associated with neuronal development and axonal transport. Normally, α-secretase cleaves about 90% of APP to form polypeptides that are non-pathogenic. In genetically determined

AD, APP is cleaved by the enzyme β-secretase and then by γ-secretase with the formation of pathological isoform Aβ-42 (Lobzin V. Yu, Kolmakova K. A., Emelin A. Yu, 2018). Accumulation of Aβ-42 in the brain leads to the formation of amyloid fibrils, which in turn form senile plaques, causing neurotoxicity and induction of tau pathology, thereby leading to neuronal death and neurodegeneration (Kametani F., Hasegawa M., 2018). It is now known that more toxic than senile plaques are soluble amyloid protein oligomers, which trigger a whole cascade of damaging mechanisms including neuroinflammatory process, oxidative stress, and excitotoxicity (Ferreira S. T., Klein W. L., 2011; Hölttä M. et al., 2013).

It is related to another widespread hypothesis to hyper-phosphorylation of tau protein (Wischik C.M. et al., 1988). Tau protein is mainly detected in axons of brain neurons. Its functions are assembly and stabilisation of microtubules, providing cytoplasmic transport function. In the case of hyper-phosphorylation, tau-protein passes into a pathological state of disturbance microtubule stabilisation and formation of filamentous structures - neurofibrillary tangles, which leads to extensive cell damage and cell death. Tau protein pathology is also observed in other neurodegenerative diseases, such as frontal-temporal lobe degeneration and parkinsonism associated with chromosome 17 (FTDP-17), progressive supranuclear palsy, corticobasal degeneration, and others.

However, despite significant advances in the study of AD pathophysiology, it has not been possible to develop an effective drug targeting Aβ-42 and tau protein. Therefore, other pathogenesis factors such as vascular dysfunction (Govindpani K. et al., 2020), oxidative stress (Cheignon C. et al., 2018), neuroinflammation (Heneka M. T. et al., 2015), and even the gut microbiota (Cryan J. F. et al., 2020) are being actively considered.

The National Institute of Neurological and Communicative Disorders and Stroke (NINCDS) established the criteria for the clinical diagnosis of AD and the Alzheimer's Disease and Related Disorders Association (ADRDA) working group in 1984 (McKhann G. et al., 1984). However, these criteria allowed diagnosing AD only at the stage of severe cognitive impairment, reaching the level of dementia.

In 2011, the National Institute on Aging and the Alzheimer's Association (NIA-AA) working group revised the criteria for AD to distinguish three stages of the disease (Jack Jr C. R. et al., 2011):

1. Preclinical AD - in the absence of clinical manifestations, AD biomarkers are detected by positron emission tomography (PET) (Aβ accumulation and/or neurodegeneration) and abnormal proteins (Aβ, phosphorylated and total tau protein) are detected in the cerebrospinal fluid.

2. Pre-demanding AD (MCI stage with neuroimaging signs of AD - prodromal AD)

3. Dementia in AD: mild, moderate and severe, determined by examination results and severity of the patient's social disadaptation

For aMCI as a prodromal stage of AD, the following criteria have been proposed (Petersen R. C., 2004; Winblad B. et al., 2004; Jack Jr C. R. et al., 2011; Albert M. S. et al., 2011):

1. Complaints of memory impairment by the patient, or noted by a loved one or doctor;

2. An indication by the patient or a loved one of a decline in cognitive function over the past year compared to the previous level;

3. Cognitive impairments detected during clinical (neuropsychological) examination;

4. No impact of cognitive deficits on daily activities (only mild problems with complex tasks are tolerated);

5. Absence of dementia.

Several neuropsychological tests, including the Logical Memory subtest of the Wechsler Memory Scale (Wechsler D., 1987; Albert M. S. et al., 2013), have been proposed to assess memory decline in this type of MCI. The most commonly used threshold for diagnosing aMCI is 1.5 standard deviations below the age norm (Petersen R. C. et al., 1999; Petersen R. C., Morris J. C., 2005).

In accordance with international diagnostic recommendations NIA-AA, DSM-5 (Diagnostic and Statistical Manual of Mental Disorders, 5th edition), ICD-10, the

combined data of anamnesis, clinical, neuropsychological and neuroimaging (CT, MRI, PET) examinations are currently used to make a lifetime diagnosis of AD.

In 2018, the NIA-AA updated and detailed its classification of biomarkers according to the Amyloid/Tau Protein/Neurodegeneration (A/T/N) system (Jack Jr C. R. et al., 2018). Due to the rapid development of neuroimaging, MRI with morphometry is of great interest, which allows to detect atrophic changes in the early stages of AD, reflecting the process of neurodegeneration (Ananyeva N. I. et al., 2018).

Thus, it is relevant to identify a biomarker that will most accurately reflect the progression from preclinical to clinical stages of AD, as well as improve the differential diagnosis with cognitive impairment of other genesis (Sperling R. A. et al., 2011).

1.1.2. Vascular cognitive impairment

Vascular cognitive impairment (VCI) are represented by the whole spectrum of vascular changes in the brain, leading to cognitive impairment of any severity, ranging from subjective cognitive decline to dementia (T O'Brien J. et al., 2003).

VCI is the second most common dementia after AD, accounting for 15% to 20% of dementia cases in North America and Europe (Rizzi L., Rosset I., Roriz-Cruz M., 2014) and approximately 30% in Asia (Chan K. Y. et al., 2013).

The major risk factors for VCI include age, family history, low level of education, arterial hypertension, diabetes mellitus, obesity, smoking, heart rhythm disorders, hypercholesterolemia, hyperhomocysteinaemia, and others. (Lin Q. et al., 2017; Van Der Flier W. M. et al., 2018; Grishina D. A., Lokshina A. Б., 2021). Less frequently, VCI develops because of cerebral vascular lesions in rheumatic diseases, the pathology of the coagulation or anti-coagulation blood system, cerebral amyloid angiopathy, hereditary arteriopathies, etc. We should note that most elderly people may have some cerebrovascular diseases in the absence of cognitive impairment.

There are 6 main pathogenetic variants of VCI: VCI due to "strategic" brain infarcts, VCI due to haemorrhagic stroke, VCI due to multi-infarct brain damage, VCI due to cerebral hypoperfusion, "subcortical variant" and combined forms of VCI

(Bogolepova A. N. et al., 2021). The "subcortical variant" is the most common pathogenetic variant of VCI and is associated with the lesion of small calibre end vessels supplying the basal nuclei and deep parts of the cerebral white matter.

Significant attention has recently been paid to the early stages of VCI, which served to introduce the term "subcortical vascular mild cognitive impairment" (svMCI) in foreign literature, which literally translates as "subcortical vascular mild cognitive impairment" (svMCI) and is considered, most often, as the prodromal stage of subcortical vascular dementia (Frisoni G. B. et al., 2002; De Mendonça A. et al., 2005; Lyu H. et al., 2019; Frantellizzi V. et al., 2020.). In the domestic literature, the most widely used terms for this condition are "dyscirculatory encephalopathy", "chronic cerebral ischaemia", "subcortical arteriosclerotic encephalopathy" (Levin O. S., 2012; Kalashnikova L. A., Gulevskaya T. S., Dobrynina L. A., 2018).

According to neuroimaging data in svMCI, signs of CSVD in the form of focal changes in the white matter of the brain, lacunar infarcts, microhemorrhages and dilated perivascular spaces are determined (Skrobot O. A. et al., 2018). Neuropsychological profile in svMCI is represented by dysregulatory type of cognitive impairment and is characterised by impairment of controlling (regulatory, executive) mental functions (Levin O. S., 2006; Levin O. S., 2012; Ghosh S., Libon D., Lippa C., 2014). The clinical picture of svMCI is usually represented by a gradual onset and slow progression, but can be combined with episodes of acute neurological symptomatology, such as dysarthria, paresis, and walking disorders (T O'Brien J. et al., 2003; Maximova M. Y., Piradov M. A., 2017). Lesion of the basal nuclei and periventricular white matter leads to functional isolation of the frontal lobes of the brain with the formation of secondary frontal dysfunction with the presence of cognitive and emotional disorders of frontal character (Zakharov V. V., Vakhnina N. V., 2014).

Thus, aMCI and svMCI may be prodromal stages of the most common types of dementia – AD dementia and subcortical vascular dementia. The emergence of modern neuroimaging techniques is of great importance for clarifying the etiology of MCI, which makes it possible to compare the results obtained with clinical data and is likely to expand the possibilities of therapeutic intervention and slow down the pathological

process at an early stage of the disease, and in some cases prevent it (Livingston G. et al., 2020).

1.2. Radiological anatomy of the hippocapmal formation

The medial regions of the temporal lobe are represented by the HF, the parahippocampal region and the amygdala complex (van Staalduinen E. K., Zeineh M. M., 2022). The HF is a key structure of the limbic system of the brain involved in many cognitive processes, including memory consolidation and recall, spatial navigation, creativity, emotion and social behaviour.

Atrophic changes in HF are known to occur in the early stages of AD, with some researchers describing changes in certain subfields even in preclinical stages (Wu J. et al., 2022). However, atrophic HF changes are also found in other neurodegenerative diseases, as well as in AD (Wong F. C. C. et al., 2021).

The term "hippocampus" was first used by the Italian anatomist and surgeon Giulio Cesare Arancius in 1587 in the first chapter of his work "De Humano Foetu Liber" (Bir S. C. et al., 2015). The term is derived from the Greek word for seahorse - "hippos" (horse) and "campus" (sea monster). A number of other terms have subsequently been proposed to describe this structure, including "silkworm", "horn of Ammon" and "ram's horn". However, it is the first name for this structure that has been most widely used in the literature to date. Arancius linked the functional significance of the open brain structure to olfaction. The connection of the hippocampus with cognitive impairment was first mentioned in the studies of V. M. Bekhterev, who in 1900 described two patients with memory disorders who had hippocampal damage (Bekhterev V. M., 1900).

The HF consists of a set of cytoarchitectonically different subfields: the hippocampus proper or ammon's horn (cornu ammonis), dentate gyrus and subicular complex (Figure 1). Some authors also refer the entorhinal cortex to the HF because of its proximity and the presence of important functional connections (Schultz C., Engelhardt M., 2014).

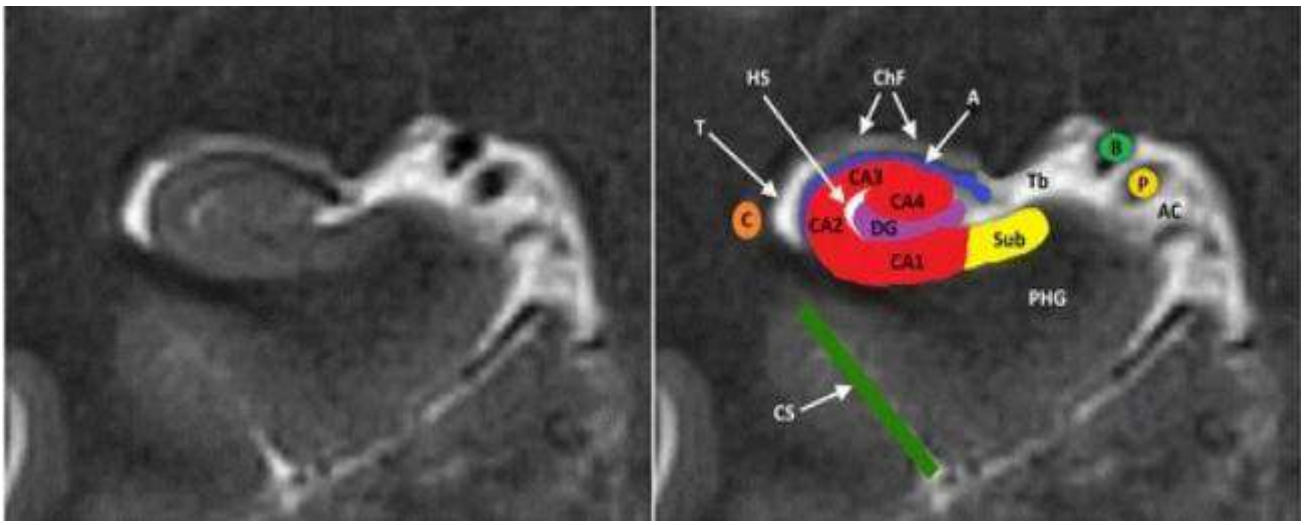

Figure 1 - MR image of the HF (T2 WI). CA1-CA4 - sectors of the hippocampus proper, DG - dentate gyrus, Hs - small cyst of the hippocampal sulcus, A - alveus, Ac – ambient cisterna, B - basal vein of Rosenthal, C - tail of the caudate nucleus, ChF – choroid fissure, CS - collateral sulcus, DG - dentate gyrus, P - posterior cerebral artery, PHG - parahippocampal gyrus, Sub - subiculum, T - temporal horn of lateral ventricle, Tb - transverse fissure of Bichat (Cited. Unforgettable, - a pictorial essay on anatomy and pathology of the hippocampus / S. Dekeyzer et al. // Insights into imaging. - 2017. - Vol. 8. - P. 200)

The HF is a C-shaped structure of grey and white matter located anteroposteriorly along the temporal horn of the lateral ventricle of the brain with a length of 4.5-5 cm. The HF is divided into 3 parts: the anterior part or head, the middle part or body, and the posterior part or tail. There are approximate boundaries of the HF parts based on coronal images. The boundary of the head and body is the area where the apex of the hippocampal hook is clearly visualised. The boundary of the tail and body of the hippocampus is the place where the vault columns (Ananyeva N. I. et al., 2015; Malykhin N. V. et al., 2017) or the hilum of the quadrigeminal plate (Berron D. et al., 2017) are most fully visualised. The head is the most voluminous part of the hippocampus and directly passes into the amygdala body. The intraventricular surface of the head forms 2 to 4 finger-like bulges (digitations). The tail is characterised by variability of shape and location of subfields against the background of variability of its curves, which causes difficulties in its segmentation.

They usually divide the hippocampus proper into 4 sectors, labelled CA1-CA4. The largest sector is CA1. Medially it borders medially with the subicular complex and dorso-laterally with CA2 (Palomero-Gallagher N. et al., 2020.).

CA2 is a relatively small region located between CA3 and CA1 that provides a connection between the entorhinal cortex and CA1 (Andrade-Talavera Y., Rodríguez-Moreno A., 2023). In the FreeSurfer 6.0 software, the CA2 and CA3 subfields are combined due to the lack of clear boundaries between them.

CA3 forms the upper contour of the hippocampus, and CA4 is located in the central sections and surrounded by the dentate gyrus.

Histologically and phylogenetically, the hippocampus proper and the dentate gyrus are referred to the archicortex. The hippocampus proper is usually distinguished by three or four layers, as opposed to six layers in the neocortex. The outermost layer of the hippocampus is represented by a thin layer of white matter (alveus) and is formed by axons emanating from the hippocampus. The next superficial layer is called stratumoriens and contains basal dendrites, pyramidal cell axons and interneurons. The middle layer, stratum pyramidale, contains pyramidal cells, which are the main cellular elements of the hippocampus. The deep layer combines stratum radiatum, lacunosum and moleculare (SRLM) and is represented by apical dendrites, axons and interneurons. In CA3, a special layer, stratum lucidum, is distinguished, in which proximal dendrites contact with axons of granular neurons of the dentate gyrus (mossy fibres).

The CA1 field bounds the subiculum medially and continues laterally along the lower part of the hippocampus, curving upwards along the temporal horn of the lateral ventricle. The CA1/CA2 boundary differentiates at the transition region to a denser and narrower layer of CA2 pyramidal cells. The CA2/CA3 boundary roughly corresponds to the extension of the CA3 pyramidal layer.

The dentate gyrus is a C-shaped structure consisting of three layers of cells: the outer molecular layer, the middle granular layer, and the inner layer of polymorphic cells, which merges with the CA4 sector. The main neurons of the dentate gyrus are granular cells. The dentate gyrus has the unique ability to proliferate neurons throughout life. This neurogenesis is important for hippocampal functions such as learning, long-

term memory, spatial memory, and mood (Rao Y. L. et al., 2022). The hippocapmal sulcus separates the dentate gyrus from the ammonic horn and subiculum.

The subiculum complex includes the subiculum, presubiculum, parasubiculum, and prosubiculum. The subiculum and CA1 do not have a clear boundary, forming a transitional zone, labelled by some authors as the prosubiculum. The subiculum is the largest region of the subiculum complex and the most rostrally located among other HF subfields. Three layers are distinguished in the subiculum: molecular, pyramidal and multiform layers. The main neurons of the subiculum are large pyramidal cells. The subiculum gives rise to the main subcortical projections to the septal complex, contiguous nucleus, anterior thalamus and mammilary nuclei, as well as projections to the entorhinal cortex. The parasubiculum is the most medial part of the subicular complex and is located between the presubiculum and the entorhinal cortex. The parasubiculum is relatively small and characterised by indistinct differentiation of layers on MRI images, unlike the presubiculum and entorhinal cortex.

The axons of pyramidal neurons of the ammon horn and subiculum continue into the white matter lining the ventricular surface of the hippocampus (alveus) and merge at its medial edge to form the fimbriae (hippocampal fringe). The fimbriae then continue into the vault and reach the corpus callosum.

The molecular layer is formed by fibres that transmit sensory information from the entorhinal cortex, which is particularly important for higher executive functions such as attention and planning (Amaral D. G. et al., 2007).

The entorhinal cortex (28 Brodmann's field) belongs to the periallocortex and has a six-layered structure typical of the neocortex. It extends rostrally to approximately the middle of the amygdala and caudally to the level of the anterior border of the lateral patellar body. Anatomically, the entorhinal cortex is subdivided into lateral and medial regions, which have a similar histological structure but differ significantly in function. The entorhinal cortex is the main interface between the hippocampus and several brain regions.

A major contribution to understanding the anatomy of the HF subfields was made by de Flores R. et al. who compared similar slices from postmortem histological

examination with high-resolution MR images (0.2 × 0.2 × 0.2 mm 3) taken perpendicular to the long axis of the HF (de Flores R. et al., 2020).

On MR images, the grey matter of the HF is characterised by an MR signal similar to the cortex and basal nuclei, except for the molecular lacunosal layer containing white matter of the perforant pathway. On T2 WI, the band of white matter of the molecular lacunosal layer is visualised as a hypointense line separating the dentate gyrus from the hippocampus proper and the subiculum, and is referred to as the 'dark band' (Berron D. et al., 2017). The subiculum also contains myelinated nerve fibres and is therefore characterised by a relatively low MR signal on T2 WI.

The arterial supply of the HF is provided by collateral branches (anterior, middle and posterior hippocampal arteries) of the posterior cerebral artery and the anterior choroidal artery. Venous outflow occurs in the intrahippocampal veins flowing into the superficial hippocampal veins, which flow into the basilar vein.

1.3. Radiological diagnostic techniques for mild cognitive impairment

Neuroimaging research methods plays an important role in planning the diagnostic examination of patients with cognitive impairment of varying severity (Johnson K.A. et al., 2012; Ananyeva N. I. et al., 2018). In recent decades, thanks to significant advances in the development of neuroimaging, it has become possible to perform differential diagnosis at an early stage of various diseases accompanied by cognitive decline.

Magnetic resonance imaging is one of the available and effective methods of diagnosing AD and VCI at early stages (Neznanov N. G. et al., 2016, 2018; Stulov I.K. et al., 2022: 244). Positron emission tomography (PET), including with the use of Aβ markers (Artemov M. V., Stanzhevsky A. A., 2020; Spano M. et al., 2023), as well as single-photon emission tomography (SPECT) (Emelin A. Y. et al., 2020; Świetlik D., Białowąs J., 2019) deserve a special role. X-ray computed tomography (CT) is inferior to brain MRI in the assessment of brain matter (Frisoni G. B., 2001) and has limited application when there are contraindications for MRI. Nevertheless, CT allows rapid

exclusion of other possible causes of cognitive impairment, such as tumour, haemorrhage and hydrocephalus, as well as detecting indirect signs of atrophic changes in the HF in general.

Magnetic resonance imaging:

One of the first papers devoted to differential diagnosis of cognitive impairment using neuroimaging methods was published by Erkinjuntti T. et al. in 1987 (Erkinjuntti T. et al., 1987). This paper described diffuse white matter changes and/or the consequences of brain infarcts in patients with vascular dementia, and noted the high sensitivity of MRI compared to CT.

MRI is widely used in the assessment of atrophic changes and focal brain lesions. With the advent of new MRI post-processing technologies, it is now possible to quantify both atrophic changes in various brain structures and focal changes.

Progressive atrophy characterises AD because of damage and death of brain neurons. Atrophic changes in the brain in AD are more pronounced than in VCI. According to histopathological studies and MR-morphometry, the earliest atrophic changes are found in medial parts of temporal lobes, especially in entorhinal cortex and HF (Braak H., Braak E., 1991; Scahill R. I. et al., 2002; Killiany R. J. et al., 2002; Neznanov N. G. et al., 2018). With further progression, the temporal neocortex is involved, and only then the process spreads to the parietal and frontal lobes (McDonald C. R. et al., 2009; Maxwell S. P., Cash M. K., Darvesh S., 2022).

It is worth noting that, in clinical practice, it usually made the diagnosis of AD when atrophic changes are already present. Even in patients at the early stage of AD (MMSE ~ 24) entorhinal cortex volumes are already reduced by ~ 20-30% and hippocampal volumes by ~ 15-25% (Schuff N. et al., 2009; Dickerson B. C. et al., 2001). The annual reduction in hippocampal volumes in early stage AD is approximately 3-5% (Schuff N. et al., 2009; Barnes J. et al., 2009), while in older adults without dementia, hippocampal atrophy is about 1-2% per year (Erickson K. I. et al., 2011). Given the described features, atrophic changes in the medial sections of the temporal lobes are used as a biomarker for AD at the stage of MCI (Albert M. S. et al., 2011; Ananyeva N. I. et al., 2017, 2018).

In neuroimaging studies of patients with suspected neurodegenerative diseases, the medial temporal lobe atrophy (MTA) scale, which is primarily focused on hippocampal atrophy (Scheltens P. et al., 1992), is widely used for approximate assessment of atrophic changes in the medial temporal lobe. This scale is based on visual assessment of the choroidal slit width, temporal horn width of the lateral ventricles and hippocampal height on coronal images at the level of the anterior pontine (Table 1, Figure 2). The score is related to age: < 75 years - a score ≥ 2 points is considered pathological, 75 years and older - a score ≤ 3 points is considered pathological.

Table 1 - Medial temporal atrophy scale

Score	Width of the choroidal fissure	Width of the temporal horn of the lateral ventricle	Hippocampal height
0	norm	norm	norm
1	↑	norm	norm
2	↑↑	↑	↓
3	↑↑↑	↑↑	↓↓
4	↑↑↑	↑↑↑	↓↓↓

Nevertheless, several pathomorphological and neuroimaging studies have shown that some of the first structures to show pathological changes in AD are the entorhinal and transentorhinal cortex, with subsequent involvement of specific HF subfields (Braak H., Braak E., 1991; Khan U.A. et al., 2014; Jessen F. et al., 2006). Thus according to one study (Kulason S. et al. 2020), based on MR morphometry, the earliest atrophic changes were found in the transentorhinal cortex 9-14 years and in the entorhinal cortex 8-11 years, before the establishment of the MCI syndrome. Therefore, Enkirch S. J. et al. proposed a new visual scale to assess entorhinal cortex atrophy (ERICA) (Enkirch S. J. et al., 2018). This scale assesses dilation of the collateral sulcus,

atrophy of the entorhinal cortex and parahippocampal gyrus on coronal images at the level of the mammilary bodies (Figure 2).

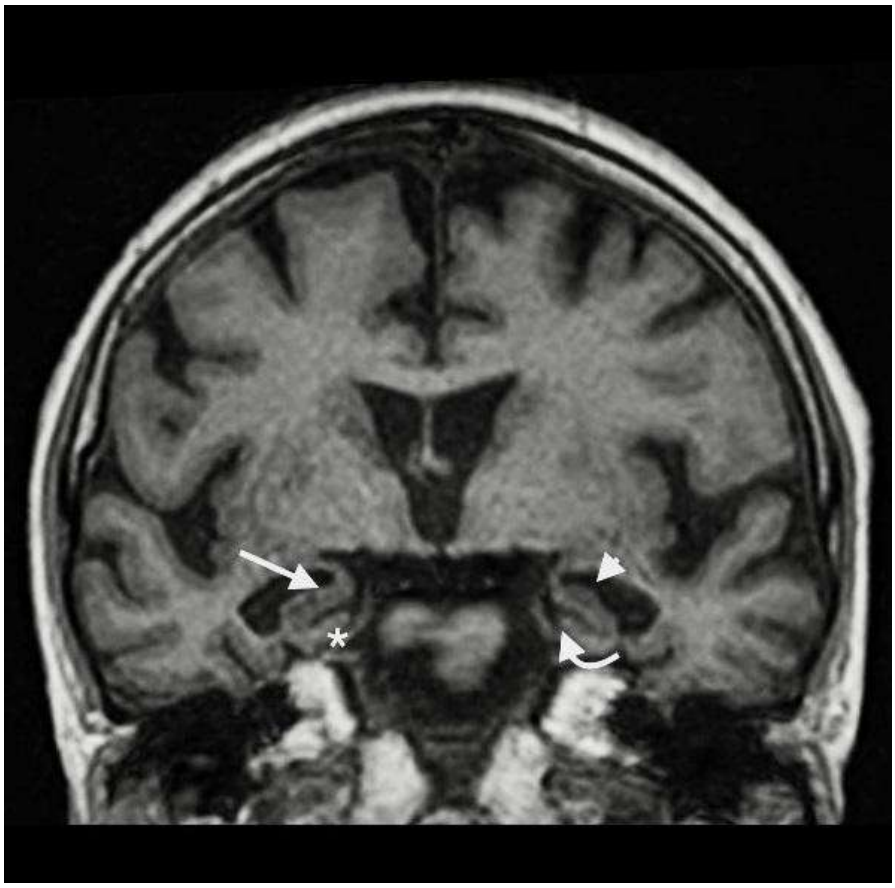

Figure 2 - Coronal image of the mediobasal regions of the temporal lobes (T1 WI) . MTA and ERICA visual scales score:. MTA=3 (arrow), MTA=4 (arrow head), ERICA=2 (asterisk) and ERICA=3 (curved arrow)

ERICA score 2 is characterised by the appearance of a gap between the entorhinal cortex and the cerebellar outline - the "tentorial gap sign" shown in Figure 2. According to the authors, an ERICA score of 2 or higher with the presence of the "tentorial gap sign" allows to distinguish between patients with subjective cognitive decline and AD at the stage of clinical manifestations with an accuracy of 91%.

In the work of Traschütz A. et al. the use of the ERICA scale had a positive predictive value (PPV) of 97% for the presence of aMCI syndrome and 83% for the presence of conversion of aMCI to dementia in AD, which was comparable to a volumetric study (Traschütz A. etal., 2020). According to Roberge X. et al. a positive

ERICA scale score (≥2-3) was associated with conversion of aMCI to dementia in AD with a sensitivity of 56% and a specificity of 78% compared to 69% and 60%, respectively, for a positive MTA scale score (≥2 for ≤75 years or ≥3 for >75 years) (Roberge X. et al., 2021).

Focal brain changes are characteristic of the "subcortical variant" of VCI on the background of CSVD. There are special standards for describing neuroimaging signs of CSVD - STRIVE (Standards for ReportIng Vascular changes on nEuroimaging), adopted in 2013 by an international group of experts (Wardlaw J. M. et al., 2013). The standardised neuroimaging signs of small vessel lesions include "recent" small subcortical infarcts, lacunae, white matter hyperintensity (WMH), dilated perivascular spaces, cerebral microhemorrhages (CMH) and brain atrophy.

The term "recent" small subcortical infarction refers to neuroimaging signs of a small infarction in the territory of a single perforating arteriole with corresponding clinical manifestations occurring in the previous few weeks. Usually such a subcortical infarction, taking into account the timing of its occurrence, is called acute or subacute, and its size is up to 20 mm in the axial plane. According to Doubal F. N. et al, up to 30% of patients with clinical symptoms of subcortical infarcts may have no neuroimaging features on MRI (Doubal F. N., Dennis M. S., Wardlaw J. M., 2011). Some subcortical infarcts are detected incidentally on neuroimaging and are referred to as asymptomatic or "dumb" brain infarcts. Most subcortical infarcts transform over time into lacunes (Poirier and Desrouesne type Ia lacunes) (Poirier J., Derouesne C., 1984). However, some subcortical infarcts transform into hyperintense foci on FLAIR MRI without cavity formation, which is described as incomplete infarction (lacunae of type Ib according to Poirier and Desrouesne classification) (Poirier J., Derouesne C., 1984; Vereshchagin N. V., Morgunov V. A., Gulevskaya T. C., 1997).

According to STRIVE criteria, a lacuna is a rounded or ovoid cavity of subcortical localisation filled with fluid similar to the MR signal of cerebrospinal fluid, with a diameter of 3 to 15 mm (Figure 3).

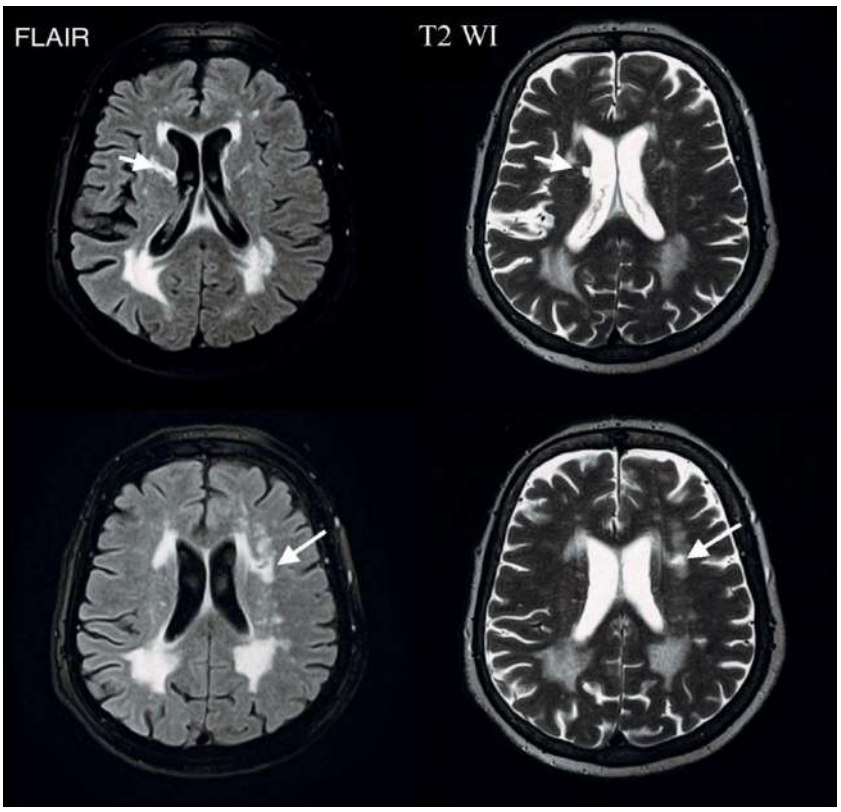

Figure 3 - MRI of the brain, axial plane (FLAIR and T2 WI). Lacunae in the basal nuclei and deep white matter of the brain (arrows).

The lacuna in the vast majority of cases corresponds to the consequence of a small cerebral infarction in the territory of a single perforating arteriole, but in rare cases may be the result of a small haemorrhage.

In contrast to lacunae, Virchow-Robin perivascular spaces (PVS) are located along the vessels, are linear (or rounded in cross-section) and up to 3mm in diameter, and usually lack a hyperintense rim on T2 WI and FLAIR MRI in the periphery (Bokura H., Kobayashi S., Yamaguchi S., 1998). However, the perivascular spaces may increase up to 10-20mm in diameter, especially in the basal nuclei. These changes are described as status cribrosum or Ét at criblé (Poirier J., Derouesne C., 1985). Although the clinical relevance of the presence of dilated PVS in the brain remains controversial, some authors have described their contribution to the development of CSVD and cognitive decline (Mills S. et al., 2007; Doubal F. N. et al., 2010; Niazi M. et al., 2018), others report no significant correlation with cognitive function (Hilal S. et al., 2018). Gertje E. C. et al. report an association of dilated PVS with CSVD severity, but no correlation with cognitive decline (Gertje E. C. et al., 2021).

WMH of presumably vascular genesis is characterised by the presence of hyperintense changes in T2 WI and FLAIR, iso- and hypointense changes on T1 WI. Fazekas F. et al proposed the scale for assessment of brain white matter changes in 1987 and is currently the most widespread (Fazekas F. et al., 1987). Using this scale, the deep white matter and periventricular white matter are studied separately, each area being graded from 0 to 3 points. It showed the different grades on the Fazekas scale in Figure 4.

Differences in the etiology and histopathology of deep and periventricular white matter lesions have been described (Fazekas F., Schmidt R., Scheltens P., 1998). Changes in the periventricular white matter are associated with demyelination, granular ependymitis and subependymal gliosis, whereas changes in the deep white matter are ischaemic in nature and contribute to the development of VCI (Fazekas F. et al., 1993).

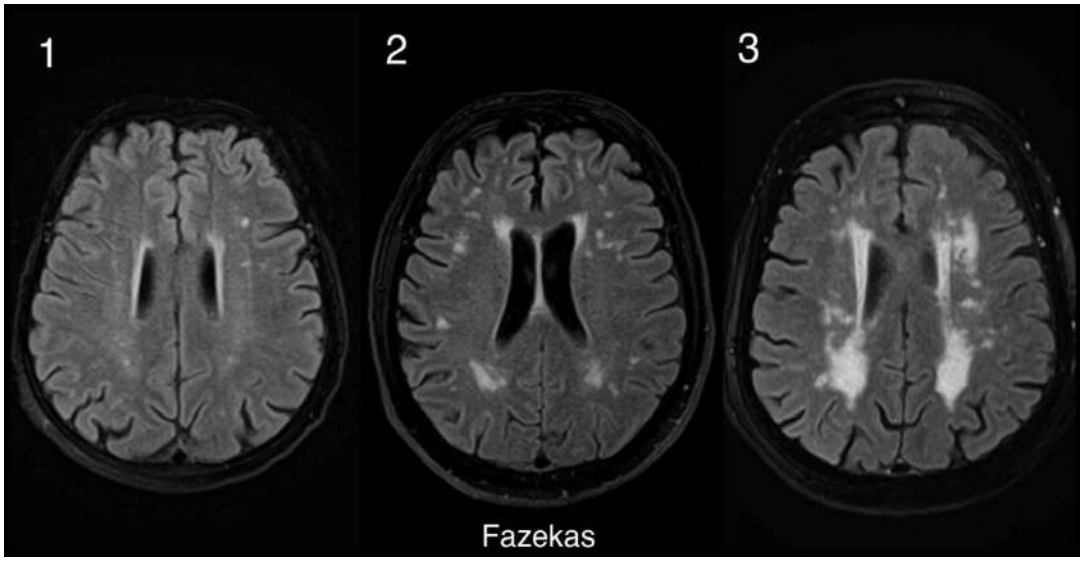

Figure 4 - Axial images of the brain (FLAIR). Stages according to Fazekas visual scale 1, 2 and 3

The following volumes have been proposed as the threshold for the volume of white matter lesions that can cause cognitive impairment: 25% of total white matter (Van Straaten E. C. W. et al., 2003; Price C. C. et al., 2005), 10 cm2 of white matter (Boone K. B. et al., 1992), 0.5% of white matter of intracranial volume (De Carli C. et al., 1995). However, there are currently no clear recommendations as to what volume to

use as a threshold for patients with VCI. It is worth noting that the statement of the International Society of Vascular Behavioral and Cognitive Disorders (VASCOG) (Sachdev P. et al., 2014) recommends paying attention to the presence of extensive and confluent lesions, which corresponds to Fazekas grade 2 and 3. The VASCOG statement also notes that the presence of lacunar infarcts (one or more) is mandatory for vascular dementia, but not for MCI stage.

Progress in the diagnosis of CMH is associated with the widespread use of blood product-sensitive pulse sequences, such as T2* gradient echo (GRE) and susceptibility weighted imaging (SWI) on MR scanners (Greenberg S. M. et al., 2009; Blitstein M. K., Tung G. A., 2007). CMH histologically represent macrophages containing haemosiderin and possessing paramagnetic properties (Fazekas F. et al., 1999; De Reuck J. et al., 2011). The relationship between the presence of CMH and the development of dementia is determined. Thus, according to Uetani H. et al., in MRI with magnetic field strength of 3.0 Tesla CMH were more often detected in patients with vascular dementia - up to 86%, less often in AD - 48%, and in patients with MCI was up to 41% (Uetani H. et al., 2013).

The etiology of CMH is quite extensive, but the two most common forms associated with small vessel pathology are hypertensive microangiopathy (HMA) and cerebral amyloid angiopathy (CAA) (Charidimou A. et al., 2016). CSVD develops on the background of long-term arterial hypertension and is caused by the lesion of small perforating arteries of the deep parts of the brain. HMA is detected in 60% of patients with arterial hypertension (AH) over 55 years of age and 80% over 85 years of age, over 55 years of age and 80% over 85 years of age. Cerebral amyloid angiopathy (CAA) is a disease caused by abnormal deposition of Aβ in the wall of cortical and leptomeningeal vessels, which can lead to both CMH and macroscopic intracerebral haemorrhage (Charidimou A. et al., 2016; Magid-Bernstein J. et al., 2022).

For CAA and AD, the lobular distribution of CMH is most typical, while HMA is characterised by a central location - in the deep white matter, basal nuclei, thalamus, brainstem, cerebellum (Vernooij M. W. et al., 2008).

Thus, structural MRI data allow us to assess atrophic changes in the brain using visual scales, as well as to detect signs of CSVD.

Diffuse-tensor magnetic resonance imaging:

Recently, the diffusion-tensor imaging (DTI) method has become widespread for the assessment of white matter pathology, which made it possible to detect microstructural abnormalities invisible on structural MRI (Egle M. et al., 2022). DTI is a modern method of lifetime assessment of the directionality of water diffusion in the human brain, which allows to evaluate white matter conductive pathways (Pronin I. N. et al., 2008). Fractional anisotropy (FA) is the most important index of the diffusion tensor and characterises the spatial orientation of white matter fibres.

With the introduction of DTI, a new perspective on AD, which was previously predominantly considered as a grey matter pathology, has emerged (Aung W. Y., Mar S., Benzinger T. L. S., 2013). A study by Huang J. et al. found white matter changes in patients with early AD in the temporal, parietal and frontal lobes that correlated with cognitive deficits (Huang J., Auchus A. P., 2007). Magalhães T. N. C. et al. found damage to the tracts of the medial temporal lobes in patients with aMCI accompanied by atrophic hippocampal changes (Magalhães T. N. C. et al., 2023).

In svMCI, a decrease in white matter FA is determined throughout the brain, with a more pronounced decrease in the corpus callosum, internal capsule, radial vein, posterior thalamic radicles, inferior longitudinal fascicles, inferior fronto-occipital fascicles, and right superior longitudinal fascicle (Zhou Y. et al., 2011; Tu M. C. et al., 2017; Wang Z. et al., 2020; Qiu Y. et al., 2021).

Thus, the use of DTI is a useful additional technique to assess white matter microstructure disorder associated with demyelination, gliosis and conduction pathway damage in neurodegenerative and cerebrovascular diseases.

Functional magnetic resonance imaging:

Patients with aMCI demonstrate impaired default mode network functioning compared to healthy individuals related to retrieval of autobiographical and episodic memories (Acharya A. et al., 2019). Reduced functional connectivity characterises this

category of patients between the hippocampus and the posterior cingulate gyrus (Dunn C. J. et al., 2014).

In svMCI, changes in the executive control network are primarily identified, and decreased connectivity in the dorsal attention network, the default mode network, and the sensorimotor network is also noted (Acharya A. et al., 2019; Chong J. S. X. et al., 2019; Fokin V. F. et al., 2020). This can be explained by a decrease in neuronal activity along the anteroposterior axis mediated by structural damage to long associative pathways and cortical-subcortical connections against the background of focal brain lesions (Dey A. K. et al., 2016).

Nevertheless, at present, the role of fMRI in the differential diagnosis of MCI of various genesis remains unclear.

Radionuclide techniques:

Functional neuroimaging, including positron emission tomography (PET) and single photon emission computed tomography (SPECT), has been used to assess metabolic and perfusion changes in different types of cognitive impairment (Oldan J. D. et al., 2021; Zheng Y., Zhou Z., 2021).

PET is a diagnostic technique of nuclear medicine that allows monitoring the distribution in the body of biologically active compounds labelled with positron-emitting radioisotopes. One of the most widely used radiopharmaceuticals (RFC) for the assessment of cerebral metabolism is 18 F-fluorodeoxyglucose (18F-FDG), due to its longest half-life and lowest emission energy.

The informativeness of 18F-FDG PET technique in different types of aMCI has been shown in a number of works (Lupanov I. A., 2014; Caminiti S. P. et al., 2018). In patients with aMCI, areas of hypometabolism are usually detected in parietal and temporal cortex, precuneus and posterior cingulate cortex (Mosconi L. et al., 2008; Herholz K. et al., 2011). Several authors have reported a negative prognostic value of 18F-FDG PET in patients with aMCI, which can be extremely useful to exclude progression to dementia (Caminiti S.P. etal., 2018; Tripathi M. et al., 2019).

The metabolic changes in 18F-FDG PET in patients with VCI differ depending on the nature and severity of the cerebrovascular process. Most often, local,

asymmetrical areas of metabolic reduction in the white matter and cortex, mainly in the frontal lobes, as well as in the subcortical structures are detected in patients with svMCI (Odinak M.M. et al., 2012; Lupanov I.A., 2014).

Neuropathological features of AD are Aβ and NFT in the brain (Jack C.R. et al., 2013). In accordance with this, specific preparations for lifetime visualisation of tau protein (Flortaucipir 18) and Aβ (Florbetaben, Florbetapir, Flutemetamol, etc.) in the brain have been developed for PET.

One of the first and most studied Aβ biomarkers is C-11 Pittsburgh Compound B (PIB), which has high sensitivity for detecting the fibrillar form of Aβ.

However, the data of PET with Aβ biomarkers for the diagnosis of AD and aMCI are ambiguous. Thus, positive results of PET with Aβ biomarkers range from 10% in individuals aged 50 years to 44% in individuals aged 90 years (Jansen W. J. et al., 2015), and in pathological studies Aβ is detected in about 30% of cognitively healthy individuals (Bennett D. A. et al., 2006). It should be noted that approximately 30% of patients with subcortical VCI are also found to have pathological Aβ deposits on PET (Lee M. J. et al., 2014). Nevertheless, negative PET results with Aβ biomarkers are a good test to exclude AD in subjects with cognitive impairment.

Single-photon emission computed tomography (SPECT) is an alternative to PET, which provides insight into regional cerebral perfusion, while being a cheaper and more accessible diagnostic method in clinical practice (Litvinenko I. V. et al., 2019).

In Russia, a technetium-99m-based radiopharmaceutical (RFC), exametazyme, is used to assess regional cerebral blood flow (Kondakov A. K. et al., 2016; Kurbanova M. M. et al., 2020). Most studies have revealed the dependence of glucose metabolism, according to FDG-PET data, with SPECT perfusion indices in certain parts of the brain according to metabolic demand.

There are specific patterns of glucose hypometabolism and hypoperfusion in the posterior cingulate cortex and precuneus in the early stages of AD with subsequent spread to the posterior temporoparietal cortex (Valotassiou V. et al., 2015).

The sensitivity and specificity of perfusion SPECT for identifying patients with AD from healthy individuals are considered to be lower compared to PET with FDG

(80% and 85% vs. 90% and 89%, respectively), but both methods have higher specificity than clinical criteria (specificity 70%) (Bloudek L. M. et al., 2011; Valotassiou V. et al., 2018). A study by Yeo J. M et al. determined the sensitivity and specificity of SPECT at 79.7% and 79.9% for the differential diagnosis of AD and frontal temporal degeneration, 74.5% and 72.4% for the differential diagnosis of AD and vascular dementia, and 70.2% and 76.2% for the differential diagnosis of AD and dementia with Lewy bodies (Yeo J. M. et al., 2013).

Thus, radionuclide techniques are effective methods for diagnosing cognitive impairment, but their use is limited by the high cost of the RFC used.

1.4. MR-morphometry of hippocampal formation in the diagnosis of mild cognitive impairment of different genesis

Currently, it is of great interest to study the atrophic changes of HF subfields, which will possibly improve the differential diagnosis of various diseases at the MCI stage (Xiong W. et al., 2023.).

The functional significance of HF was first mentioned in the studies of V.M Bekhterev, who described in 1900 two patients with memory impairment with hippocampal damage (Bekhterev V., 1900).

Analysis of HF volumes using MR morphometry has been successfully applied in many neuropsychiatric diseases. However, the segmentation of HF subfields has long been performed manually, which is time-consuming and leads to measurement errors because it is highly dependent on the researcher. Van Leemput K. et al. developed a computational method for fully automated HF subfield segmentation based on a Bayesian modelling approach implemented in the publicly available FreeSurfer software (Van Leemput K. et al., 2009).

Using the FreeSurfer 6.0 software version it is possible to obtain volumetric indices of 12 HF subfields: sectors of the ammonic horn (CA1, CA3, CA4), dentate gyrus (granule cells and molecular layer of the dentate gyrus - GC-ML-DG). - granule

cells and molecular layer of the dentate gyrus (GC-ML-DG), subiculum, presubiculum, parasubiculum, molecular layer of the hippocampus, hippocampus-amygdala transition area (HATA), hippocampal sulcus, fimbriae and hippocampal tail. It is worth noting that the FreeSurfer 6.0 version compared to the previous FreeSurfer 5.3 version is a more reliable, versatile and anatomically accurate tool for segmentation of HF subfields (Whelan C. D. et al., 2016).

According to the data of pathomorphological studies, the neurodegenerative process in AD has certain stages associated with intracellular accumulation of NFT and first described by Braak H. and Braak E. (Braak H., Braak E., 1991). The earliest changes resulting from NFT accumulation occur in the transentorhinal cortex and entorhinal cortex, which corresponds to the preclinical stages of AD (Braak H., Braak E., 1991; Schönheit B., Zarski R., Ohm T.G., 2004). The process then moves to CA1 and the subiculum of the HF, and as the disease progresses, spreads to the remaining HF subfields (Figure 5). Neocortex is usually affected at late stages of AD (stages V, VI according to Braak H. and Braak E.).

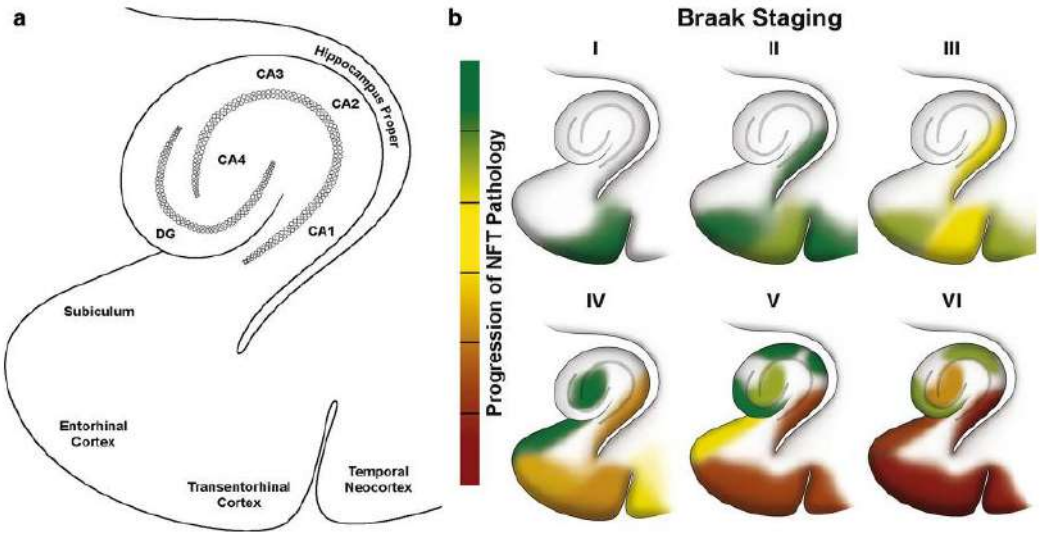

Figure 5 - anatomy of hippocampal formation subfields (a), distribution of neurofibrillary tangles, Braak stages (b)
(Cited inThe basis of cellular and regional vulnerability in Alzheimer's disease / Mrdjen D. et al. //Acta Neuropathologica. - 2019. - №138. - P. 734)

Atrophic HF changes are considered the most confirmed and widely used biomarker of AD according to MRI (Neznanov N. G., 2016; Csukly G. et al., 2016; Andreev E. V., 2017). However, data from recent studies show that specific changes in specific HF subfields may be a more sensitive biomarker than total HF volume and applied at the aMCI stage. For example, Wu J. et al. described atrophic changes in specific HF subfields even in preclinical stages of AD (Wu J. et al., 2022). According to most neuroimaging studies, the subiculum, CA1, and entorhinal cortex are the most vulnerable HF subfields for neurodegenerative process in AD (Apostolova L. G. et al., 2010; Tran T. T. et al., 2022). However, other studies have shown reduced volumes of CA3 and dentate gyrus in patients with aMCI (Yassa M. A. et al., 2010), or CA2/CA3 (Hanseeuw B. J. et al., 2011). Thus, at present, the MR-semiotics of atrophic changes in the HF subfields in aMCI remains poorly studied and the results are often contradictory.

It is worth noting that atrophic changes in the HF are also found in other neurodegenerative diseases, as well as in VCI (Van de Pol L. et al., 2011). For example, in svMCI, several studies have found decreased volumetric measures of the subiculum, CA1, CA4, molecular layer and dentate gyrus (Wong F. C. C. et al., 2021; He M. et al., 2022). In a recent longitudinal study, the annual rate of subiculum atrophy was shown to be significantly higher in individuals with a high rate of progression of white matter hyperintensity on MRI (Pin G. et al., 2021). Disruption of calcium homeostasis, oxidative stress, neuroinflammation and other pathophysiological mechanisms involved in ischaemic/hypoxic injury contribute to damage and death of HF neurons.

Atrophic changes in the HF are also determined in hippocampal sclerosis in the elderly, which is due to preferential neuronal damage and gliosis in CA1 and subiculum (Jicha G. A., Nelson P. T., 2019). In this pathology, HF changes are more pronounced compared to AD and are disproportionate to the degree of cognitive impairment. MRI in T2WI mode usually shows an increase in MR signal from the hippocampus in combination with a decrease in its volume.

Separately, it is necessary to note the potential application of MR-morphometry of HF in monitoring and evaluating the effectiveness of therapy in patients with MCI. Recently, the neuroplasticity of HF has been studied with the aim of slowing cognitive

decline and potentially delaying the onset of dementia (Scarmeas N., 2017; Yassine H. N., Schneider L. S., 2017). For example, a study by Ten Brinke L. F. et al. found an increase in hippocampal volumes in patients with MCI who performed aerobic exercise for 6 months (Ten Brinke L. F. et al., 2015). Erickson K. I. et al. conducted a study of the effects of aerobic exercise on the hippocampus in older adults without cognitive impairment. This study revealed a preferential increase in the volume of dentate gyrus, subiculum and CA1 (Erickson K. I. I. et al., 2011). Similar data were obtained by Broadhouse K. M. et al. who demonstrated an increase in CA1 and subiculum volumes and improved cognitive function in patients with MCI who performed intensive weight-bearing exercise for 6 months (Broadhouse K. M. et al., 2020).

In recent years, there has been a progressive increase in the number of publications devoted to artificial intelligence and, in particular, machine learning, in the diagnosis of cognitive impairment (Shang Q. et al., 2022; Stulov et al., 2023: 239; Zubrikhina M. O. et al., 2023). In a number of studies, the use of machine learning algorithms with the inclusion of HF subfields in the diagnostic model has shown high accuracy for predicting the development of Alzheimer-type dementia in patients with MCI syndrome (Izzo J. et al., 2020; Kwak K. et al., 2022).

Thus, the use of timely diagnosis of diseases leading to cognitive impairment at an early stage will make it possible to modify risk factors and prescribe therapy, which is of great importance in the prognosis of patients with MCI. It is assumed that by avoiding the impact of risk factors, it is possible to prevent or slow down the development of dementia up to 40% of cases (Livingston G. et al., 2020).

Consequently, the comparative study on studying and comparing the nature of atrophic process of HF subfields in MCI of different genesis is an actual scientific task.

CHAPTER 2. MATERIALS AND RESEARCH METHODS

2.1. General characteristics of the studied patients

The work was performed in the radiology department and geriatric psychiatry department of the National Medical Research Centre for psychiatry and neurology named after V. M. Bekhterev. We examined a total of 146 people. The study revealed patients who did not fulfil the criteria of the main sample (15 with dementia, 16 with depression, 19 with mixed cognitive impairment, 5 with consequences of large infarcts or infarcts in the strategic zone, 1 with signs of amyloid angiopathy, 1 with extracerebral mass), who were excluded during further investigation.

The present study included the results of examination of 90 people. The main group consisted of patients with MCI syndrome, including 30 patients with aMCI (mean age 71.67±6.93 years), 30 patients with svMCI (mean age 75.67±5.29). The control group consisted of 30 conditionally healthy volunteers (mean age 71,50±5,43).

The general characteristics of the patients are summarised in Table 2.

Table 2 - Distribution of patients by diagnosis, age and sex

Surveyed groups	Number of people in the group	Men		Women		Age, average. (years)
		Abs. number	%	Abs. number	%	
aMCI	30	9	30	21	70	71,67±6,93
svMCI	30	9	30	21	70	75,67±5,29
control	30	14	46,7	16	53,3	71,50±5,43

Table 2 shows that patients with aMCI were generally younger (71.67±6.93 years) than patients with svMCI (75.67±5.29), which may be due to the peculiarities of manifestation of neurodegenerative diseases. The mean age of patients in the aMCI group and the control group did not differ statistically.

It skewed the gender distribution towards females in all groups studied; however, there were no statistically significant differences between the groups in this respect.

We assessed the level of education in points as follows: 1 point - did not study; 2 points - primary education; 3 points - secondary education; 4 points - specialised secondary education; incomplete higher education - 5 points; higher education - 6 points; academic degree - 7. In all three groups education was not lower than secondary education, no statistically significant differences between the groups were determined. Data on the level of education are presented in Table 3.

Table 3 - Characterisation of examined patients by educational level Me [LQ; UQ]

	aMCI	svMCI	control	p-value
Level of education (points) Me[LQ;UQ]	5[4;6]	6[4;6]	6[4;6]	0,23

Table 3 shows that there were no statistically significant differences in the level of education between the groups.

All patients underwent clinical and neurological, neuropsychological, laboratory and neuroimaging studies.

Inclusion criteria for the main group:

1. established syndrome of MCI according to clinical and neuropsychological examination (F06.7)
2. age 60-85 years
3. signed voluntary informed consent of the research participant

Criteria for non-inclusion:

1. dementia with MMSE score<24
2. depressive symptoms with a Beck Depression Scale score > 20
3. cognitive impairment due to other causes, such as brain neoplasia, hydrocephalus, consequences of infarcts in the large artery basin as well as in strategic

areas, mental illness, epilepsy, parkinsonism, endocrine diseases (thyroid disorders, decompensated diabetes mellitus, hyperprolactinaemia), alcohol or drug abuse, traumatic brain injury.

4. visual impairment, severe aphasia and motor impairments that do not allow for clinical assessment and neuropsychological testing

Exclusion Criteria:

1. patient refusal to undergo the trial
2. presence of ferromagnetic materials in the body

The Petersen R., Touchon J. (Petersen R., Touchon J., 2005) criteria were used to diagnose MCI syndrome, which include:

1. complaints of cognitive impairment by the patient or noted by family members
2. indication by the patient or people close to the patient (informant) of a decline in cognitive function from a previous level within the last year
3. cognitive impairments detected in clinical (neuropsychological) examinations
4. no impact of cognitive deficits on daily activities (only mild problems with complex tasks are tolerated)
5. absence of dementia

We then divided all patients with MCI syndrome into two groups (aMCI and svMCI) using additional criteria. This division is based on the theory that most patients with aMCI progress to AD and patients with svMCI to subcortical vascular dementia.

Patients with aMCI met the criteria of The National Institute on Aging and the Alzheimer's Association (Albert M. S. et al., 2011), in the absence of clinically significant changes on brain MRI (single foci were allowed). The clinical and neuropsychological profile of patients with aMCI was characterised by progressive memory impairment with relative preservation of other cognitive functions.

It referred patients to the svMCI group if the clinical and neuropsychological profile of MCI was consistent with the dysregulatory type of MCI and signs of CSVD according to STRIVE criteria.. The dysregulatory type of MCI is characterised by signs

of frontal lobe dysfunction and is the most typical variant for patients with CSVD (Levin O. S., Chimagomedova A. Sh., 2022). Among the complaints of this group of patients, difficulties in performing tasks related to planning and thinking were noted.

The control group included conditionally healthy individuals with no history of neurological or psychiatric disorders, no cognitive complaints and no acute pathology on MR images of the brain (single vascular foci were allowed).

Clinical-neurological and neuropsychological examinations were performed jointly by a neurologist, a psychiatrist and a neuropsychologist.

Obtained written informed consent from all participants.

The requirements of international and domestic bodies in the field of organisation of scientific research and ethical standards were met when including patients with MCI syndrome and subjects from the control group: the subject's awareness and consent to the full examination and confidentiality (Declaration of the World Medical Association "Ethical Principles of Scientific Medical Research Involving Human Subjects" with amendments, 2000, Helsinki; "Rules of Clinical Practice in the Russian Federation", approved by the Ministry of Health of the Russian Federation, approved by the Ministry of Health of the Russian Federation, 2000, Helsinki).

The study was conducted with the permission of the local ethical committee of of the National Medical Research Centre for Psychiatry and Neurology named after V. M. Bekhterev (protocol No 3 of 18.03.2021).

2.2. Clinical and neurological examination

All patients were examined together with a psychiatrist and a neurologist, including general and neurological examination, complaints, life and disease history (taking into account the level of education and professional skills, hereditary history, cerebrovascular diseases, arterial hypertension, acute cerebrovascular disorders, concomitant diseases, intoxications, head injuries, etc.). We paid special attention to the duration and nature of the course of the disease. Anamnesis data was supplemented with information from relatives and close people.

2.3. Neuropsychological methods of examination of patients

All patients underwent extended neuropsychological testing to clarify the state of cognitive functions. A neuropsychologist performed testing in a separate room with sufficient lighting and exclusion of external sound stimuli. The following methods were used:

1. The Mini Mental State Examination (MMSE) (Folstein M. F., Folstein S. E., Mc Hugh P. R., 1975) was used to identify and assess the severity of cognitive impairment. The maximum number of points in this scale is 18. To conditionally determine the severity of cognitive impairment, the following scores were established: 28-30 points - normal, 24-27 points - mild cognitive impairment, 20-23 - mild dementia, 11-19 - moderate dementia, less than 10 points - severe dementia. Patients with a score of 23 or less on the MMSE scale were not included in the study.

2. "Frontal Assessment Battery" (FAB) (Dubois B. et al., 2000) - used to assess regulatory functions. The maximum number of points is 18.

3. The Clock Drawing Test (CDT) (Sunderland T. et al.,1989)-used to assess visual-spatial function

4. Wechsler Memory Scale (WMS) (Wechsler D. A., 1945) - used to investigate memory

5. The Beck Depression Inventory (BDI) (Beck A. T. et al., 1961) was used to exclude depressive disorders that could affect cognitive function. Patients with a total score of 20 or more were not included in the study.

2.4. Laboratory methods of research

Laboratory diagnostics was performed on the basis of clinical diagnostic laboratory and included biochemical blood analysis with glucose and cholesterol testing. Hypercholesterolaemia was defined at the level of total cholesterol >5.2 mmol/l in accordance with the excess of the upper reference value (Dolgov V. V., Menshikov

V. V., 2012). To exclude endocrine diseases that can lead to cognitive impairment, hormones were determined: thyroxine, triiodothyronine, thyroid hormone, prolactin.

2.5. Neuroimaging techniques

MRI of the brain of all patients was performed on an Atlas Exelart Vantage XGV MR scanner (Toshiba, Japan) with a magnetic field induction of 1.5 Tesla using a standard 8-channel head coil, followed by visual assessment of the obtained MR images and their post-processing.

2.5.1. Methods of magnetic resonance imaging of the brain

For brain MRI, standardised sequences (T1-, T2-weighted images (WI), FLAIR, T2* and DWI) were used to perform a preliminary assessment of the brain.

Additionally, we performed a targeted study of the mediobasal regions of the temporal lobes using T2 WI-oblique Cor and FLAIR-oblique Cor with a slice thickness of 2.2 mm perpendicular to the long axis of the hippocampus.

High-resolution T2 WI is thought to allow more accurate assessment of the internal structure of the HF compared to T1 WI.

On high-resolution T2 WI, the radial lacunosum and molecular layer (SRLM) separating the dentate gyrus from the hippocampus and subiculum proper is clearly visualised.

A pulsed T1 gradient echo 3D-MPRAGE pulse sequence with a 1mm isotropic voxel was used for subsequent MR morphometry.

The total scanning time per patient took approximately 32 minutes.

Technical parameters of pulse sequences are presented in Table 4.

Table 4 - Technical parameters of pulse sequences

PS	TR, ms	TE,ms	FoV, mm	Number of slices	Cutting thickness,mm	Flip	Time
Sag T2	4300	105	250	20	5.6	90	1:48
Ax T1-MPRAGE	12	5	256	150	1	20	9:32
Ax T2	7704,1	105.0	240	36	3.0	90	3:13
Ax FLAIR	10000	105.0	250	33	4.0	90	4:10
Ax DWI	5900	100.0	250	20	6.0	90	0:36
Ax T2* HEMO	857,9	25.0	240	23	5.0	25	2:25
Oblique Cor T2 WI	14640	120	240	60	2.2	90	6:15
Oblique Cor FLAIR	8000	105	220	33	2.2	90	3:52

Note: PS-pulse sequence; Sag - sagittal plane; Ax - axial plane; Oblique Cor - oblique coronal plane; HEMO - T2*-weighted gradient echo - gradient echo sequence; T1-MPRAGE - Magnetisation Prepared - RApid Gradient Echo - 3D with pre-magnetization of inversion pulses; FLAIR - fluid attenuated inversion recovery - inversion-recovery sequence with long inversion time; DWI - diffusion weighted imagery; TR - time of repetition; TE - time echo; FoV - field of view; Flip - rotation angle of the hydrogen proton axis at the RF pulse.

Lacunae were counted in the subcortical structures and white matter, then their number was summarised and expressed as a score. If there were less than 5 lacunae, the patient received a score of 1 point, if there were more than 5 lacunae - 2 points, if there were no lacunae - 0 points.

T2* PS was used to detect CMH. If less than 5 CMH were present, the patient was scored 1 point, if more than 5 CMH were present, 2 points were scored, and if none were present, 0 points were scored.

Enlarged perivascular spaces (PVS) were defined as linear and rounded structures with a diameter of more than 3 mm. Measurements were performed on two slices (at the level of basal nuclei and at the level of semiovascular centres) performed in the axial plane using T2 WI, and then the scores were summed. In the presence of less than 10 dilated PVS, the patient received a score of 1 point, in the presence of more than 10 dilated PVS - 2 points, in their absence - 0 points.

The volume of hyperintense white matter (WMH) was estimated using the Fazekas visual scale separately for deep and periventricular white matter, and then the scores were summed. The boundary for separation of foci in the deep and periventricular white matter was 13 mm from the walls of the lateral ventricles (De Carli C. et al., 2005). To evaluate focal changes in the periventricular white matter, the following criteria were used: 0 - absent; 1 - "caps" or thin lines; 2 - moderate "halo"; 3 - irregular periventricular zones extending to the deep white matter foci in the deep white matter were evaluated accordingly: 0 - absent; 1 - pinpoint foci; 2 - foci beginning to merge; 3 - large merging zones.

2.5.2. Post-processing of acquired images

Postprocessing was performed using the FreeSurfer 6.0 software (http://surfer.nmr.mgh.harvard.edu/), which allows to perform in a fully automatic mode not only the analysis of quantitative indices of the cortex, white matter and various brain structures, but also to obtain volumes of 12 subfields of the HF: sectors of the ammon horn (CA1, CA3, CA4), dentate gyrus (granule cells and molecular layer of the dentate gyrus - GC-ML-DG), subiculum, presubiculum, parasubiculum, molecular layer of the dentate gyrus. - granule cells and molecular layer of the dentate gyrus (GC-ML-DG), subiculum, presubiculum, parasubiculum, molecular layer of the hippocampus, hippocampus-amygdala transition area (HATA), hippocampal sulcus, fimbriae, and hippocampal tail.

This software uses built-in digital atlases of brain structures (Desikan-Killiany atlas, Destrieux atlas) to analyse morphometry results.

Postprocessing was performed on a personal computer (4-core Intel Core i 5 processor, operating frequency 2.3 GHz, RAM 16 GB) in the Linux Ubuntu 16.04.1 LTS environment. The obtained 3D-MPRAGE files in DICOM (Digital Imaging and Communications in Medicine) format were converted to NIFTI (Neuroimaging Informatics Technology Initiative) format using the MRI Convert software package. The MR morphometry results were visualised using the Freeview package built into FreeSurfer 6.0.

The FreeSurfer 6.0 software was used to quantitatively assess various cortical regions, subcortical structures, HF and its subfields, the volume of hypointense foci, and the intracranial volume (ICV). The fraction of hypointense foci was defined as the volume of hypointense foci (mm3)/ICVx100. The digital results were exported to Microsoft Excel, which was used to build a patient database.

2.6. Methods of statistical processing

Statistical analysis were performed using data that were converted from a database in Microsoft Excel to IBM SPSS Statistics 20 statistical package.

Preliminary analysis included examining the distributions of demographic and clinical data in the aMCI, svMCI, and control groups. The level of significance in all cases was considered sufficient to reject the null hypothesis at $p \leq 0.05$.

The arithmetic mean and standard deviation, M(σ), and median (Me) were used as measures of central tendency.

Normality of distributions was established using the Shapiro-Wilk criterion, differences in the frequencies of gradations of nominal features in three groups were established using the Z-criterion with the Bonferroni correction, differences in the central tendencies of rank features were analysed using the Kraskell-Wallis criterion with the subsequent use of the Mann-Whitney criterion and the Bonferroni correction.

One-factor analysis of variance (ANOVA) was used to compare the mean of the three groups followed by multiple comparisons using Tukey's criterion if the variances

were homogeneous and Tamhane's criterion otherwise. The homogeneity of dispersions was assessed by Leven's criterion.

With two compared groups, Student's test was applied if the distribution of signs was normal or Mann-Whitney test if it was not normal.

Differences in mean quantitative data in the three study groups were investigated using covariance (ANCOVA) adjusted for age, sex, education and intracranial volume. Pre-selection of the estimated covariates for covariance analysis in the groups was done using Spearman's correlation coefficient and Goodman and Kraskel's gamma Goodman and Kraskel's correlation coefficient.

The Spearman correlation coefficient was used to analyse the relationship because the distributions of the traits were not normal. For correlation analysis, HF subfield volumes were adjusted to intracranial volume using regression residuals analysis.

Constructing a decisive classification rule for the differential diagnosis of aMCI and svMCI classes was solved using binary logistic regression. ROC analysis was used to assess the quality of the obtained equations and to select the cut-off point.

CHAPTER 3. RESULTS OF THE STUDY

3.1. Results of clinical, neurological and neuropsychological examination of patients

It summarised the general clinical examination data for risk factor assessment in the MCI and control groups in Table 5.

Table 5 - Characterisation of examined patients by type and frequency of risk factors.

Risk factors	Surveyed groups						p-value
	aMCI		svMCI		control		
	Abs. number	%	Abs. number	%	Abs. number	%	
Hypercholesterolaemia	12	40	17	56,7	7	23,3	0,03 b
Arterial hypertension	26	86,7	26	86,7	15	50	<0.001 a,b
Type II diabetes mellitus	1	3,3	7	23,3	4	13,3	0,07

Significant differences a -between aMCI and control, b -between svMCI and control

When analysing clinical data, arterial hypertension was detected in the vast majority of patients with aMCI and svMCI to an equal extent. Hypercholesterolaemia was more frequently detected in patients with aMCI. Patients with diabetes mellitus predominated in the aMCI group.

It presented the data on the study of the neuropsychological profile of the patients in Table 6.

Table 6 - Comparison of groups according to the mean scores of neuropsychological examination of patients on MMSE, clock drawing test and frontal assessment battery (scores, M±σ)

Methodology	aMCI	svMCI	Control	p-value
MMSE	25,73±1,05	26,77±0,92	28,87±0,65	<0,01a <0.001b,c
Clock drawing test	7,83±1,54	8,30±1,66	9,07±0,81	<0,05b
Frontal assessment battery	14,23±1,80	14,80±2,13	17,07±1,12	<0.001b,c

Significant differences: a - between svMCI and aMCI, b - aMCI and control, c - between svMCI and control

As can be seen from the data in the presented table, the subjects in the aMCI group differed in their MMSE test scores from the control group. The Clock Drawing Test and the Frontal Dysfunction Battery showed statistically significant decreases in both groups of patients with MCI compared to the control group, but there were no significant differences between the aMCI and svMCI groups.

It presented the results of the neuropsychological examination of the patients using the Wechsler Memory scale in Table 7.

Table 7 - Comparison of groups by mean scores of neuropsychological examination of patients on the Wechsler Memory scale (scores, M±σ)

Wechsler Memory Scale (subtests)	aMCI	svMCI	Control	p-value
I. Personal and public data	5,47±0,68	5,93±0,12	6,00±0,11	<0,01a,b

II. Orientation	4,33±0,71	4,50±0,70	5,00±0,12	<0,01b <0,05c
III. Mental control	3,57±1,72	4,47±1,37	5,20±1,17	<0,01b
IV. Logical memory	3,52±1,78	6,50±2,37	10,10±2,32	<0.001a,b,c
V. Digits	10,13±1,46	9,50±1,57	11,03±1,18	<0,01c
Va. Short-term Memory capacity (direct order digitisation)	5,63±0,80	5,67±0,96	6,17±0,71	-
Vb. Working Memory capacity (reverse order digitisation)	4,50±0,77	4,13±0,81	4,87±0,73	<0,01c
VI. Visual retention	5,87±2,14	7,37±2,52	7,80±2,85	<0,05b
VII. Paired associations (associative memory)	9,23±2,42	11,37±3,30	15,43±2,53	<0.001b,c <0,05a
VIIa. Paired associations Easy	7,32±1,32	7,83±1,13	8,43±0,76	<0,05b
VIIb. Paired associations Hard	1,92±1,55	3,57±2,51	7,00±2,13	<0,001b <0,01c <0,05a
Equivalent to intelligence index memories	95,60±9,99	110,23±12,08	124,93±10,85	<0.001a,b,c

Significant differences: a - between aMCI and svMCI, b - aMCI and control, c - between svMCI and control

When comparing the Wechsler Memory scale scores, differences between the aMCI and control groups were found in almost all subtests, except for the "Digits", "Working Memory capacity (reverse order of digits)" and "Short-term memory capacity (direct order of digits)" subtests, which indicates lower logical, visual and associative memory scores in the aMCI group compared to the control group.

When comparing the Wechsler Memory scale scores, differences between the svMCI and control groups were found in several subtests, namely: "Orientation", "Logical Memory", "Digits", "Working Memory capacity (reverse order of digits)", "Paired associations" (associative memory), "Paired associations Hard" and "Intelligence-equivalent Memory index", which indicates lower indices of logical, working and associative memory in the svMCI group compared to the control group.

In the aMCI group, lower scores on the subtests of Personal and Social Data, Logical Memory, Visual Retention, Paired Associations, Paired Associations Hard, and Intelligence Equivalent Memory Score were found compared to the psucr group.

3.2. Results of conventional magnetic resonance imaging of the brain

The standardised STRIVE report was used to assess CSVD by neuroimaging.No recent small subcortical infarcts were detected in the study groups. MRI signs were CSVD included: WMH, lacunes, dilated perivascular spaces (PVS), cerebral microhemorrhages (CMH). The data on lacunae, dilated PVS and CMH are presented in Table 8.

Table 8 - Frequency of lacunae, dilated perivascular spaces, cerebral microhemorrhages in the studied groups

MRI signs	aMCI	svMCI	Control	p-value
Lacunae :				0.002 a,b
<5	2 (6,7%)	4 (13,2%)	0	
>5	0	4 (13,2%)	0	

Microhemorrhages:				0,51
<5	0	1(3,3%)	0	
>5	1(3,3%)	1(3,3%)	0	
Dilated PVS				0,37
<10	9(30%)	10(33%)	7(23,3%)	
>10	2(6,7 %)	4(13,3%)	2(6,7%)	

Significant differences: a - between aMCI and svMCI, b - aMCI and control

Lacunae were detected in 8 patients in the svMCI group, their number varied from 2 to 9. Single lacunae were detected in 2 patients in the aMCI group. The lacunae were localised mainly in the area of basal nuclei. No lacunae were found in the control group.

CMH were detected only in 2 patients in the svMCI group and in 1 patient in the aMCI group. In the control group there were no CMH.

The degree of WMH severity was assessed in scores using the Fazekas visual scale separately for the periventricular and deep white matter, and then the scores were summed. The Fazekas scale data for aMCI, svMCI, and control groups are presented in Figures 6, 7, and 8.

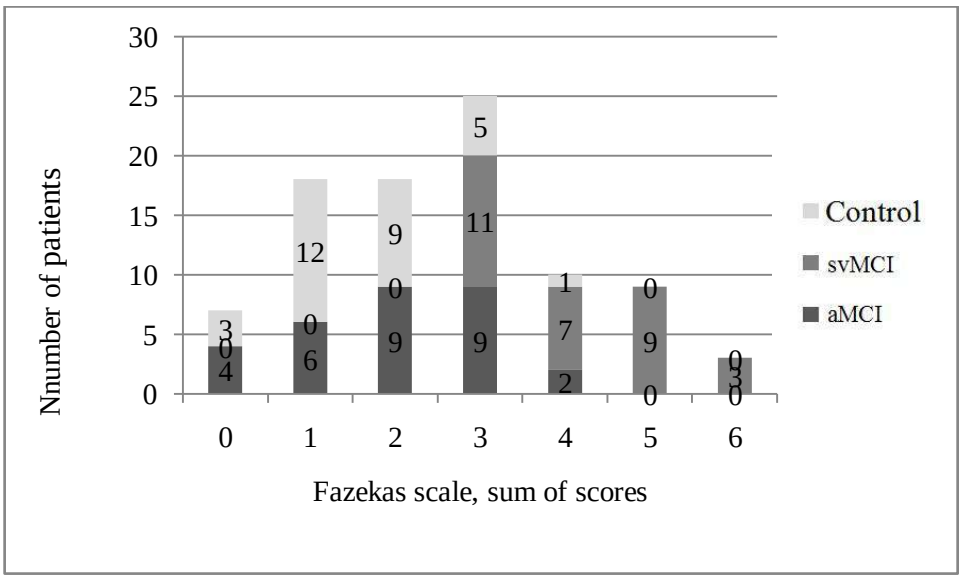

Figure 6 - Sum of Fazekas scale scores in the three groups

The severity of WMH was consistently higher in the svMCI group. The median value of the sum of Fazekas scores was 4 points in the svMCI group, 2 points in the aMCI group, and 2 points in the control group. There were no statistically significant differences between the aMCI and control groups on the Fazekas scale.

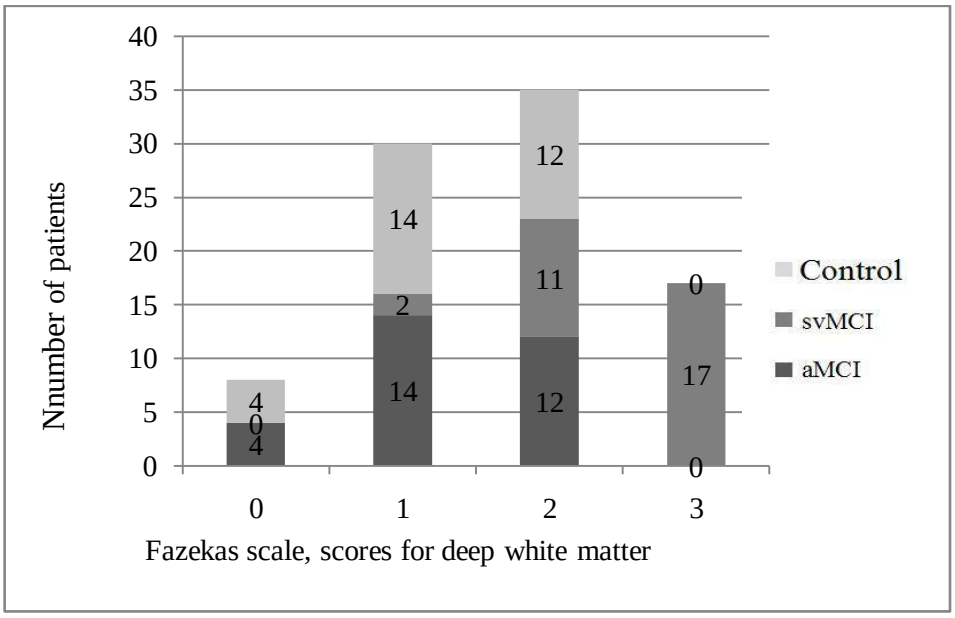

Figure 7 - Fazekas deep white matter lesion scores in the three groups

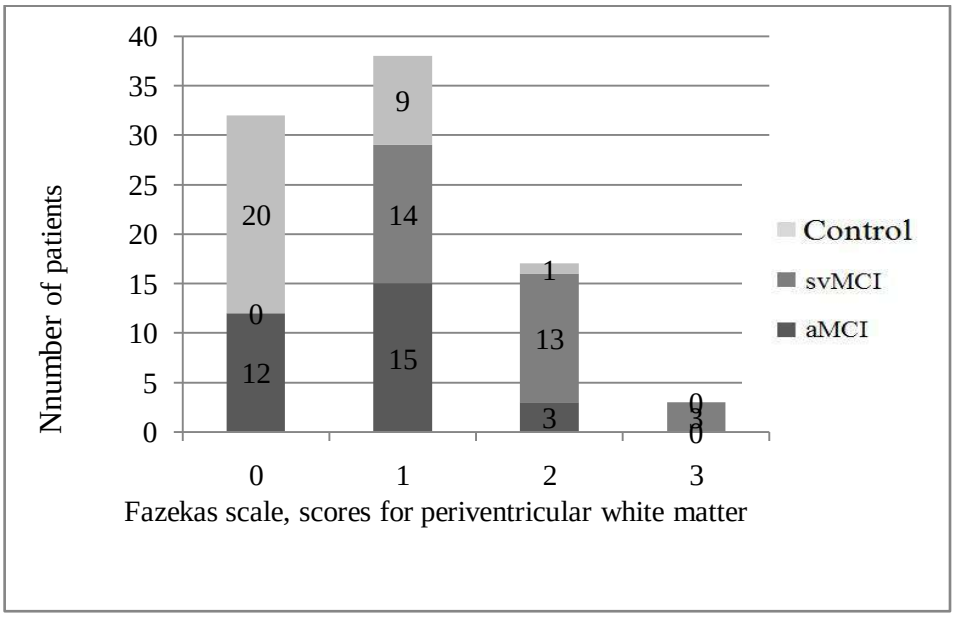

Figure 8 -Evaluation of periventricular white matter lesions according to the Fazekas scale in the three groups

As shown in Figures 6, 7, and 8, in the svMCI group, changes were predominant in the deep white matter (Me=3) and were less pronounced in the periventricular white matter (Me=2).

The MTA and ERICA scales were used for visual assessment of hippocampal and entorhinal cortex atrophy. Data on visual scales are presented in Figure 9 and Table 9.

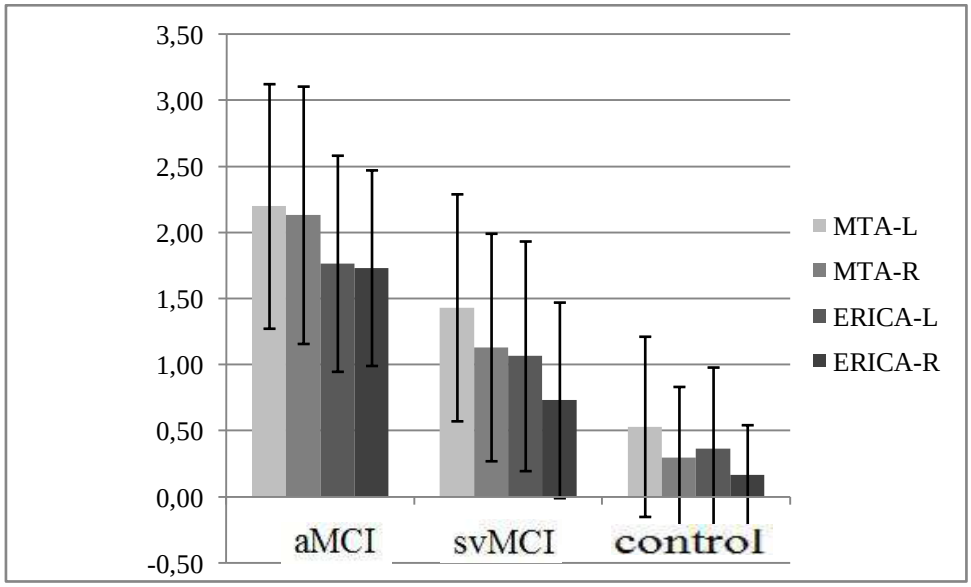

Figure 9 - Graph of hippocampal and entorhinal cortex atrophy assessment by MTA and ERICA visual scales in the three groups

Table 9 - Assessment of hippocampal and entorhinal cortex atrophy by MTA and ERICA visual scales in the three groups (scores, M±σ)

Visual scales, right (R) and left (L) hemisphere	aMCI	svMCI	Control	p-value
MTA - L	2,20±0,92	1,43±0,86	0,53±0,68	<0.001b,c 0,002a
MTA - R	2,13±0,97	1,13±0,86	0,30±0,53	<0.001a,b,c
ERICA - L	1,77±0,82	1,07±0,87	0,37±0,61	<0,001b 0,002 a,c
ERICA - R	1,73±0,74	0,73±0,74	0,17±0,38	<0.001 a,b 0,003 c

Significant differences: a - between aMCI and svMCI, b - aMCI and control, c - between svMCI and control

As can be seen from the graph in Figure 9 and Table 9, the highest scores on the MTA and ERICA scales were observed in patients with aMCI.

3.3. Results of magnetic resonance morphometry of the brain

MR-morphometric analysis was performed to assess quantitative indices of different brain sections, including HF subfields, as well as to study the volume of focal changes in the brain matter.

3.3.1. Results of magnetic resonance morphometry of focal brain changes

To clarify the severity of vascular lesion of the brain matter, MR-morphometry was used to measure the volume of hypointense foci with determination of the fraction of foci from the ICV; the obtained data are presented in Figures 10 and 11.

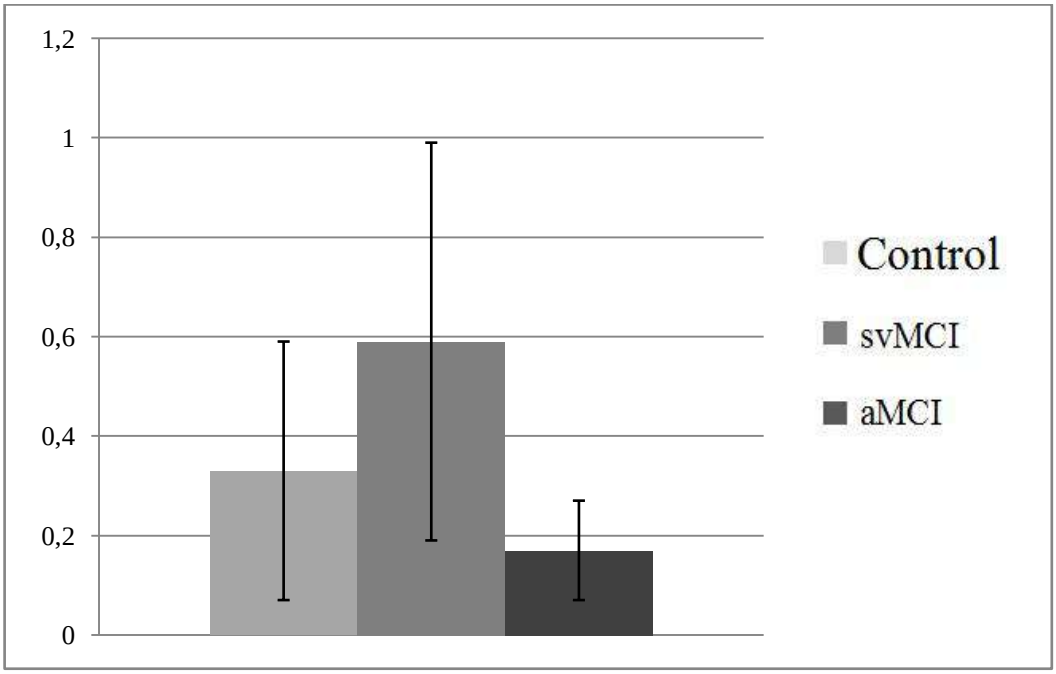

Figure 10 - Average fraction of hypointense foci in the brain matter in the three groups

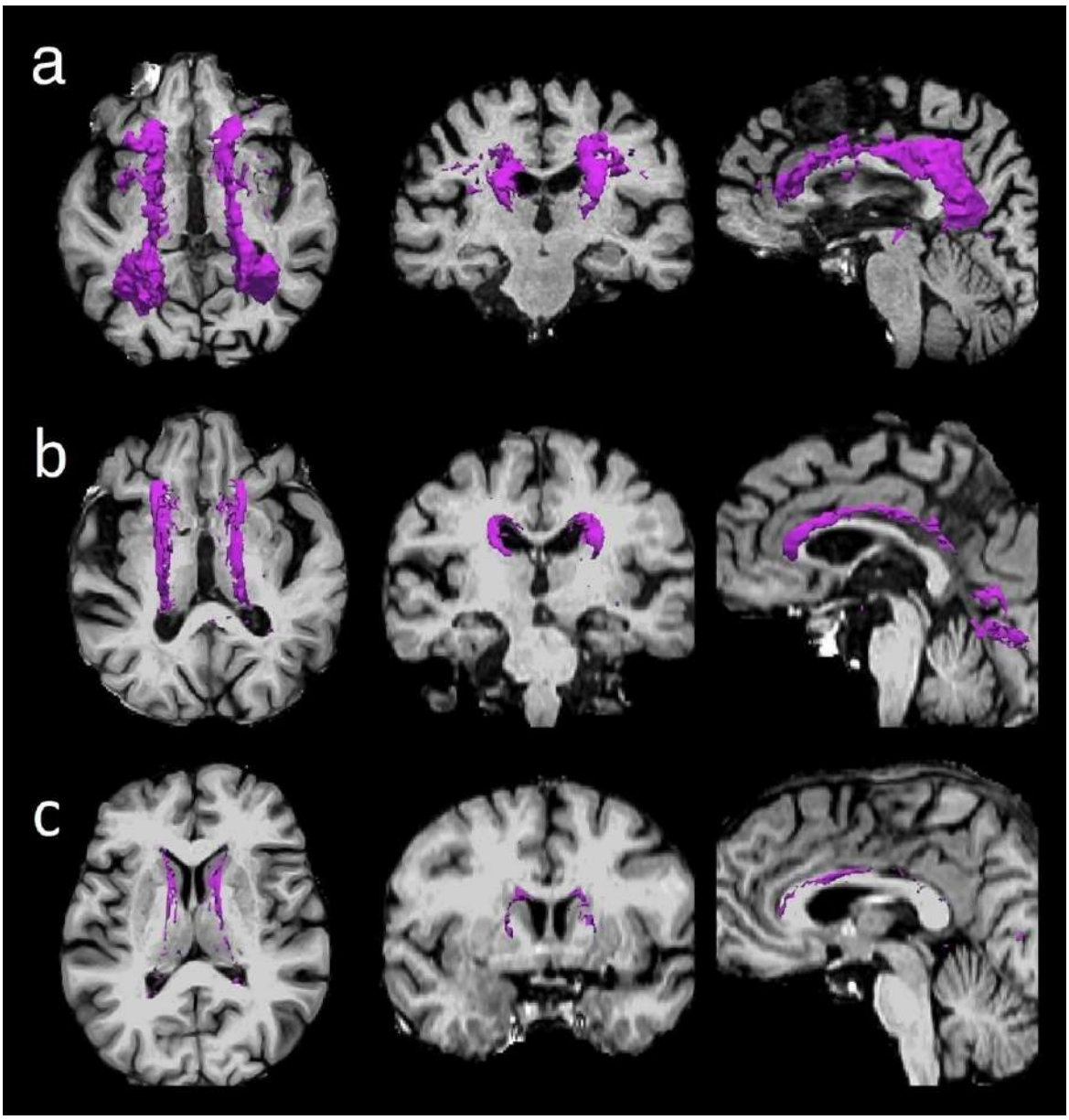

Figure 11 - Differences in the volume of T1-hypointense foci in the three groups. Focal changes in patient M. with svMCI, 80 years old, card number 31559 (a), patient K. with aMCI, 71 years old, card number 31755 (b) and conditionally healthy volunteer D., 79 years old, card number 31685 (c)

The mean volume fraction of hypointense foci in the svMCI group was 0.59±0.40 of the intracranial volume, which was significantly higher than in the aMCI group (0.33±0.26, $p<0.05$) and the control group (0.17±0.10, $p<0.001$).

When comparing the Fazekas score for periventricular white matter, deep white matter, and the sum of scores with the fraction of hypointense foci, significant positive correlations were found in all groups, as shown in Table 10.

Table 10 - Correlations between Fazekas scores and the fraction of hypointense foci in the brain.

Localisation		Volume of hypointense foci Spearman correlation coefficient (r), p<0.05		
		aMCI	svMCI	Control
Fazekas Scale, points	DWM	0,61	0,60	0,37
	PWM	0,62	0,67	0,74
	DWM+PWM	0,68	0,79	0,64

Note: DWM - deep white matter, PWM - periventricular white matter

Table 10 clearly shows that there is a mild positive correlation between the volume of hypointense foci and Fazekas scale scores for WMH in the deep white matter in the control group (r=0.37), in other cases the strength of correlation is significantly higher.

The correlation between the sum of Fazekas scores and the volume of hypointense foci in the brain is graphically shown in Figure 12.

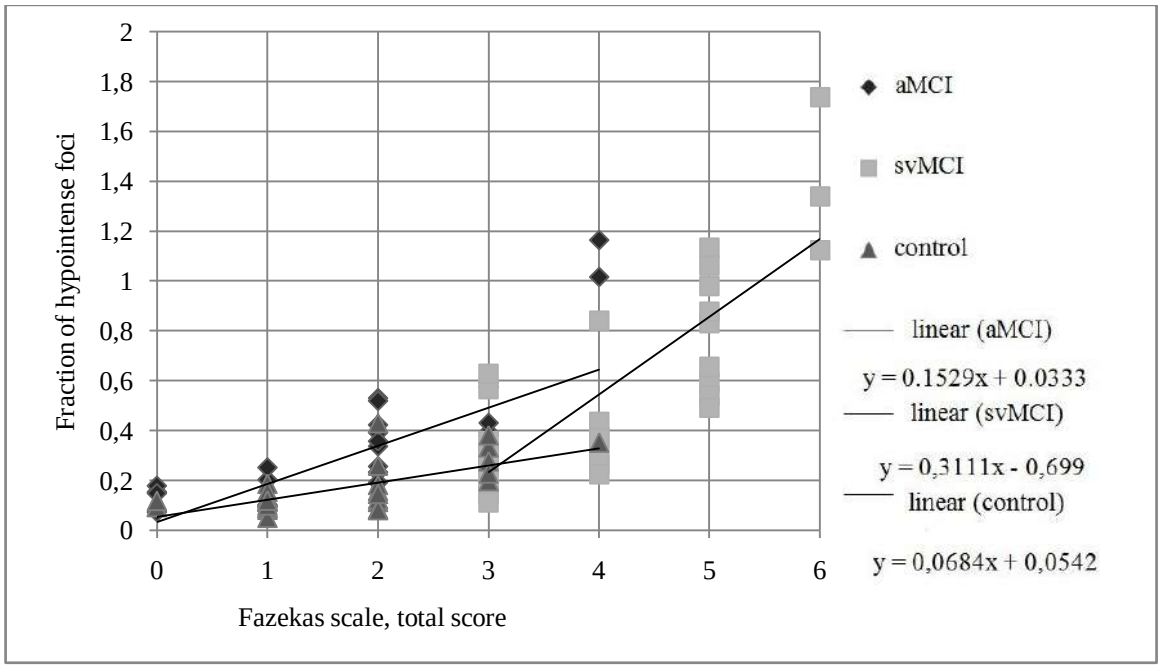

Figure 12 - Graph of dependence of the sum of Fazekas scores and white matter lesion volume

3.3.2. Results of magnetic resonance morphometry of anatomical structures of the brain

In patients with MCI syndrome compared to the control group, ventricular dilation and increased cerebrospinal fluid (CSF) volume were determined as a manifestation of atrophic changes in the brain (Table 11).

Table 11 - Volumetric changes of brain structures in patients of three groups (M±σ)

Structure	aMCI, mm3	svMCI, mm3	control, mm3	p-value
	1	2	3	
Right lateral ventricle	17798,49 ±8343,62	16165,73 ±8606,29	10783,14 ±5493,67	0,002 (1,3) 0,022 (2,3)
Left lateral ventricle	18902,72 ±9346,59	17279,57 ±9857,51	12552,20 ±7264,43	0,021 (1,3)
III ventricle	2027,09 ± 638,87	1897,05 ±638,64	1499,03 ± 521,89	0,003 (1,3) 0,036 (2,3)
CSF	1406,94 ±401,78	1387,88 ±412,40	1124,78 ±294,1	0,013 (1,3) 0,023 (2,3)
Right amygdala	1143,61 ±292,36	1373,45 ±290,65	1413,1 ±279,6	0,0004 (1,3) 0,006 (1,2)
Left amygdala	1014,66 ±261,92	1178,86 ±261,65	1309,66 ±262,19	0,0004 (1,3)
Right hippocampal formation	2669,51 ±392,10	3014,83 ±391,72	3244,36 ±392,54	0,0004 (1,3) 0,003 (1,2)
Left hippocampal formation	2605,74 ±360,55	2945,66 ±360,18	3233,30 ±360,93	0,0004 (1,3) 0,001 (1,2) 0,008 (2,3)

As follows from Table 11, when analysing volumetric indices of subcortical structures in patients with MCI syndrome, in comparison with the control group, a decrease in the total volume of the left HF was determined.

We found a statistically significant decrease in the volume of both amygdala bodies in the aMCI group compared to the control group. It should also be noted that the

aMCI group showed a decrease in the volume of the right amygdala compared to the svMCI group.

In MR-morphometric analysis of the cerebral cortex in the aMCI group, statistically significant differences, compared with the control group, were found in the thickness of the cortex of the individual gyrus of both temporal lobes and the cortex of both fusiform gyrus (Table 12).

Table 12 - Quantitative changes in cortical thickness parameters in patients of the three groups (M±σ)

Cortical area	aMCI, mm	svMCI, mm	control, mm	p-value
	1	2	3	
Right parahippocampal gyrus	2,02±0,30	2,29±0,30	2,39±0,30	0,0004 (1,3) 0,002 (1,2)
Left parahippocampal gyrus	2,12±0,33	2,3±0,35	2,46±0,35	0,001 (1,3)
Right fusiform gyrus	2,22±0,18	2,4±0,18	2,47±0,18	0,0004 (1,3) 0,001 (1,2)
Left fusiform gyrus	2,35±0,19	2,45±0,19	2,58±0,19	0,0004 (1,3) 0,034 (2,3)
Right middle temporal gyrus	2,39±0,19	2,58±0,19	2,62±0,19	0,0004 (1,3) 0,0004 (1,2)
Left middle temporal gyrus	2,42±0,22	2,59±0,22	2,7±0,22	0,0004 (1,3) 0,007 (1,2)
Left superior temporal gyrus	2,33±0,19	2,37±0,19	2,50±0,19	0,004 (1,3) 0,027 (2,3)
Right inferior temporal gyrus	2,5±0,25	2,61±0,17	2,72±0,21	0,0004 (1,3)
Left inferior temporal gyrus	2,64±0,20	2,70±0,20	2,82±0,21	0,004 (1,3)
Left entorhinal cortex	2,50±0,35	2,78±0,38	3,02±0,25	0,0004 (1,3) 0,004 (1,2)
Right entorhinal cortex	2,56±0,43	3,0±0,38	2,95±0,39	0,001 (1,3) 0,0004 (1,2)
Caudal part of the right middle frontal gyrus	2,4±0,17	2,36±0,17	2,46±0,13	0,036 (2,3)

A mild decrease in the thickness of the left superior temporal gyrus and left fusiform gyrus was observed in the svMCI group compared to the control group, but less pronounced compared to the aMCI group. Also in the svMCI group there was a decrease in the thickness of the caudal cortex of the right middle frontal gyrus, which was not detected in the aMCI group.

3.3.3. Results of magnetic resonance morphometry of the hippocampal formation of patients with amnestic mild cognitive impairment

Analysis of covariance (ANCOVA) was used to examine volumetric indices of HF subfields in patients of all groups, taking into account age, sex, education level and intracranial volume.

When analysing the obtained HF volumetric subfields, errors in fimbriae segmentation were noted. The low reliability of fimbriae segmentation has been previously reported in a number of studies, and is likely due to its small size and partial volume effect (Worker A. et al., 2018; Brown E. M. et al. 2022). Thus, it was decided to exclude this structure from further analysis.

The atrophic changes of the HF subfields in patients in the aMCI group compared to the control group are clearly shown in Figure 13 and Tables 13,14.

Table 13 - Volumetric changes in the subfields of the right hippocampal formation in the aMCI group compared to the control group (M±σ)

Structure	aMCI, mm3	Control, mm3	% reduction in V	p-value
The tail of the hippocampus	438,54± 70,88	513,59±70,93	14,6	0,0004
Subiculum	312,77±54,94	403,77±54,99	22,5	0,0004
CA1	513,67±79,31	609,00±79,42	15,6	0,0004

Hippocampal sulcus	184,29±36,15	209,65±36,15	12,1	0,024
Presubiculum	235,80±41,63	301,26±41,68	21,7	0,0004
Parasubiculum	52,80±12,82	62,82±12,82	15,9	0,026
Molecular layer	427,26±68,85	528,81±68,96	19,2	0,0004
Dentate gyrus	233,44±40,31	278,07±40,37	16	0,0004
CA3	169,40±33,19	199,03±33,25	14,9	0,003
CA4	197,22±41,94*	241,54±26,09*	18,3	0,001*
HATA	46,56±11,17	55,24±11,23	15,7	0,01
The hippocampal formation as a whole	2669,51±392,10	3244,36±392,54	17,7	0,0004

*Significant differences were found only in women

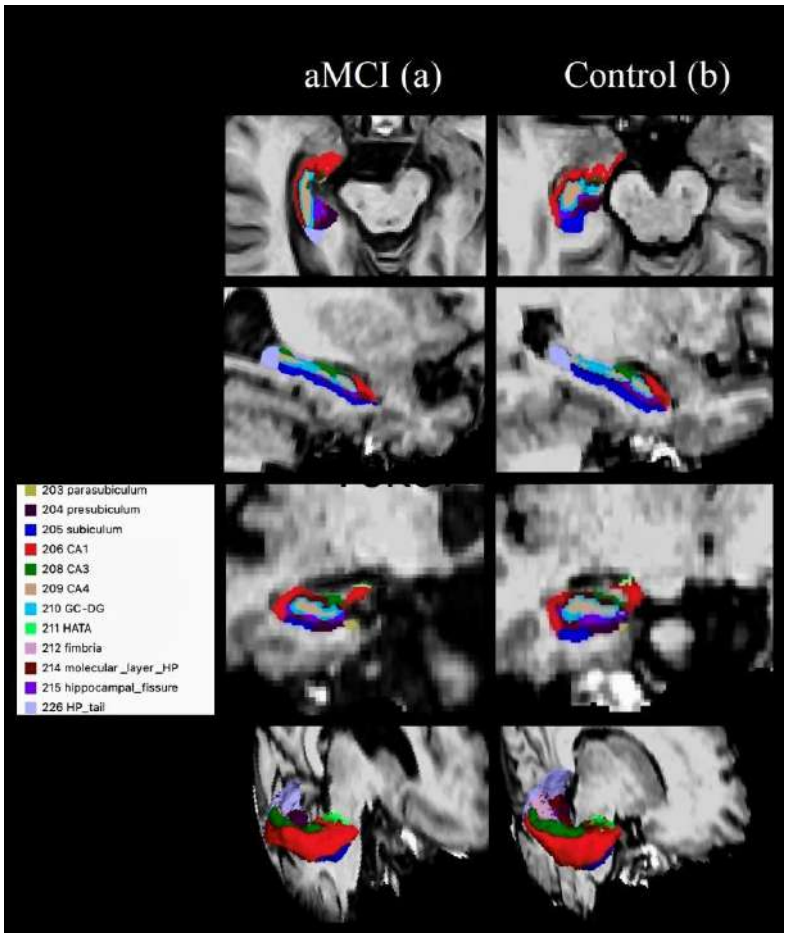

Figure 13 - Segmentation of subfields of the right hippocampal formation: a - patient K., 71 years old, with aMCI (card number 31529), b - conditionally healthy volunteer D., 79 years old (card number 31555).

It follows from the data of Table 13 that when analysing volumetric changes in the aMCI group, a decrease in volumetric indices of all subfields of the right HF was determined, except for CA4 in men. It should be noted that the decrease in the right subiculum volume was more pronounced (by 22.5%) than the total volume of the right HF (by 17.7%).

Table 14 - Volumetric changes in the left hippocampal formation in the aMCI group compared to the control group (M±σ)

Structure	aMCI, mm3	Control, mm3	% reduction in V	p-value
The tail of the hippocampus	414,27±65,89	491,11±66,06	15,6	0,0004
Subiculum	319,57±54,44	413,64±54,50	22,7	0,0004
CA1	494,81±74,44	596,53±74,49	17,1	0,0004
Hippocampal sulcus	168,21±38,94	205,30±39	18,1	0,001
Presubiculum	257,87±44,75	323,91±44,80	20,4	0,0004
Molecular layer	418,31±63,97	528,11±64,03	20,8	0,0004
The dentate gyrus	217,23±35,38	273,54±35,38	20,5	0,0004
CA3	151,99±28,48	191,25±28,65	20,5	0,0004
CA4	189,45±31,11	237,66±31,17	20,2	0,0004
HATA	46,00±9,8	56,21±9,8	18,1	0,0004
The hippocampal formation as a whole	2605,74±360,55	3233,30±360,93	19,4	0,0004

As it follows from Table 14, statistically significant atrophic changes of the left HF were found practically in all subfields except for the parasubiculum, but the greatest

extent was determined by the decrease in the volume of the left subiculum (by 22.7%) compared to the total volume of the left HF (19.4%).

When analysing the thickness and volume of the entorhinal cortex in patients with aMCI and the control group, significant differences were found on both sides, presented in Tables 15 and 16, Figure 14.

Table 15 - Volumetric changes in entorhinal cortex in the aMCI group compared to the control group (M±σ)

Structure	aMCI, mm3	Control, mm3	% reduction in V	p-value
Left entorhinal cortex	1305,23±394,17	1825,24±394,23	28,5	0,0004
Right entorhinal cortex	1360,14±349,32	1711,03±349,76	20,5	0,001

Table 16 - Changes in entorhinal cortex thickness in the aMCI group compared to the control group (M±σ)

Structure	aMCI, mm	Control, mm	p-value
Left entorhinal cortex	2,50±1,86	3,02±2,14	0,0004
Right entorhinal cortex	2,56±2,35	2,95±2,08	0,001

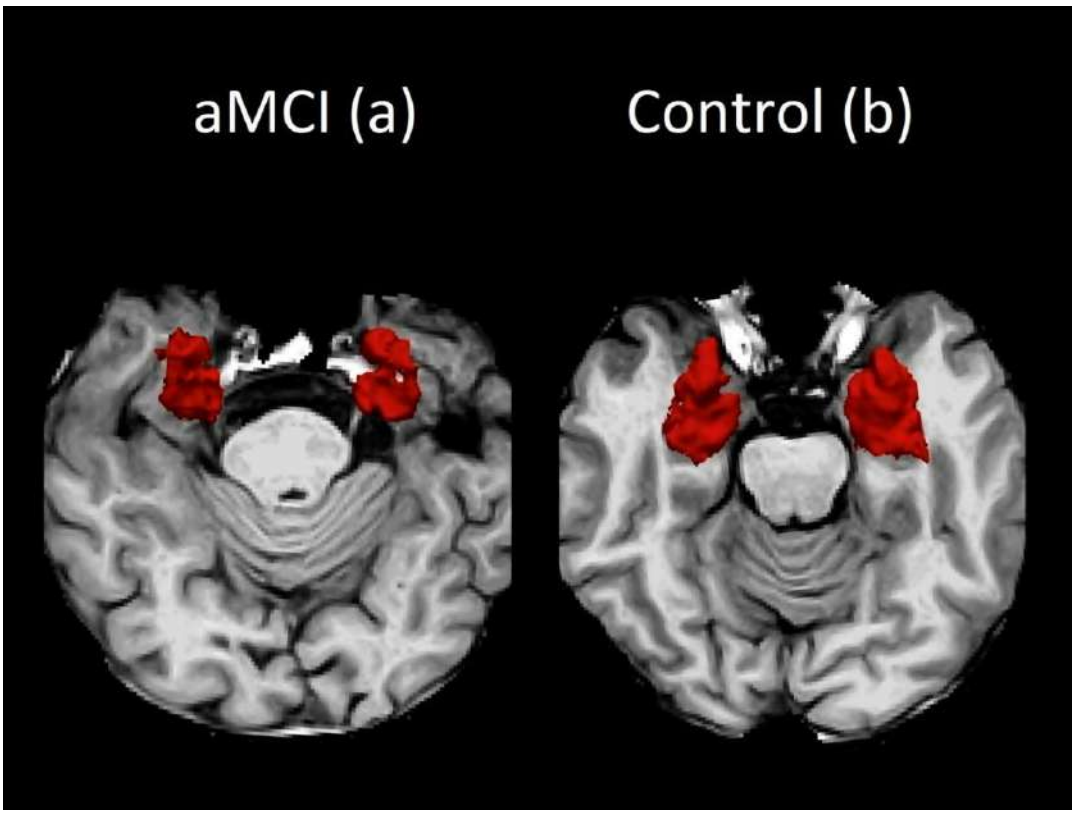

Figure 14 - Volumes of right and left entorhinal cortex: a - patient K., 73 years old, with aMCI (card no. 31521), b - conditionally healthy volunteer D., 79 years old (card no. 31555).

It follows from the data of Tables 15 and 16 that more significant differences in quantitative indices in the aMCI group were determined for the left entorhinal cortex ($p<0.0004$). The decrease in the volume of the left entorhinal cortex and the volume of the right entorhinal cortex compared to the control group was 28.5% and 20.5%, respectively.

3.3.4. Results of magnetic resonance morphometry of the hippocampal formation of patients with subcortical vascular mild cognitive impairment

Statistically significant atrophic changes in HF in patients in the svMCI group are presented in Table 17 and Figure 15.

Table 17 - Volumetric changes in the left hippocampal formation in the svMCI group compared to the control group (M±σ)

Structure	svMCI, mm3	Control, mm3	% reduction in V	p-value
Subiculum	374,96±54,39	413,64±54,50	9,4	0,022
Presubiculum	293,26±44,69	323,91±44,80	9,5	0,028
Molecular layer	480,01±63,92	528,11±64,03	9,1	0,014
Dentate gyrus	245,93±35,33	273,54±35,38	10,1	0,01
CA4	217,97±31,11	237,66±31,17	8,3	0,048
HATA	48,45±9,8	56,21±9,8	13,8	0,009
The hippocampal formation as a whole	2945,66±360,18	3233,30±360,93	8,9	0,008

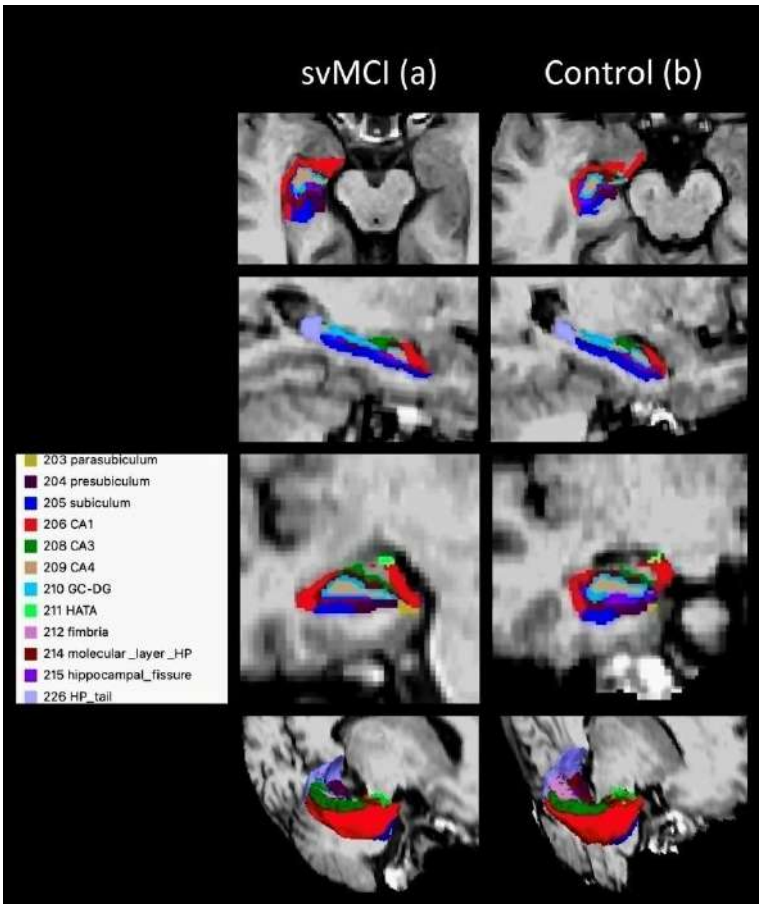

Figure 15 - Segmentation of subfields of the left hippocampal formation: a - patient B., 73 years old, with svMCI (card no. 31463), b - conditionally healthy volunteer D., 79 years old (card no. 31555).

It follows from the data presented in the table that when analysing volumetric changes in the svMCI group, a decrease in volumetric indices of several subfields of the left HF is determined, namely: subiculum, presubiculum, molecular layer, dentate gyrus, CA4 and HATA. However, when analysing the volumetric indices of the right HF, statistically significant differences were found only for the presubiculum (Table 18). There were no statistically significant differences in quantitative measures of entorhinal cortex in svMCI and control groups.

Table 18 - Volumetric changes of the right presubiculum in the svMCI group compared to the control group (M±σ)

Structure	svMCI, mm3	Control, mm3	% reduction in V	p-value
Presubiculum	272,78±41,63	301,26±41,68	9,5	0,029

3.3.5. Comparison of quantitative indices of hippocapmal formation of patients with mild cognitive impairment of different genesis

When comparing the volumes of HF subfields in the aMCI and svMCI groups, there was a statistically significant decrease in the volumes of several subfields in the aMCI group presented in Tables 19 and 20.

Table 19 - Volumetric changes in the left hippocampal formation in the aMCI group compared to the svMCI group (M±σ)

Structure	aMCI, mm3	svMCI, mm3	% reductions V	p-value
The tail of the hippocampus	414,27±65,89	463,30±67,59	10,6	0,019

Subiculum	319,57±54,44	374,96±54,39	14,8	0,0004
CA1	494,81±74,44	554,61±74,33	10,8	0,007
Hippocampal sulcus	168,21±38,94	193,45±39,98	13,5	0,05
Presubiculum	257,87±44,75	293,26±44,69	12,1	0,009
Molecular layer	418,31±63,97	480,01±63,92	12,9	0,001
Dentate gyrus	217,23±35,38	245,93±35,33	11,7	0,007
CA3	151,99±28,48	173,88±28,48	12,6	0,012
CA4	189,45±31,11	217,97±31,11	13,1	0,002
The hippocampal formation as a whole	2605,74±360,55	2945,66±360,18	11,5	0,001

As shown in Table 19, the aMCI group had the most pronounced decrease in left subiculum volume (by 14.8%).

Table 20- Volumetric changes in the right hippocampal formation in the aMCI group compared to the svMCI group (M±σ)

Structure	aMCI, mm3	svMCI, mm3	% reduction in V	p-value
Subiculum	312,77±54,94	374,84±54,88	16,6	0,0004
CA1	513,67±79,31	572,47±79,26	10,3	0,015
Presubiculum	235,80±41,63	272,78±41,63	13,6	0,003
Parasubiculum	52,80±12,82	63,14±12,82	16,4	0,007
Molecular layer	427,26±68,85	486,85±68,79	12,2	0,004
The hippocampal formation as a whole	2669,51±392,10	3014,83±391,72	11,5	0,003

Table 20 shows that in the aMCI group, the reduction in right subiculum (by 16.6%) and right presubiculum volume (by 16.4%) was most pronounced.

When analysing the quantitative parameters of the entorhinal cortex of patients with aMCI and svMCI, a statistically significant decrease in the volume and thickness of the right and left entorhinal cortex in the aMCI group was determined, presented in Tables 21 and 22.

Table 21 - Changes in entorhinal cortex thickness in the aMCI group compared to the svMCI group (M±σ)

Structure	aMCI, mm	svMCI, mm	p-value
Left entorhinal cortex	2,50±1,86	2,78±2,08	0,004
Right entorhinal cortex	2,56±2,35	3,0±2,03	0,0004

Table 22 - Volumetric changes in entorhinal cortex in the aMCI group compared to the svMCI group (M±σ)

Structure	aMCI, mm3	svMCI, mm3	% reduction in V	p-value
Left entorhinal cortex	1305,23±394,17	1659,60±393,45	21,4	0,002
Right entorhinal cortex	1360,14±349,32	1713,49±348,95	20,6	0,001

As shown in Table 22, a significant decrease in the volume of the left entorhinal cortex (by 21.4%) and right entorhinal cortex (by 20.6%) was detected in the aMCI group compared to the svMCI group.

3.3.6. Evaluation of the relationship between the volume of the subfields of the hippocapmal formation and the volume of hypointense foci in the brain matter

We performed correlation analysis to determine the correlation between the severity of white matter lession and atrophic changes of the HF subfields. In the aMCI group, statistically significant negative correlations of volumetric indices of several HF subfields with the fraction of hypointense foci were revealed, as shown in Table 23.

Table 23- Correlations between the decrease in the volumes of hippocapmal formation subfields and the fraction of hypointense foci in the brain in the aMCI group.

Structure	Volume of hypointense foci (fraction of ICV) Spearman correlation coefficient (r), p<0.05	
	On the left	On the right
Subiculum	-0,54	-0,40
Presubiculum	-0,40	-0,44
Molecular layer	-0,53	-
CA1	-0,40	-
CA3	-0,43	-
CA4	-0,45	-
The dentate gyrus	-0,49	-
Entorhinal cortex	-0,41	-0,41

When analysing the obtained data, negative correlations between the severity of cerebral vascular lesions and atrophic changes in several subfields of the right and left HF can be distinguished, with a decrease in the volumes of the subiculum, presubiculum and entorhinal cortex being observed on both sides.

We found no statistically significant correlations in the svMCI group and the control group.

3.3.7. Evaluation of the relationship of visual rating scale indices of medial temporal atrophy and entorhinal cortex atrophy with volumetric indices of hippocampal formation and entorhinal cortex

In correlation analysis, the visual scale scores of medial temporal atrophy (MTA) were negatively correlated with HF volume in patients with MCI syndrome, but no statistically significant correlations were found in the control group (Table 24).

Table 24 - Correlations between MTA visual scale scores and hippocampal formation volume.

Visual scale (points)	Volume of hippocampal formation (mm3) Spearman correlation coefficient (r), p<0.05	
	aMCI	svMCI
MTA on the right	- 0,52	- 0,37
MTA on the left	- 0,52	- 0,54

Entorhinal cortex atrophy visual scale (ERICA) scores were negatively correlated with entorhinal cortex volume in the three patient groups (Table 25).

Table 25 - Correlations between ERICA visual scale scores and hippocampal formation volume

Visual scale (points)	Entorhinal cortex volume (mm3) Spearman correlation coefficient (r), p<0.05		
	aMCI	svMCI	control
ERICA on the right	- 0,53	- 0,45	- 0,40

ERICA on the left	- 0,64	- 0,65	- 0,39

3.3.8. Evaluation of correlations of the volume of hypointense foci in the brain matter with the indicators of neuropsychological examination

To clarify the relationship between impaired cognitive functioning and the volume of white matter lesions, a correlation analysis of the studied parameters was carried out in all the studied groups.

A negative correlation was found between the indicators of the frontal assessment battery and the fraction of hypointense foci in the subjects in the control group ($r=-0.38$, $p<0.05$), graphically presented in Figure 16.

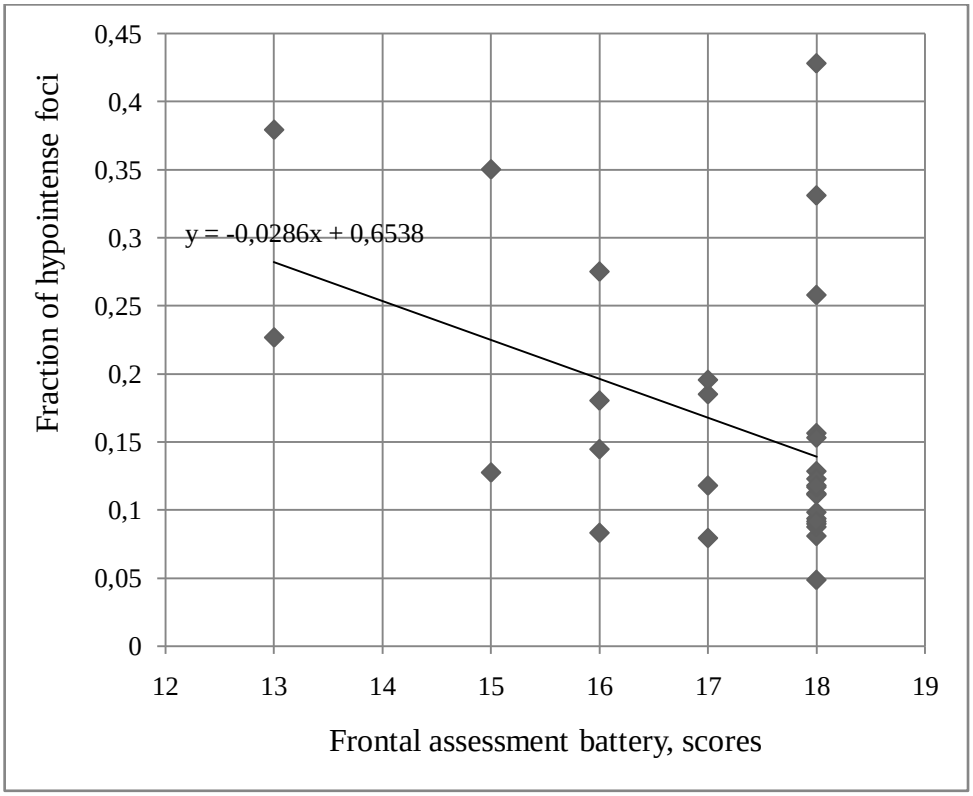

Figure 16 - Graph of the relationship between the indicators of the frontal assessment battery and the fraction of hypointense foci in the control group

No significant correlation between the volume of white matter lesion and the indicators of neuropsychological examination in patients with MCI syndrome was revealed.

3.3.9. Evaluation of correlations between the volume of the hippocapmal formation subfields and neuropsychological examination indices

Taking into account the insufficient study of regional changes in the HF in relation to cognitive impairment, it was of interest to study the relationship between the indicators of neuropsychological tests and the volumes of HF subfields. The indicators of cognitive functions in patients with MCI that were reduced compared to the control group were selected for analysis.

According to the data of correlation analysis In the group with svMCI, statistically significant positive correlations were found between the scores of the "Paired Associations Easy" subtest of the Wechsler Memory Scale with left subiculum ($r= 0.47$; $p<0.05$), left molecular layer ($r= 0.41$; $p<0.05$) and left CA4 ($r=0.40$; $p<0.05$) volumes graphically presented in Figure 17.

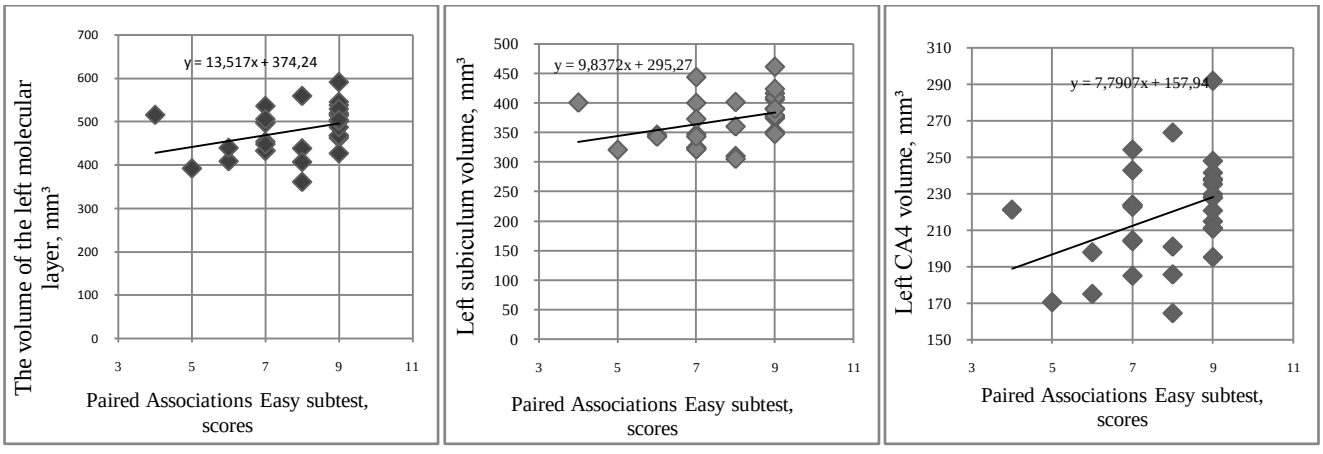

Figure 17 - Graph of correlation between the "Paired Associations Easy" subtest scores and the volumes of the subfield hippocapmal formation in the svMCI group

Statistically significant positive correlations were found between the scores of the "Paired Associations Hard" subtest of the Wechsler Memory scale with the volume of the left dentate gyrus ($r=0.39$; $p<0.05$) in the aMCI group, graphically presented in Figure 18.

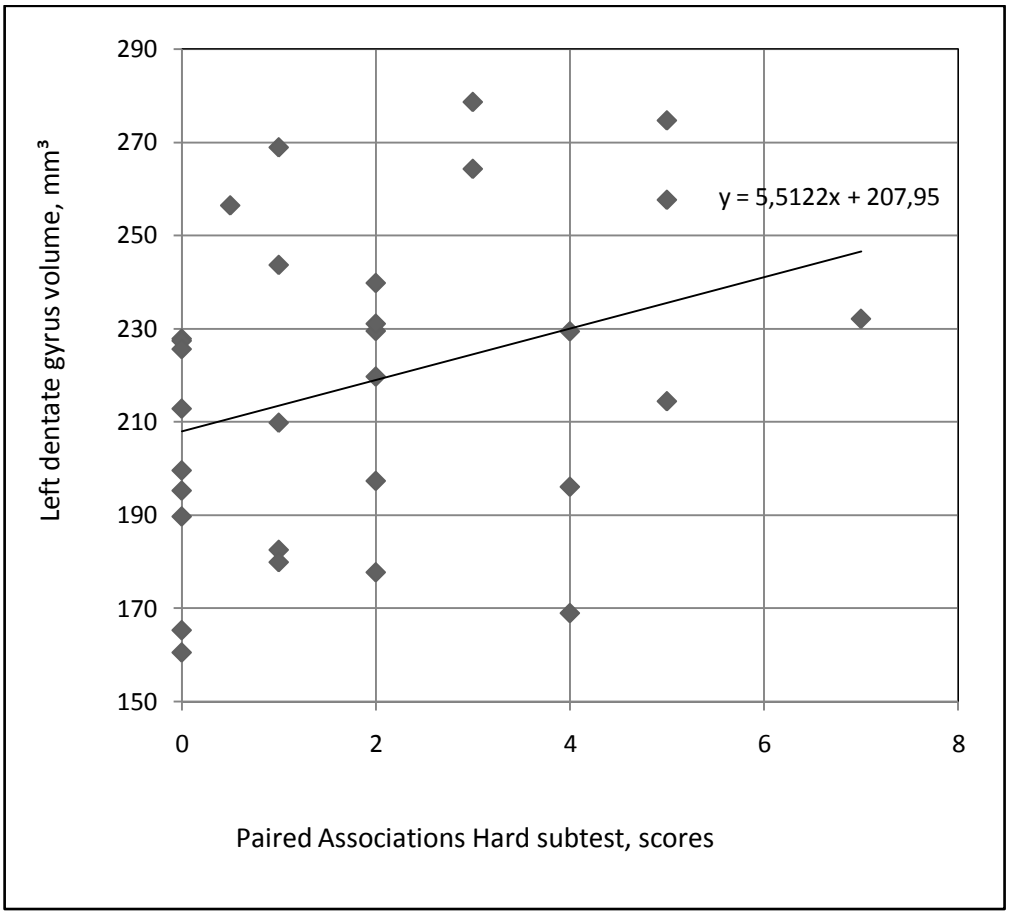

Figure 18 - Graph of correlation between the "Paired Associations Hard" subtest scores and the volume of the left dentate gyrus in the aMCI group

In the aMCI group, significant positive correlations were found between the scores of the "Visual Retention" subtest of the Wechsler Memory scale with the volumes of several HF subfields, graphically presented in Figure 19.

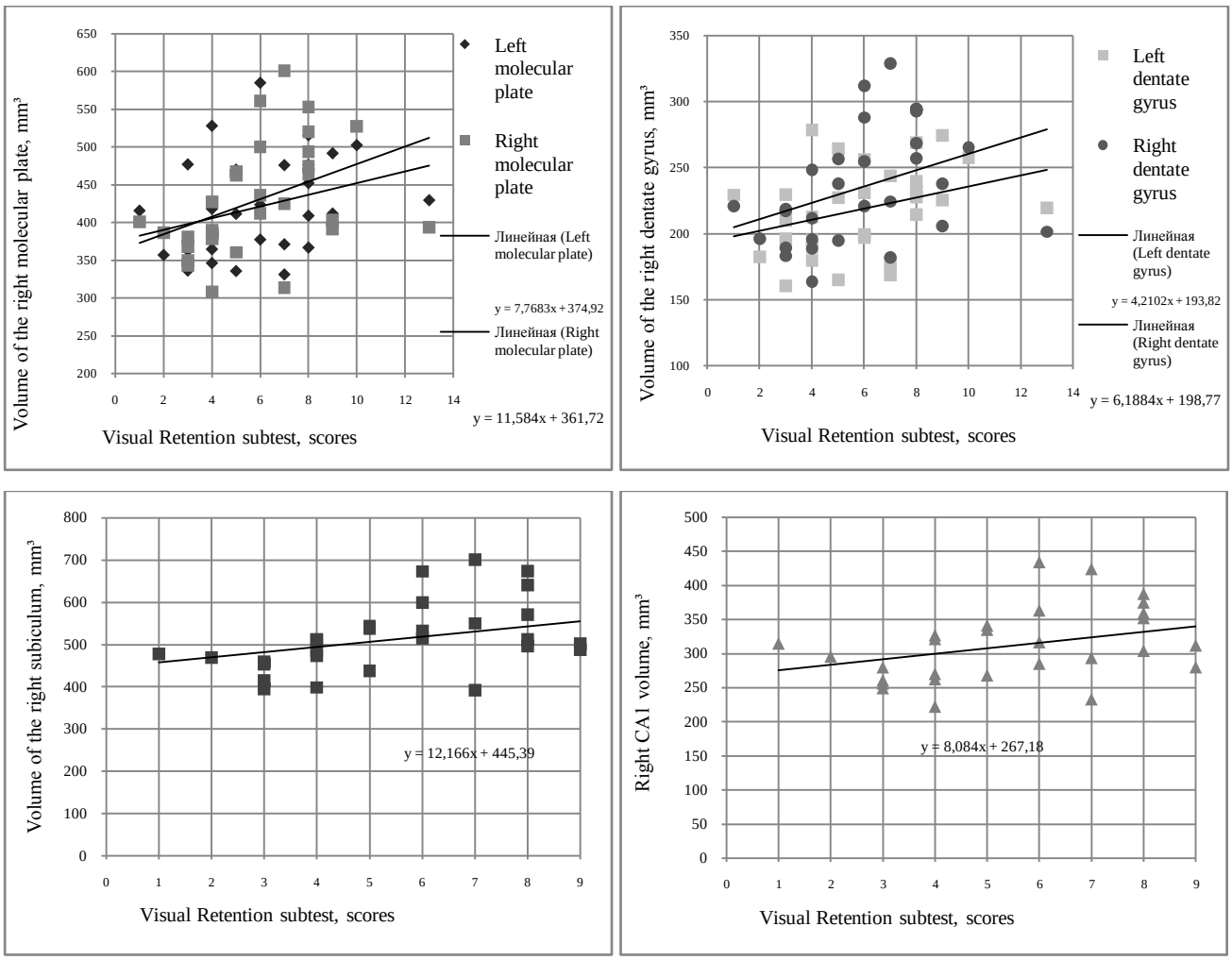

Figure 19 - Graphs of correlation between the scores of the "Visual Retention" subtest and the volumes of the subfields of the hippocapmal formation in the aMCI group

As can be seen from the graphs in Figure 19, the strongest positive correlations were determined with the right subiculum ($r=0.46$; $p<0.05$), right CA1 ($r=0.52$; $p<0.05$), right molecular lamina($r=0.56$; $p<0.05$), and right dentate gyrus ($r=0.49$; $p<0.05$).

3.4. Binary logistic regression and ROC analysis in the differential diagnosis of mild cognitive impairment of different genesis

Within the framework of solving the task of the study to clarify the possibilities of differential diagnostics of MCI of various genesis using MR-morphometry data, binary logistic regression was constructed and ROC-analysis was performed.

To evaluate the variants of the obtained binary logistic equations, we used accuracy - the percentage of the sum of correct solutions for both classes out of the total number of observations. The highest accuracy rate (73.3%) was achieved when the right subiculum was used as a variable, as well as when two variables were combined - the volume of the left subiculum and the thickness of the right entorhinal cortex (Tables 26 and 27).

Table 26 - Classification table for the combination of left subiculum volume and right entorhinal cortex thickness, where observed group membership rates (1 = aMCI, 2 =svMCI) are contrasted with those predicted from the calculated model

Observables		Predicted		
		Group		Percentage good decisions
		aMCI	svMCI	
Group	aMCI	21	9	70%
	svMCI	7	23	76,7%
Accuracy				73,3%

Table 27 - Classification table for right subiculum volume with observed group membership rates (1 = aMCI, 2 =svMCI) contrasted with those predicted from the calculated model

Observables		Predicted		
		Group		Percentage good decisions
		aMCI	svMCI	
Group	aMCI	23	7	76,7%
	svMCI	9	21	70%
Accuracy				73,3%

Next, ROC analysis was performed for both the right subiculum variant and the combination of left subiculum volume and right entorhinal cortex thickness, calculating the area under the ROC curve (AUC criterion) (Figure 20).

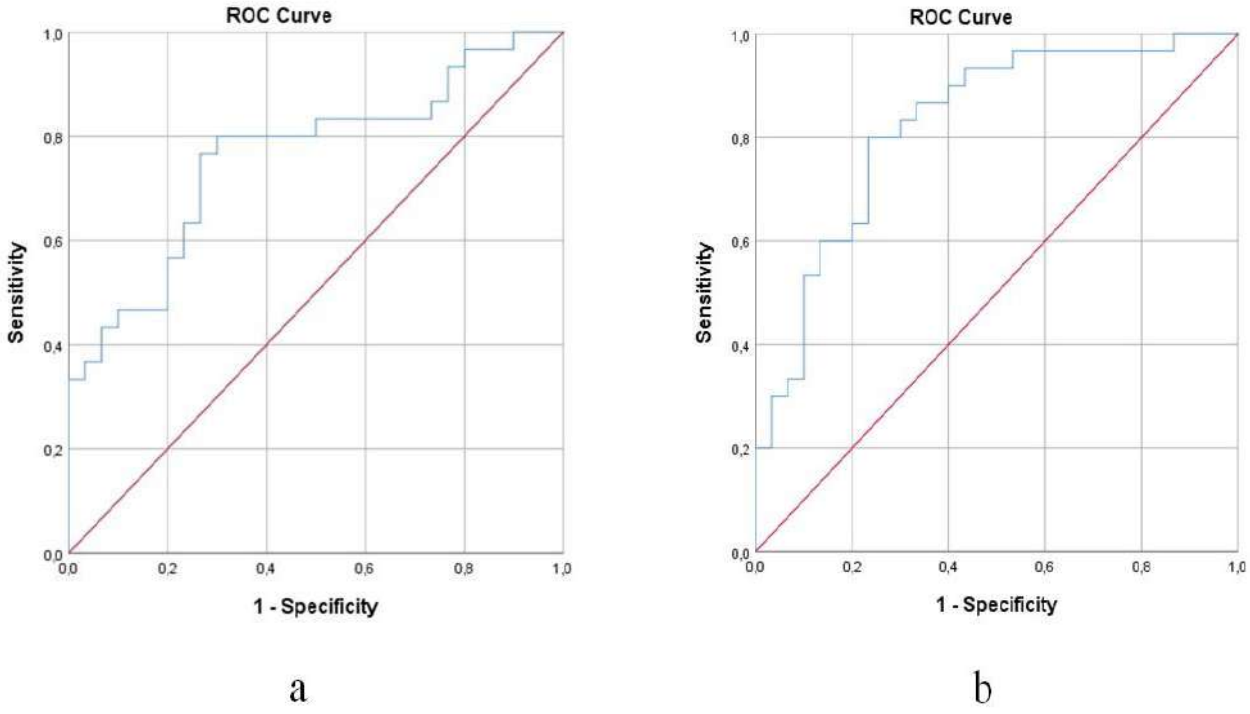

Figure 20 -ROC curves in the differential diagnosis of aMCI from svMCI: a - for right subiculum volume (AUC=0.761); b - for the combination of left subiculum volume and right entorhinal cortex thickness (AUC=0.824)

In ROC analysis, the largest area under the curve (AUC=0.824) in the differential diagnosis of aMCI from svMCI was determined for the combination of left subiculum volume and right entorhinal cortex thickness.

To clarify the advantage of the selected features over the total HF volume, similar steps were performed for the right and left HF volumes and their combinations, presented in Table 28.

Table 28 - Classification table for right and left hippocampal formation volumes, in which known group membership indices (aMCI and svMCI) are compared with those predicted on the basis of the calculated model

Variables	Recognition accuracy of aMCI and svMCI	AUC
Right hippocampal volume formations	60%	0,684

Left hippocampal volume formations	65%	0,718
The combination of the volumes of the right and of the left hippocampal formations	68,3%	0,722

Thus, the combination of left subiculum volume and right entorhinal cortex thickness, chosen as features, has the highest percentage of correct solutions and area under the curve compared to the total HF volumes.

Since patients in the aMCI group had significantly fewer vascular foci than those in the svMCI group ($p<0.05$), in the next step, another variable, the fraction of hypointense foci, was added to the selected combination of two variables (left subiculum volume and right entorhinal cortex thickness) (Table 29).

Table 29 - Classification table for left subiculum volume, right entorhinal cortex thickness and hypointense foci fraction, in which known group membership indices (aMCI and svMCI) are compared with those predicted on the basis of the calculated model

Observables		Predicted		
		Group		Percentage of correct decisions
		aMCI	svMCI	
Group	svMCI	6	24	80%
	aMCI	27	3	90%
Accuracy				85%

As Table 29 shows, the accuracy rate with this combination of the three variables increased to 85%. The ROC curve is plotted (Figure 21).

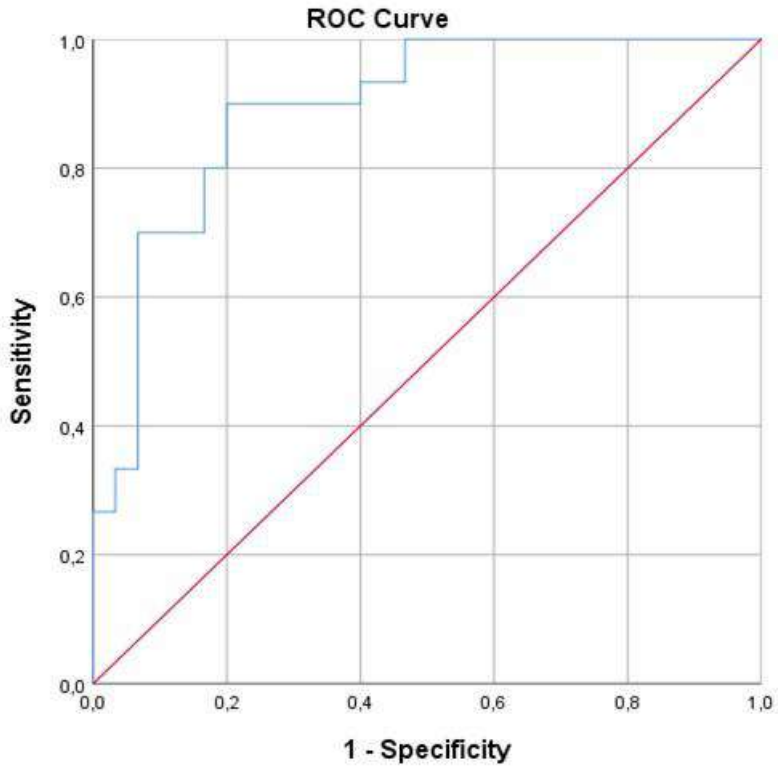

Figure 21 -ROC curve for the combination of left subiculum volume, right entorhinal cortex thickness and hypointense foci fraction in the differential diagnosis of aMCI from svMCI

In ROC analysis with a variant combination of three variables, an increase in AUC to 0.892±0.042 was observed.

In order to improve the differential diagnosis of aMCI from svMCI, a method using a binary logistic regression equation is proposed for use (1):

$$p = \frac{1}{1+e^{-(b_0+b_1x_1+b_2x_2+b_3x_3)}} \quad (1)$$

Where:

b_0 - constant

b_1 , b_2 , b_3 - values of coefficients of variables obtained during the construction of binary logistic regression (table)

x_1 , x_2 , x_3 - value of variables for a particular observation

p - probability that this observation belongs to the target class

Table 30 - Coefficient values for selected variables

coefficient	Variables	Coefficient values
b_0	Constant	14,678
b_1	Left subiculum volume, mm^3	-0,0171
b_2	Right entorhinal cortex thickness, mm	-2,4824
b_3	Fraction of hypointense foci (volume of foci/ICVx100)	-4,3096

Taking into account the coefficient values for the selected variables from Table 30, the formula takes the form (2):

$$p = \frac{1}{1+e^{-(14,678-0,017x_1-2,482x_2-4,310x_3)}} \quad (2)$$

Determination of the MCI variant is performed by calculating the probability according to this formula by substituting the values of the features included in the model, obtained during the examination of a particular patient. The calculation can be performed using a calculator. The value of $p \geq 0.5$ allows assigning the patient to the aMCI group, and the value of $p < 0.5$ - to svMCI.

The model has a sensitivity of 90%, specificity of 80%, and accuracy of 85%.

CHAPTER 4. DISCUSSION OF RESULTS

The results of the performed thesis work as a whole confirm the previously published materials, and also add new information about the presence of specific atrophic changes in MCI of different genesis.

In this study, risk factors for pathologies associated with cognitive impairment, namely arterial hypertension, diabetes mellitus and hypercholesterolaemia, were assessed in all patients. Whitmer R. A. et al. found that the presence of arterial hypertension, diabetes mellitus and hypercholesterolemia was associated with a 20-40% increased risk of dementia (Whitmer R. A. et al., 2005).

The presence of arterial hypertension in patients was equally common in the aMCI and svMCI groups. Arterial hypertension is the most common and proven risk factor for VCI associated with CSVD (Gnedovskaya E. V. et al., 2020; Gulevskaya T. S., Anufriev P. L., Tanashyan M. M., 2022). One of the characteristic markers of CSVD according to MRI is WMH, which reflects chronic ischaemia and is of great importance in cognitive impairment. In a longitudinal study by Verhaaren B. F. J. et al. in patients with uncontrolled arterial hypertension there was a more pronounced annual progression of WMH in comparison with patients receiving antihypertensive therapy (Verhaaren B. F. J. et al., 2013).

Numerous studies have shown that arterial hypertension aggravates the pathogenesis and accelerates the progression of AD (Iadecola C., Gottesman R. F., 2018; Ungvari Z. et al., 2021). Such features of pathogenesis on the background of chronic hypertension include disruption of the blood-brain barrier, activation of microglia, development of neuroinflammation, as well as dysfunction of the glymphatic system, which contributes to the formation of amyloid plaques and increased neurotoxicity (Bowman G. L. et al., 2018; Rasmussen M. K., Mestre H., Nedergaard M., 2018).

Hypercholesterolemia and diabetes mellitus, as one of the main risk factors for cerebrovascular diseases, were predominant in patients in the svMCI group. Information

about the significance of hypercholesterolemia in the development of focal brain changes (WMH) is contradictory (Kim J. S., 2021). Thus, in a study by Zhuang F. J. et al. found an association of WMH severity with age, smoking, diabetes mellitus and arterial hypertension, but no association with hypercholesterolaemia was found (Zhuang F. J. et al., 2018). Similar results were obtained in a study by Jimenez-Conde J. et al. which also reported a possible protective function of hyperlipidaemia against CSVD (Jimenez-CondeJ. et al., 2010). Conflicting results have also been obtained on the association of lacunar infarcts with the presence of hypercholesterolaemia (Kim J. S., 2021). Nevertheless, hypercholesterolemia is one of the main risk factors for atherosclerosis underlying cardiovascular and cerebrovascular diseases (Drapkina O. M. et al., 2022).

Thus, the data of this study show that modification of risk factors is the most important task in patients with MCI of both vascular and neurodegenerative genesis.

The degree of WMH severity according to the Fazekas visual scale and the fraction of hypointense foci obtained using FreeSurfer software was expectedly higher in the svMCI group than in the aMCI group and control group, with changes predominating in the deep white matter. The pathogenesis of deep white matter lesions is mainly based on arteriosclerosis of small vessels associated with vascular risk factors, the leading place of which is occupied by arterial hypertension (Rostrup E. et al., 2012; Johansen M. C. et al., 2021). In arteriosclerosis, necrosis of myocytes of the middle sheath of small arteries, fibrinoid necrosis and lipohyalinosis are observed, which leads to thickening of the vessel wall and narrowing of their lumen, hypoperfusion and development of ischaemic brain damage (Gayfutdinov R. T., 2020 ; Gulevskaya T. S., Anufriev P. L., Tanashyan M. M., 2022).

Changes in the periventricular white matter are to a greater extent caused by haemodynamic disorders against the background of the peculiarities of its blood supply and anatomical topography of white matter tracts. These disorders can be associated with atherosclerosis of large arteries and venous collagenosis (Johansen M. C. et al., 2021; Hannawi Y. et al., 2022). Linear periventricular halos and "caps" located less than 3mm from the ventricles are predominantly non-ischaemic in nature and are mainly

associated with damage to the ependymal layer with subependymal gliosis and demyelination.

Despite the fact that one of the most important neuroimaging markers of CSVD is the FLAIR MRI white matter hypointensity, the significance of white matter hypointensity on T1WI remains poorly understood. However, it is believed that white matter hypointensity determined on T1WI reflects a more severe lesion compared to hyperintensity on FLAIR, which is mainly due to more severe demyelinating damage and axonal death (Riphagen J. M. et al., 2018).

In this study, the fraction of hypointense foci obtained using FreeSurfer software in T1 WI mode was statistically significantly correlated with Fazekas scale scores in all groups (Stulov I.K. et al., 2023: 241). Previously, similar correlations of hypointense foci with the Fazekas scale were found in a number of studies (Cedres N. et al., 2020; HotzI. et al., 2022). It is worth noting that in the present study, weaker correlations (r=0.37) were found between the hypointense deep white matter fraction and Fazekas scale scores in the control group. These findings may indirectly explain the lower sensitivity of FreeSurfer in detecting small foci on T1 WI, especially in deep white matter, which is also supported by previous studies (Hotz I. et al., 2022; Riphagen J. M. et al., 2018; Wei K. et al., 2019).

Despite the simplicity of using the Fazekas visual scale in the assessment of white matter lesions in CSVD, it is not suitable for longitudinal studies , and the results are investigator-dependent (Prins N. D. et al., 2004). Therefore, the quantification of focal changes in the white matter using software in an automated mode has recently become of particular interest.

Most software packages are based on FLAIR MR images, as this MR is optimal for detecting focal changes. However, pathomorphological and neuroimaging comparisons have shown that focal measurements in FLAIR mode may overestimate changes in the periventricular white matter due to the high concentration of interstitial fluid associated with increased blood-brain barrier permeability, while underestimating changes in the deep white matter (Riphagen J. M. et al., 2018; Hotz I. et al., 2022).

A number of studies have found significant positive correlations between hypointense white matter volumes in T1 WI mode using the FreeSurfer software package and hyperintense white matter volumes in FLAIR mode obtained using different software packages (Riphagen J. M. et al., 2018; Olsson E. et al., 2013; Leritz E. C. et al., 2014; WeiK. et al., 2019). However, the obtained volumes of hypointense white matter using T1 WI, were smaller than those obtained using FLAIR (Riphagen J. M. et al., 2018; Wei K. et al., 2019). A recent study by Dadar M. et al. also highlights the need to validate hypointense white matter volumes obtained using FreeSurfer due to possible errors in the delineation of white and grey matter boundaries, especially at the level of the caudate nucleus (Dadar M. et al., 2021).

However, the undoubted advantage of MR morphometry using FreeSurfer based on T1 3D-MPRAGE is the ability to obtain quantitative measures of the cerebral cortex and subcortical brain structures and a higher signal-to-noise ratio compared to FLAIR (Thyreau B. et al., 2022).

Thus, the use of FreeSurfer software allows us to study both focal changes in CSVD and to perform quantitative analysis of various anatomical structures in the brain.

Of particular interest is the determination of the relationship between the disturbance of neuropsychological indicators and the severity of focal brain changes due to CSVD. When performing correlation analysis, statistically significant negative relationships were found between the indicators of the frontal dysfunction battery and the hypointense white matter fraction in the control group, which may indicate the dependence of the indicators of executive function and the degree of white matter lesion in conditionally healthy elderly people. Nevertheless, no correlations between the hypointense white matter fraction and indicators of cognitive impairment were found in the aMCI and svMCI groups.

However, incomplete correspondence of the total volume of white matter lesions to the severity of cognitive impairment has been described earlier in other studies. Thus, in the studies of Jiang J. et al. and Smith E. E. et al. it was found that the decline in cognitive function indices can correlate with white matter lesions of certain brain localisations, but not with the total volume of white matter lesions (Smith E. E. et al.,

2011; Jiang J. et al., 2018). Rizvi B. et al. found an association between the severity of WMH in occipital brain regions with decreased verbal and delayed memory performance and reduced volumes of the dentate gyrus and CA1 (Rizvi B. et al., 2023). Also, a number of studies emphasise the greater importance of periventricular white matter lesions in cognitive impairment than deep white matter lesions (Jiang J. et al., 2018; Armstrong N. J., et al., 2020).

Thus, in patients with CSVD at the MCI stage, it is not so much the total volume of white matter lesion as the localisation of the lesion in the brain that is of greater importance in the impairment of cognitive functions. We can also assume that there are certain factors of brain resistance to cerebrovascular diseases and neurodegenerative processes, such as cognitive reserve and brain reserve that allow maintaining the level of cognitive functions (Mok V. C. T. et al. 2017; Koberskaya N. N., Tabeeva G. R., 2019).

In the aMCI group, statistically significant negative correlations of the volume indices of several HF subfields with the fraction of hypointense white matter foci were revealed. We found no such correlations between the svMCI and control groups. We should note that the results of studies on the dependence of white matter lesion with atrophic changes of HF are few and contradictory. Thus, some studies determined the relationship between the volume of white matter lesion and hippocampal atrophy (Crane D.E. et al., 2015; Fiford C. M. et al., 2017). However, other studies have reported no such correlation (Gattringer T. et al., 2012; Nosheny R. L. et al., 2015). In a study by Van Etten E. J. et al. reduced hippocampal volume in APOE ε4 carriers was associated with WMH in the temporal lobes but not other brain localisations (Van Etten E. J. et al., 2021).

Thus, the findings suggest that the interaction between neurodegenerative and vascular processes may go beyond an additive effect and may acquire a synergistic character, contributing to more pronounced atrophic changes in HF and memory impairment.

Currently, the visual scale of medial temporal atrophy (MTA), is widely used in patients with cognitive impairment, as it allows indirect assessment of atrophic changes

in the mediobasal sections of the temporal lobes, primarily the hippocampus (Neznanov N.G., 2016). The recently proposed entorhinal cortex atrophy scale (ERICA), has not yet become as widespread as the MTA scale. Nevertheless, according to a recent study by Roberge X. et al., the ERICA scale is superior to the MTA scale in predicting the conversion of aMCI to AD (Roberge X. et al., 2021).

In this study, MTA scale scores were negatively correlated with total HF volume and ERICA scores were negatively correlated with entorhinal cortex volume in patients with MCI syndrome. A recent study by Loreto F. et al. also found significant negative correlations between MTA scale scores and corresponding hippocampal volumes (Loreto F. et al., 2023).

Thus, the use of visual scales in routine practice suggests atrophic changes in the mediobasal regions of the temporal lobes in this category of patients. The obtained differences of visual scales in the aMCI and svMCI groups may suggest the possible use of these scales in the differential diagnosis of these conditions.

In the morphometric analysis of cortical thickness, the main differences in the aMCI group compared to the svMCI and control groups were determined by the cortical thickness of the middle temporal gyrus, parahippocampal and fusiform gyrus of both cerebral hemispheres. Similar results were obtained by a number of authors (Sun P. et al., 2019; Artemov M. V., Stanzhevsky A. A., 2020). In the work of Csukly G. et al., it was shown that a decrease in cortical thickness of the parahippocampal and fusiform gyrus allows to distinguish aMCI from the non-amnestic form of MCI (Csukly G. et al., 2016).

Also in the aMCI group there was a rather symmetrical decrease in the volume of the amygdaloid bodies, which is considered specific for AD at an early stage (Damulina A. I., Konovalov R. N., Kadykov A. S., 2015; Artemov M. V., Stanzhevsky A. A., 2020). The main functions of the amygdala are the formation of emotional reactions (primarily fear), participation in memory and decision-making processes, which is due to the presence of connections with the prefrontal cortex, temporal cortex and hippocampus (Sawada M. et al., 2022).

When analysing volumetric indices of HF between the aMCI group and the control group, statistically significant differences were detected both in the total volume of the right and left HF and practically in all subfields. Despite the significant differences in volumetric indices between the groups, there was a greater bilateral decrease in the volumes of the subiculum, presubiculum, and molecular layer of the HF (Stulov I. K. et al., 2022: 240; Stulov I. K. et al., 2023: 242). These results are in agreement with a number of previously conducted studies (Carlesimo G. A. et al., 2015; Khan W. et al., 2015; Zhao W. et al., 2019; Hari E. et al., 2022; Huang Y. et al., 2022).

Kwak K. et al. in developing a method for differential diagnosis of the progressive form of MCI (pre-AD) from the stable form of MCI using a convolutional neural network found that the subiculum, presubiculum, CA1 and molecular layer had the greatest impact on model performance than other subfields of the HF (Kwak K. et al., 2022). In addition, Zeng Q. et al. found that the characteristic pattern of atrophic changes of HF in the progressive form of MCI was also a decrease in the subiculum and molecular layer (Zeng Q. et al., 2021).

Left parasubiculum volumes did not differ significantly between the aMCI and control groups, as previously described by Zhao W. et al. (Zhao W. et al., 2019). Also, similar data were obtained in a study by He P. et al. in which there were no significant differences in parasubiculum volumes between the aMCI, Alheimer-type dementia and control groups, which may indicate the relative resistance of this subfield to the neurodegenerative process (He P. et al., 2022).

Most studies have considered CA1, presubiculum and subiculum subfields as biomarkers of early AD (Carlesimo G. A. et al., 2015; Khan W. et al., 2015; Zhao W. et al., 2019; Hari E. et al., 2022.). Nevertheless, some studies have reported selective vulnerability of CA2-3, CA4 and dentate gyrus (BroadhouseK. M. et al., 2019; Baek M. S. et al., 2022). Such conflicting data may be due to both different criteria for selecting of patients wiht cognitive impairment and HF segmentation methods.

In this study, despite statistically significant differences in CA1 between the aMCI and control groups, the decrease in the volume of this subfield was less pronounced than that of the subiculum and presubiculum. Khan W. et al reported

similar findings where they demonstrated greater accuracy of presubiculum volume reduction in predicting the progression of aMCI in AD than total HF volume ((Khan W. et al., 2015). Carlesimo G. A. et al. showed that the largest area under the curve (AUC), for the difference between the aMCI and control, and aMCI and Alheimer's type dementia groups had subiculum and presubiculum, while CA1 had the lowest AUC (Carlesimo G. A. et al., 2015).

Atrophic changes in the entorhinal cortex, according to pathomorphological data, occur at an earlier stage of AD than atrophy of the hippocampus proper and are detected already at the stage of subjective cognitive decline. This allowed some authors to consider the decrease in quantitative indicators of the entorhinal cortex as a potential biomarker of AD (Khan U. A. et al., 2014; Zhou M. et al., 2016; Enkirch S.J. et al., 2018).

In the conducted study, a significant decrease in the volume and thickness of the entorhinal cortex was revealed in the aMCI group compared to the control group (Stulov I.K. et al., 2023: 239). Thus, the volume of the left entorhinal cortex was reduced by 28.5%, and the volume of the right entorhinal cortex by 20.5%. These results are consistent with the data of the study by Jessen F. et al., where a decrease in entorhinal cortex volume was found in patients with subjective cognitive impairment by 18%, in patients with MCI by 26%, and in patients with dementia in AD by 44% (Jessen F. et al., 2006).

The earliest changes in the entorhinal cortex occur in layer II, which is confirmed by studies in humans and primates (Gómez-Isla T. et al., 1996; Long J.M. et al., 2020). In a recent pathomorphological study of elderly individuals aged 80 years with unique episodic memory (SuperAgers), it was found that the content of NFT in layer II of the entorhinal cortex was lower and neurons were larger than in individuals of the same age category with average cognitive abilities and in patients with aMCI (Nassif C. et al., 2022).

The main entrance to the hippocampus is from layer II of the entorhinal cortex, the axons of which connect with dendrites of cells of the granular layer of the dentate gyrus forming a perforant pathway (Augustinack J. C. et al., 2010). Neurons of the

granular layer of the dentate gyrus connect to CA3 by mossy fibres, and CA3 neurons contact the dendrites of CA1 pyramidal cells via Schaffer collaterals. CA1 then connects to the subiculum and closes the pathway, with the result that the subiculum is seen as the exit region. However, there are also short pathways, such as neurons of layer III of the entorhinal cortex projecting to CA1 and the subiculum (temporal-ammonic pathway). Damage to the perforant pathway occurs in the early stages of AD, extending from the entorhinal cortex to the dentate gyrus (Gómez-Isla T. et al., 1996; Carlesimo G. A. et al., 2015).

Thus, there is an uneven decrease in the quantitative indices of the HF and entorhinal cortex subfields at the stage of aMCI, which may be responsible for damage to the perforant pathway and a decrease in memory processes.

We know that atrophic changes of HF are characteristic not only for AD and aMCI, but are also observed in subcortical vascular dementia and svMCI (Kril J. J. et al., 2002; Nishio K. et al., 2010). The sensitivity of HF to ischaemic and hypoxic lesions has been described previously in a number of papers, yet studies of regional HF atrophy in svMCI are limited (Wong F. C. C. et al., 2021; He M. et al., 2022; Johnson A. C., 2023).

When analysing the volumetric parameters of the HF in the svMCI group compared to the control group, a moderate decrease in both the total volume of the left HF and the volume of several of its subfields (within 8.3-13.8%) was observed, namely: subiculum, presubiculum, dentate gyrus, CA4, and the hippocampal-amygdala transition region. Also in the svMCI group a decrease in the volume of the right presubiculum was found compared to the control group, while no statistically significant differences in the total volume of the right HF were detected. There were no statistically significant differences in quantitative indicators of the entorhinal cortex between the svMCI and control groups.

According to recent studies, the subiculum is one of the most vulnerable subfields of the HF to ischaemic process. These data are reflected in several papers using MR morphometry and also confirmed by rodent studies (Nishio K. et al., 2010; Pin G. et al., 2021). It is possible that this sensitivity is related to the presence of numerous receptors

to glucocorticoids in the subiculum, which may enhance ischaemic neuronal damage (Pin G. et al., 2021).

Some studies have reported regional atrophic changes of the HF in svMCI. For example, the study by Li X. et al. revealed decreased volumes of the subiculum, presubiculum, CA4 and dentate gyrus (Li X. et al., 2016). Wong F. C. C. et al. found decreased volumes of the subsiculum, CA1, CA4, molecular layer, and dentate gyrus, which has been attributed to impaired episodic memory and executive function in individuals with svMCI (Wong F. C. C. et al., 2021).

Thus, the results obtained in this study were generally consistent with the data of previous studies. Nevertheless, the role of atrophic changes in the hippocampal-amygdala transition region in VCI is still unclear.

The most pronounced differences between aMCI and svMCI groups according to MR-morphometry and ROC-analysis were determined by quantitative indices of subiculum and entorhinal cortex. The findings may indicate that these structures are associated with the earliest deposition of NFT in and characterised more vulnerable to the neurodegenerative process than to ischaemia (Stulov I. K. et al. 2022: 244; Schönheit B., Zarski R., Ohm T. G., 2004; Scher A. I. et al., 2011 ; Kim G. H. et al., 2015). Thus, atrophic changes of HF subfields are detected already at the stage of aMCI and svMCI, and the distribution patterns of HF subfield atrophy can be used for differential diagnosis of MCI of different genesis.

Today, modern trends in medicine include the development and implementation of new diagnostic solutions based on artificial intelligence, and in particular, machine learning. Large databases of medical data are being actively created and medical decision support systems are being developed for the diagnosis and treatment of various diseases. The introduction of machine learning is also noted for processing neuroimaging research data (Trufanov G. E., Efimtsev A. Yu., 2023). Machine learning algorithms are able to analyse large databases, detect patterns and classify objects, which allows increasing the accuracy of differential diagnostics. One of the machine learning algorithms is binary logistic regression, which we applied in the study to develop a model for differential diagnosis of MCI of different genesis. We use binary

logistic regression when the dependent variable can take only two values, which allows us to estimate the probability of a patient belonging to one of two classes.

The variables obtained by MR morphometry were used to develop a model for differential diagnosis of aMCI from svMCI. At the first stage, we selected the variables that showed the highest decision accuracy (73.3%), namely, the right subiculum, as well as the combination of two variables - the volume of the left subiculum and the thickness of the right entorhinal cortex (Stulov I.K. et al., 2023: 238). However, the largest area under the curve (AUC=0.824) was obtained for the combination of left subiculum volume and right entorhinal cortex thickness. It is worth noting that atrophic changes in the subiculum and entorhinal cortex appeared to be the most pathognomonic for aMCI, probably due to neurodegeneration and neuronal death. At the same time, patients in the aMCI group had a significantly lower number of vascular foci than in the svMCI group ($p<0.05$), which allowed us to use the hypointense foci fraction as a third variable, improving the decision accuracy rate to 85% (AUC=0.892) (Stulov I.K. et al., 2023: 239).

Thus, based on the obtained data on MR-semiotics of atrophy of HF subfields and focal lesions of the brain white matter, it was possible to develop a model for differential diagnosis of aMCI from svMCI.

The existence of features of cytoarchitectonics of HF subfields and the presence of certain connections between them suggest that different subfields may process different types of memory (Mueller S.G. et al., 2011). Nevertheless, the interrelationships of regional changes in HF with cognitive impairments remain poorly studied and have recently been of scientific interest.

Recent studies have reported that visual memory impairment is a key marker of HF integrity and may have diagnostic value at different stages of AD (Oltra-Cucarella J. et al., 2019; Huang Y. et al., 2022).

In this paper, statistically significant positive correlations of the "Visual Retention" indexes of the Wechsler Memory scale with the volumes of some HF subfields in the aMCI group, namely, with the right subiculum, CA1 on the right, molecular layer and dentate gyrus on both sides. The strongest positive correlations

were found with the subfields of the right HF. These data suggest that atrophic changes in the described HF subfields are associated with visual memory impairment in patients with aMCI.

A study by Huang Y. et al. found positive correlations of visual memory performance with the volumes of the subiculum, CA1, molecular layer, and dentate gyrus, which generally supports the results of the present work (Huang Y. et al., 2022). Similar correlations of visual memory performance were also found by Zammit A. R. et al. for the subiculum and CA1 (Zammit A. R. et al., 2017).

In the present study, the decrease in visual memory indices was predominantly associated with atrophic changes in the subfields of the right HF. This feature was previously reported in the works of several authors (Burgess N., Maguire E. A., O'Keefe J., 2002; Ono S. E. et al., 2019; Ezzati A. et al., 2016).

The medial temporal lobes also play a significant role in associative memory (Shing Y. L. et al. L. et al., 2011; Bender A. R., Daugherty A. M., Raz N., 2013; Daugherty A. M., Flinn R., Ofen N., 2017). However, the specific contribution of specific HF subfields in associative memory formation is also still unexplored.

In the aMCI group, statistically significant positive correlations of the "Paired Associations Hard" subtest of the Wechsler Memory scale with the volumes of the left dentate gyrus were obtained, and in the svMCI group, positive correlations of the Paired Associations Easy subtest of the Wechsler Memory scale with the volumes of the left subiculum, left molecular layer, and CA4 on the left side were obtained. These data suggest that atrophic changes in these subfields of the left HF are associated with verbal associative memory impairment in patients with MCI syndrome (Stulov I. K., 2022: 243).

The specific role of CA3, CA4, and dentate gyrus in associative memory formation in both healthy individuals and patients with cognitive decline has previously been found by a number of researchers (Mueller S. G. et al., 2011; Shing Y. L. et al., 2011; Bender A. R., Daugherty A. M., Raz N., 2013; Daugherty A. M., Flinn R., Ofen N., 2017). Also, in a study using fMRI it was shown that CA3 and dentate gyrus

presumably perform the encoding of novel associations (face-name), whereas the subiculum is involved in retrieving learnt associations (Zeineh M. M. et al., 2003).

Thus, MR-semiotics of atrophic changes of the HF subfields in patients with the syndrome of MCI of neurodegenerative and vascular genesis was determined and data on the role of atrophic changes of the HF subfields in impairment of various types of memory were obtained. A model of differential diagnostics of MCI of different genesis using MR-morphometry data and the method of binary logistic regression with high sensitivity (90%) and specificity (80%) was developed.

GENERAL CONCLUSION

Alzheimer's disease and subcortical vascular cognitive impairment are the most common causes of cognitive decline, which raises the interest of identifying them in the pre-demanding stage.

According to the data of pathomorphological studies, stages of AD development associated with the patterns of NFT distribution in the brain have been described (Braak H., Braak E., 1991). NFT deposits are first detected in the transentorhinal cortex, entorhinal cortex, hippocampus, then spread to the adjacent parts of temporal neocortex, association cortex and only at late stages are detected in the rest of the neocortex. NFT has a neurotoxic effect, causing dysfunction and death of neurons, which is accompanied by atrophic changes. The HF is the most susceptible to neurodegenerative process, and its atrophic changes are considered by most researchers as a biomarker for AD. Nevertheless, according to a number of studies, the vulnerability of HF to chronic ischaemic process has been shown, which complicates differential radial diagnosis (Li X. et al., 2016; Gulyaeva N. V., 2021; Wong F. C. C. et al., 2021). It is also worth noting that the HF consists of various subfields with specific features of cytoarchitectonic structure and functioning, the lesion of which on the background of neurodegenerative and vascular diseases is poorly studied.

Currently, due to the rapid development of neuroimaging techniques and the development of special software for image processing, it is now possible to study specific subfields of the HF in vivo.

This study allowed us to describe the distribution of atrophic changes of individual HF subfields characteristic of aMCI and svMCI.

The common features for patients with MCI syndrome are a decrease in the total volume of the left HF and the volume of only one subfield (presubiculum) of the right HF. These data, presumably, may indicate a greater vulnerability of the left HF to vascular and neurodegenerative processes.

HF volumetric indices in the svMCI group were intermediate between HF volumetric indices in the aMCI and control groups. It was possible to identify pathognomonic atrophic changes in certain subfields of the HF for svMCI - subiculum, presubiculum, molecular layer, dentate gyrus, CA4 and the region of transition of the hippocampus to the amygdala of the left HF and presubiculum of the right HF.

In aMCI, despite atrophic changes in the majority of subfields of both HF, predominant involvement of both subiculums in the pathological process was revealed. There was also a pronounced decrease in quantitative indices of the entorhinal cortex on both sides, characteristic of patients with aMCI, according to a number of neuroimaging and pathomorphological studies.

The revealed differences in quantitative indices of subiculum and entorhinal cortex in aMCI and svMCI suggested that these structures are more vulnerable to the neurodegenerative process than to the chronic ischaemic process, which is probably due to the accumulation of NFT at the early stage of AD.

The results of the study showed that atrophic changes of HF subfields are detected already at the stage of MCI, and we can use the distribution patterns of atrophy of HF subfields for differential diagnostics of MCI of neurodegenerative and vascular genesis.

In the aMCI group, compared to the svMCI and control groups, there was a decrease in the volume of the amygdala, which is considered to be specific for AD at an early stage. The amygdala, as well as the HF, belongs to the limbic system and is involved in the formation of emotions and memory processes.

The obtained correlations of MTA and ERICA visual scales with the volumes of mediobasal compartments of temporal lobes, as well as significant differences in the indices of these scales between the groups of patients with MCI can speak about the expediency of their application in everyday clinical practice for differential diagnostics of MCI.

Quantitative indices of the volume of cerebral vascular lesions (hypointense on T1 WI) and their fraction relative to the intracranial volume, characteristic of patients with MCI of different genesis and control subjects, were obtained in the course of the

work. In the correlation analysis no correlations between the fraction of cerebral vascular lesions and indices of neuropsychological testing in patients with MCI were revealed, which is probably due to the brain and cognitive reserve. However, positive correlations between the fraction of foci in the brain and indicators of the frontal assessment battery in individuals in the control group were determined.

We obtained unique data on the relationship between the severity of focal changes in the brain and atrophic changes in certain subfields of the HF in patients with aMCI. This may suggest that the presence of cerebral vascular lesions on the background of neurodegenerative process enhances the progression of atrophic changes with probable deterioration of cognitive functions.

The role of atrophic changes in the subfields of the hippocampal formation with disorders of different types of memory was determined. Thus, visual memory impairment in patients with aMCI was associated with atrophic changes in certain subfields of the right HF (subiculum, CA1, molecular layer, dentate gyrus). Verbal associative memory impairment in patients with svMCI is associated with atrophic changes in certain subfields of the left HF (subiculum, molecular layer, CA4), and in patients with aMCI - with the left dentate gyrus Thus, the unique contribution of each individual HF subfield in memory formation in patients with different types of cognitive impairment was demonstrated.

Using binary logistic regression and ROC analysis, the advantage of using certain HF subfields in the differential diagnosis of aMCI and svMCI over total HF is shown.

On the basis of the data obtained at MR-morphometry with the use of binary logistic regression the model of differential diagnostics of MCI of different genesis is developed, which is important, taking into account the search of new diagnostic solutions on the basis of artificial intelligence and machine learning.

Thus, MR-morphometry of the brain with evaluation of HF subfields is a promising and effective method for differential diagnostics of MCI of different genesis in clinical practice.

CONCLUSIONS

1. The use of an optimised brain MRI protocol, supplemented by MR morphometry using FreeSurfer 6.0 software and assessment of hippocampal formation subfields, improves the accuracy of differential diagnosis of mild cognitive impairment of various genesis.

2. Common features that distinguish amnestic and subcortical mild cognitive impairment from physiological aging are a decrease in the total volume of the left hippocampal formation (by 19.4% and 8.9%, respectively) and right presubiculum (by 21.7% and 9.5% , respectively).

3. Amnestic mild cognitive impairment compared to physiological aging is characterised by a more pronounced decrease in volume measures of the subiculum (by 22.5% on the right and 22.7% on the left) and entorhinal cortex (by 28.5% on the right and 20.5% on the left) than by a decrease in total hippocampal formation (by 17.7% on the right and 19.4% on the left)

4. Pathognomonic signs for subcortical vascular mild cognitive impairment are a decrease in the volume of the left hippocampal formation due to the subiculum, presubiculum, dentate gyrus, molecular layer, CA4 and the area of hippocampal to amygdala transition. Decreased volume of entorhinal cortex and total volume of the right hippocampal formation is not characteristic for subcortical vascular mild cognitive impairment.

5. The specificity of the atrophic process causes impairment of different types of memory in patients with mild cognitive impairment: visual memory - with a predominant decrease in the volumes of subfields of the right hippocampal formation, verbal associative memory - with a decrease in the volumes of subfields of the left hippocampal formation.

6. The developed diagnostic model based on the binary logistic regression method using MR morphometry data allows distinguishing patients with amnestic mild cognitive impairment from patients with subcortical mild cognitive impairment with high sensitivity (90%) and specificity (80%).

PRACTICAL GUIDANCE

1. MR-morphometry with subsequent assessment of the localisation of the atrophic process of the hippocampal formation subfields allows to optimise the differential diagnosis of mild cognitive impairment of different genesis.

2. It is recommended to use FreeSurfer software version 6.0 and higher for MR brain morphometry in patients with mild cognitive impairment syndrome.

3. Multidisciplinary approach with MRI with MR morphometry, clinical and neurological examination and neuropsychological testing allows to increase the accuracy of diagnosis and to predict the development of the disease in the future.

4. To develop models of differential diagnostics of mild cognitive impairment of various genesis using MR-morphometry data, it is reasonable to apply machine learning algorithms, which is of topical importance, taking into account the search for new diagnostic solutions.

PROSPECTS FOR FURTHER DEVELOPMENT OF THE TOPIC

The prospects for further development of the topic are related to the use of big data sets (Big data) and the introduction of artificial intelligence technologies.

In addition, it is reasonable to study the value of functional MRI to clarify changes in functional connectivity and features of the cerebral connectome, as well as diffusion-tensor MRI to assess microstructural damage to brain matter in patients with mild cognitive impairment.

To improve the accuracy of differential diagnosis of mild cognitive impairment, it is necessary to apply an integrated approach, including in the model the data of structural and functional neuroimaging, neuropsychological testing and laboratory examination (concentration of Aβ, tau-protein in cerebrospinal fluid), as well as to increase the statistical power of the study.

LIST OF SYMBOLS

aMCI - amnestic mild cognitive impairment

AD - Alzheimer's disease

WI - weighted images

ICV - intracranial volume

WMH - white matter hyperintensity

HF - hippocampal formation

PS - pulse sequence

MR - magnetic resonance

MRI - magnetic resonance imaging

NFT - neurofibrillary tangles

SPECT - single photon emission computed tomography

PVS - perivascular liquor spaces

svMCI - subcortical vascular mild cognitive impairment

PET - positron emission tomography

MCI - mild cognitive impairment

CSVD - cerebral small vessel disease

CMH - cerebral microhemorrhages

Aβ - beta-amyloid.

DWI - diffusion weighted imagine;

FAB - Frontal Assessment Battery (a battery of tests to assess frontal dysfunction)

FLAIR - Fluid Attenuated Inversion-Recovery - (pulse sequence)

MMSE - Mini Mental State Examination (Brief Mental Status Examination)

STRIVE - Standards for ReportIng Vascular changes on nEuroimaging

LIST OF REFERENCE

1. Acharya, A. White matter hyperintensities relate to basal ganglia functional connectivity and memory performance in aMCI and SVMCI / A. Acharya [et al. Acharya [et al.] // Frontiers in Neuroscience. - 2019. - Vol. 13. - Article number:1204. - URL: https://doi.org/10.3389/fnins.2019.01204

2. Albert, M. S. The diagnosis of mild cognitive impairment due to Alzheimer's disease: recommendations from the National Institute on Aging Alzheimer's Association workgroups on diagnostic guidelines for Alzheimer's disease / M. S. S. Albert [et al.] // Alzheimer's & Dementia. - 2011. - Vol. 7, № 3. - P. 270-279.

3. Alzheimer, A. Uber eigenartige Erkrankung der Hirnrinde / A. Alzheimer // Allgemeine Zeitschrift für Psychiatrie und psychisch-gerichtliche Medizin. - 1907. - Bd. 64. - S. 146-148.

4. Alzheimer's Association. 2018 Alzheimer's Disease Facts and Figures:World Alzheimer's Report // Alzheimer's & Dementia. - 2018. - Vol. 14, № 3. - P. 367-429.

5. Amaral, D. G. The dentate gyrus: fundamental neuroanatomical organisation (dentate gyrus for dummies) / D. G. Amaral. G. Amaral, H. E. Scharfman, P. Lavenex // Progress in Brain Research. - 2007. - Vol. 163. - P. 3-22.

6. Ananyeva, N. I. Changes in the volume of brain structures in the aspect of physiological aging / N. I. Anan'eva, L. V. Lukina, E. V. Andreev [et al.] // Radiation diagnostics and therapy. - 2022. - № S (13). - P. 19-20.

7. Ananyeva, N. I. Detection of neuroimaging biomarkers at the early stage of Alzheimer's disease / N. I. Anan'eva, E. V. Andreev, L. R. Akhmerova [et al.] // Diagnosis and treatment of mental and narcological disorders: modern approaches: a collection of methodological recommendations; compiled by N. V. Semenova. N. V. Semenova. - SPb.: Publishing and printing company "Kosta", 2018. - P. 112-125.

8. Ananyeva, N. I. Hippocampus: radial anatomy, variants of the structure / N. I. Ananyeva, R. V. Ezhova, I. E. Galsman [et al.] // Radiation diagnostics and therapy. - 2015. - № 1. - P. 39-44.

9. Ananyeva, N. I. MRI in clarifying the internal structure of the hippocampus in the norm and in a number of mental diseases / N. I. Ananyeva, E. V. Andreev, L. R. Akhmerova [et al.] // S. S. Korsakov Journal of Neurology and Psychiatry. - 2019. - Vol. 119, № 5-2. - P. 210-211.

10. Ananyeva, N. I. MR-morphometry of subfields and subregions of the hippocampus in norm and in a number of mental diseases / N. I. Ananyeva, E. V. Andreev, T. A. Salomatina [et al] // Radiation diagnostics and therapy. - 2019. - № 2. - P. 50-58.

11. Ananyeva, N. I. Opportunities of specialised structural MRI of the brain using visual assessment of atrophic changes in various brain structures and voxel morphometry in early diagnosis of Alzheimer's disease / N. I. Ananyeva, N. M. Zalutskaya, I. K. Stulov [et al] // V. M. Bekhterev School: from origins to the present: Proceedings of the All-Russian scientific and practical conference with international participation, dedicated to the 160th anniversary of the birth of V. M. Bekhterev and the 110th anniversary of V. M. Bekhterev SPb NIPNI. - SPb.: Alta Astra, 2017. - P. 229-232.

12. Ananyeva, N. I. Role of hippocampal neuroimaging in the diagnosis of Alzheimer's disease at an early stage / N. I. Ananyeva, N. M. Zalutskaya, N. G. Neznanov [et al] // Radiation diagnostics and therapy. - 2019. - № 1 (S). - P. 18-19.

13. Andrade-Talavera, Y. Kainate receptors in the CA2 region of the hippocampus / Y. Andrade-Talavera, A. Rodríguez-Moreno // Neural Regeneration Research. - 2023. - Vol. 18, № 2. - P. 320-321.

14. Andreev, E. V. Application of MR voxel-based morphometry in the assessment of brain atrophic changes in the diagnosis of the early stage of dementia of the Alzheimer type / E. V. Andreev, N. I. Ananyeva, Y. A. Beltseva [et al] // Davidenkov Readings: Congress with international participation (September 28-29, 2017, St. Petersburg): a collection of abstracts. - St. Petersburg. : "Man and his health", 2017. - P. 14-15.

15. Apostolova, L. G. Subregional hippocampal atrophy predicts Alzheimer's dementia in the cognitively normal / L. G.. G. Apostolova [et al.] // Neurobiology of

Aging. - 2010. - Vol. 31, № 7. - P. 1077-1088.

16. Armstrong, N. J. Common genetic variation indicates separate causes for periventricular and deep white matter hyperintensities / N. J. J. Armstrong [et al.] // Stroke. - 2020. - Vol. 51, № 7. - P. 2111-2121.

17. Artemov, M.V. Application of magnetic resonance morphometry and positron emission tomography in the diagnosis of Alzheimer's disease / M.V. Artemov, A.A. Stanzhevsky // Visualisation in medicine. - 2020. - Vol. 2, № 3. - P. 22-27.

18. Astakhova, E. A. Relationship of bioelectrical activity and structural changes in the hippocampus in temporal lobe pharmacoresistant epilepsy / E. A. Astakhova, S. E. Cherenkova, E. V. Marchenko [et al.] // Translational Medicine. - 2021. - Vol. 8, № 2. - P. 5-13.

19. Augustinack, J. C. Direct visualisation of the perforant pathway in the human brain with ex vivo diffusion tensor imaging / J. C. Augustinack [et al.] // Frontiers in Human Neuroscience. - 2010. - Vol. 4. - P. 42-56.

20. Aung, W. Y. Diffusion tensor MRI as a biomarker in axonal and myelin damage / W. Y. Y. Aung, S. Mar, T. L. S. Benzinger // Imaging in Medicine. - 2013. - Vol. 5, № 5. - P. 427-440.

21. Baek, M. S. Association of hippocampal subfield volumes with amyloid-beta deposition in Alzheimer's disease / M. S. S. Baek [et al.] // Journal of Clinical Medicine. - 2022. - Vol. 11, № 6. - Article number: 1526. - URL: https:// doi:10.3390/jcm11061526

22. Beck, A. T. An inventory for measuring depression / A. T. T. Beck [et al.] // Archives of General Psychiatry. - 1961. - Vol. 4, № 6. - P. 561-571.

23. Behrman, S. Diagnosing and managing mild cognitive impairment / S. Behrman, V. Valkanova, C. L. Allan // The Practitioner. Behrman, V. Valkanova, C. L. Allan // The Practitioner. - 2017. - Vol. 261, № 1804. - P. 17-20.

24. Bekhterev, V. M. Demonstration of eines Gehirns mit Zerstörung der vorderen und inneren Theile der Hirnrinde beider Schläfenlappen / V. M. M. Bekhterev // Neurologie Zentralblatt. - 1900. - Vol. 19. - P. 990-991.

25. Bender, A. R. Vascular risk milds associations between hippocampal

subfield volumes and memory / A. R. R. Bender, A. M. Daugherty, N. Raz // Journal of Cognitive Neuroscience. - 2013. - Vol. 25, № 11. - P. 1851-1862.

26. Bennett, D. A. Neuropathology of older persons without cognitive impairment from two community-based studies / D. A. Bennett [et al.]// Neurology. - 2006. - Vol. 66,№ 12. - P. 1837-1844.

27. Berron, D. A protocol for manual segmentation of medial temporal lobe subregions in 7 Tesla MRI / D. Berron [et al.] // NeuroImage: Clinical. - 2017. - Vol. 15. - P. 466-482.

28. Bir, S. C. Julius Caesar Arantius (Giulio Cesare Aranzi, 1530-1589) and the hippocampus of the human brain: the history behind the discovery / S. C. Bir. C. Bir [et al.] // Journal of Neurosurgery. - 2015. - Vol. 122, № 4. - P. 971-975.

29. Blitstein, M. K. MRI of cerebral microhemorrhages / M. K. K. Blitstein, G. A. Tung // American Journal of Roentgenology. - 2007. - Vol. 189, № 3. - P. 720-725.

30. Bloudek, L. M. Review and meta-analysis of biomarkers and diagnostic imaging in Alzheimer's disease / L. M. M. Bloudek [et al.] // Journal of Alzheimer's Disease. - 2011. - Vol. 26,№ 4. - P. 627-645.

31. Bogolepova, A. N. Clinical recommendations "Cognitive impairment in elderly and senile patients" / A. N. Bogolepova, E. E. Vasenina, N. A. Gomzyakova [et al] // S. S. Korsakov Journal of Neurology and Psychiatry. - 2021. - Vol. 121, № 10-3. - P. 6-137.

32. Bokura, H. Distinguishing silent lacunar infarction from enlarged Virchow-Robin spaces: a magnetic resonance imaging and pathological study / H. Bokura, S Kobayashi, S Yamaguchi // Journal of Neurology. - 1998. - Vol. 245, № 2. - P. 116-122.

33. Boone, K. B. Neuropsychological correlates of white-matter lesions in healthy elderly subjects: a threshold effect / K. B. Neuropsychological correlates of white-matter lesions in healthy elderly subjects: a threshold effect. B. Boone [et al.] // Archives of Neurology. - 1992. - Vol. 49, № 5. - P. 549-554.

34. Bowman, G. L. Blood-brain barrier breakdown, neuroinflammation, and cognitive decline in older adults / G. L. L. Bowman [et al.] // Alzheimer's & Dementia. - 2018. - Vol. 14, № 12. - P. 1640-1650.

35. Braak, H. Neuropathological stageing of Alzheimer-related changes / H. Braak, E. Braak // Acta Neuropathologica. - 1991. - Vol. 82, № 4. - P. 239-259.

36. Broadhouse, K. M. Hippocampal plasticity underpins long-term cognitive gains from resistance exercise in MCI / K. M. M. Broadhouse [et al.] // NeuroImage: Clinical. - 2020. - Vol. 25. - Article number: 102182. - URL: https://doi: 10.1016/j.nicl.2020.102182

37. Broadhouse, K. M. Memory performance correlates of hippocampal subfield volume in mild cognitive impairment subtype / K. M. M. Broadhouse [et al.] // Frontiers in Behavioral Neuroscience. - 2019. - Vol. 13. - Article number: 259.- URL: https://doi: 10.3389/fnbeh.2019.00259

38. Brown, E. M. Test-retest reliability of FreeSurfer automated hippocampal subfield segmentation within and across scanners / E. M. M. Brown [et al.] // Neuroimage. - 2020. - Vol. 210. - Article number: 116563. - URL: https://doi: 10.1016/j.neuroimage.2020.116563

39. Burgess, N. The human hippocampus and spatial and episodic memory / N. Burgess, E. A. Maguire, J. O'Keefe // Neuron. Burgess, E. A. Maguire, J. O'Keefe // Neuron. - 2002. - Vol. 35, № 4. - P. 625-641.

40. Caminiti, S. P. FDG-PET and CSF biomarker accuracy in prediction of conversion to different dementias in a large multicentre MCI cohort / S. P. P. Caminiti [et al.] // NeuroImage: Clinical. - 2018. - Vol. 18. - P. 167-177.

41. Carlesimo, G. A. Atrophy of presubiculum and subiculum is the earliest hippocampal anatomical marker of Alzheimer's disease / G. A. A. Carlesimo [et al.] // Alzheimer's & Dementia: Diagnosis, Assessment & Disease Monitoring. - 2015. - Vol. 1, № 1. - P. 24-32.

42. Cedres, N. Predicting Fazekas scores from automatic segmentations of white matter signal abnormalities / N.Cedres [et al.] //Aging (Albany NY). - 2020. - Vol. 12, № 1. - P. 894-901.

43. Certificate of state registration of the database No. 2023621026 Russian Federation. Magnetic resonance morphometry of the brain with assessment of hippocampal formation in mild cognitive impairment of different genesis / N. I.

Anan'eva, L. V. Lukina, I. K. Stulov, N. Y. Safonova, D. O. Vuks; applicant and right holder Federal State Budgetary Institution "V. M. Bekhterev National Medical Research Centre for Psychiatry and Neurology" of the Ministry of Health of the Russian Federation. - No. 2023620642; applied for. 10.03.2023; publ. 29.03.2023.

44. Chan, K. Y. Epidemiology of Alzheimer's disease and other forms of dementia in China, 1990-2010: a systematic review and analysis / K. Y. Y. Chan [et al.] // Lancet. - 2013. - Vol. 381,№ 9882. - P. 2016-2023.

45. Charidimou, A. White matter hyperintensity patterns in cerebral amyloid angiopathy and hypertensive arteriopathy / A. Charidimou [et al. Charidimou [et al.]// Neurology. - 2016. - Vol. 86,№ 6. - P. 505-511.

46. Cheignon, C. Oxidative stress and the amyloid beta peptide in Alzheimer's disease / C. Cheignon [et al. Cheignon [et al.] // Redox biology. - 2018. - Vol. 14. - P. 450-464.

47. Cherenkova, S. E. Pharmacoresistant temporal lobe epilepsy: the relationship between epileptiform activity and structural changes in the hippocampus / S. E. Cherenkova, E. V. Marchenko, A. M. Aleksandrov [et al.] // Translational Medicine. - 2020. - Vol. 7, № 6. - P. 46-54.

48. Chong, J. S. Amyloid and cerebrovascular burden divergently influence brain functional network changes over time / J. S. S. X Chong [et al.] // Neurology. - 2019. - Vol. 93, № 16. - P. e1514-e1525.

49. Clinical Laboratory Diagnostics: National Manual. In 2 vol. Vol. 1 / ed. by V.V. Dolgov, V.V. Menshikov. - Moscow: GEOTAR-Media, 2012. - 928 p.

50. Crane, D. E. Gray matter blood flow and volume are reduced in association with white matter hyperintensity lesion burden: a cross-sectional MRI study / D. E. E. Crane [et al.] // Frontiers in Aging Neuroscience. - 2015. - Vol. 7. - Article number: 131. - URL: https://doi.org/10.3389/fnagi.2015.00131

51. Cryan, J. F. The gut microbiome in neurological disorders / J. F. F. Cryan [et al.] // Lancet Neurology. - 2020. - Vol. 19, № 2. - P. 179-194.

52. Csukly, G. The differentiation of amnestic type MCI from the non-amnestic types by structural MRI / G. Csukly [et al.] // Frontiers in Aging Neuroscience. - 2016. -

Vol. 8. - Article number: 52. - URL: https://doi: 10.3389/fnagi.2016.00052

53. Dadar, M. Beware of white matter hyperintensities causing systematic errors in FreeSurfer gray matter segmentations! / M. Dadar [et al.] // Human Brain Mapping. - 2021. - Vol. 42, № 9. - P. 2734-2745

54. Damulina, A. I. Significance of voxel-based morphometry in the study of mild cognitive impairment / A. I. Damulina, R. N. Konovalov, A. S. Kadykov // Annals of Clinical and Experimental Neurology. - 2015. - Vol. 9, №. 3. - P. 42-48.

55. Daugherty, A. M. Hippocampal CA3-dentate gyrus volume uniquely linked to improvement in associative memory from childhood to adulthood / A. M. Daugherty. M. Daugherty, R. Flinn, N. Ofen // Neuroimage. - 2017. - Vol. 153. - P. 75-85.

56. De Carli, S. Anatomical mapping of white matter hyperintensities (WMH) exploring the relationships between periventricular WMH, deep WMH, and total WMH burden / S. de Carli [et al.] // Stroke. - 2005. - Vol. 36, № 1. - P. 50-55.

57. De Flores, R.Characterisation of hippocampal subfields using ex vivo MRI and histology data: Lessons for in vivo segmentation / R.de Flores [et al.] // Hippocampus. - 2020. - Vol. 30, № 6. - P. 545-564.

58. De Mendonça, A.Clinical significance of subcortical vascular disease in patients with mild cognitive impairment / A.de Mendonça [et al.] // European Journal of Neurology. - 2005. - Vol. 12, № 2. - P. 125-130.

59. De Oliveira, F. F. Assessment of risk factors for earlier onset of sporadic Alzheimer's disease dementia / F. F. de Oliveira [et al] // Neurology India. F. de Oliveira [et al.] // Neurology India. - 2014. - Vol. 62, № 6. - P. 625-630.

60. De Reuck, J. Comparison of 7.0-T T2*-magnetic resonance imaging of cerebral bleeds in post-mortem brain sections of Alzheimer patients with their neuropathological correlates / J. de Reuck [et al.] // Cerebrovascular Diseases. - 2011. - Vol. 31, № 5. - P. 511-517.

61. De Simone, M. S. Predicting progression to Alzheimer's disease in subjects with amnestic mild cognitive impairment using performance on recall and recognition tests / M. S. de Simone. S. de Simone [et al.] // Journal of Neurology. - 2019. - Vol. 266, № 1. - P. 102-111

62. Deckers, K. Target risk factors for dementia prevention: a systematic review and Delphi consensus study on the evidence from observational studies / K. Deckers. Deckers [et al.] // International Journal of Geriatric Psychiatry. - 2015. - Vol. 30, № 3. - P. 234-246.

63. Dekeyzer, S. "Unforgettable", - a pictorial essay on anatomy and pathology of the hippocampus / S. Dekeyzer [et al.] // Insights into Imaging. - 2017. - Vol. 8. - P. 199-212.

64. Dickerson, B. C. MRI-derived entorhinal and hippocampal atrophy in incipient and very mild Alzheimer's disease / B. C. Dickerson [et al.] // Neurobiology of Aging. - 2001. - Vol. 22, № 5. - P. 747-754.

65. Doubal, F. N. Characteristics of patients with minor ischaemic strokes and negative MRI: a cross-sectional study / F. N. Doubal. N. Doubal, M. S. Dennis, J. M. Wardlaw // Journal of Neurology, Neurosurgery & Psychiatry. - 2011. - Vol. 82, № 5. - P. 540-542.

66. Doubal, F. N. Enlarged perivascular spaces on MRI are a feature of cerebral small vessel disease / F. N. Doubal. N. Doubal [et al.] // Stroke. - 2010. - Vol. 41, № 3. - P. 450-454.

67. Drapkina, O. M. Prevention of chronic non-infectious diseases in the Russian Federation. National Guidelines / O. M. Drapkina, A. V. Kontsevaya, A. M. Kalinina [et al.] // Cardiovascular therapy and prevention. - 2022. - Vol. 21, № 4. - P. 5-232.

68. Dubois B. The FAB: a frontal assessment battery at bedside / B. Dubois [et al.] // Neurology. - 2000. - Vol. 55, № 11. - P. 1621-1626.

69. Dubois, B. Preclinical Alzheimer's disease: definition, natural history, and diagnostic criteria / B. Dubois [et al] // Alzheimer's & Dementia. Dubois [et al.] // Alzheimer's & Dementia. - 2016. - Vol.12, No. 3. - P. 292-323.

70. Dunn, C. J. Deficits in episodic memory retrieval reveal impaired default mode network connectivity in amnestic mild cognitive impairment / C. J. Dunn. J. Dunn [et al.] // NeuroImage: Clinical. - 2014. - Vol. 4. - P. 473-480.

71. Edwards, G. A. Modifiable risk factors for Alzheimer's disease / G. A. A.

Edwards [et al.] // Frontiers in Aging Neuroscience. - 2019. - Vol. 11. - Article number: 146. - URL: https://doi.org/10.3389/fnagi.2019.00146

72. Edwards, G. A., 3rd Amyloid-beta and tau pathology following repetitive mild traumatic brain injury / G. A. Edwards, 3rd, I. Moreno-Gonzalez, C. Soto // Biochemical and Biophysical Research Communications. - 2017. - Vol. 483, № 4. - P. 1137-1142.

73. Egle, M. Prediction of dementia using diffusion tensor MRI measures: the OPTIMAL collaboration / M. Egle [et al.] // Journal of Neurology, Neurosurgery & Psychiatry. - 2022. - Vol. 93, № 1. - P. 14-23.

74. Emelin, A. Yu. cerebral perfusion in patients with Alzheimer's disease and mixed dementia / A. Yu. Emelin, V. Yu. Lobzin, K. M. Naumov [et al.] // Izvestia of the Russian Military Medical Academy. - 2020. - VOL. 39, NO. S3-2. - P. 70-73.

75. Emelin, A. Yu. Possibilities of diagnostics and treatment of cognitive impairment at non-demanding stages / A. Yu. Emelin // Neurology, neuropsychiatry, psychosomatics. - 2020. - Vol. 12, №. 5. - P. 70-73.

76. Enkirch, S. J. The ERICA score: an MR imaging-based visual scoring system for the assessment of entorhinal cortex atrophy in Alzheimer's disease / S. J. Enkirch [et al] // Radiology. J. Enkirch [et al.] // Radiology. - 2018. - Vol. 288, № 1. - P. 226-333.

77. Erickson, K. I. Exercise training increases size of hippocampus and improves memory / K. I. I. Erickson [et al.] // Proceedings of the National Academy of Sciences. - 2011. - Vol. 108, № 7. - P. 3017-3022.

78. Erkinjuntti, T.Do white matter changes on MRI and CT differentiate vascular dementia from Alzheimer's disease? / T. Erkinjuntti [et al.] // Journal of Neurology, Neurosurgery & Psychiatry. - 1987. - Vol. 50, №1. - P. 37-42.

79. Evans, T. E. Subregional volumes of the hippocampus in relation to cognitive function and risk of dementia / T. E. E. Evans [et al.] // Neuroimage. - 2018. - Vol. 178. - P. 129-135.

80. Ezzati, A. Differential association of left and right hippocampal volumes with verbal episodic and spatial memory in older adults / A. Ezzati [et al. Ezzati [et al.]

// Neuropsychologia. - 2016. - Vol. 93. - P. 380-385.

81. Fan, L. New insights into the pathogenesis of Alzheimer's disease / L. Fan [et al.] // Frontiers in neurology. - 2020. - Vol. 10. - Article number: 1312. - URL: https://doi.org/10.3389/fneur.2019.01312

82. Fazekas, F. Histopathologic analysis of foci of signal loss on gradient-echo T2*-weighted MR images in patients with spontaneous intracerebral hemorrhage: evidence of microangiopathy-related microbleeds / F. Fazekas. Fazekas [et al.] // American Journal of Neuroradiology. - 1999. - Vol. 20, № 4. - P. 637-642.

83. Fazekas, F. MR signal abnormalities at 1.5 T in Alzheimer's dementia and normal aging / F. Fazekas [et al.] // American Journal of Neuroradiology. - 1987. - Vol. 8, № 3. - P. 421-426.

84. Fazekas, F. Pathologic correlates of incidental MRI white matter signal hyperintensities / F. Fazekas [et al.] // Neurology. - 1993. - Vol. 43, № 9. - P. 1683-1683.

85. Fazekas, F. Pathophysiologic mechanisms in the development of age-related white matter changes of the brain / F. Fazekas, R. Schmidt, P. Scheltens // Dementia and Geriatric Cognitive Disorders. Fazekas, R. Schmidt, P. Scheltens // Dementia and Geriatric Cognitive Disorders. - 1998. - Vol. 9 (Suppl. 1). - P. 2-5.

86. Ferreira, S. T. The Aβ oligomer hypothesis for synapse failure and memory loss in Alzheimer's disease / S. T. T. Ferreira, W. L. Klein // Neurobiology of Learning and Memory. - 2011. - Vol. 96, № 4. - P. 529-543.

87. Fiford, C. M. White matter hyperintensities are associated with disproportionate progressive hippocampal atrophy / C. M. M. Fiford [et al.] // Hippocampus. - 2017. - Vol. 27, № 3. - P. 249-262.

88. Fokin, V. F. Resting neural networks in cognitive decline in patients with dyscirculatory encephalopathy / V. F. Fokin, N. M. Ponomareva, R. V. Konovalov [et al] // Annals of Clinical and Experimental Neurology. - 2020. - Vol. 14, № 4. - P. 39-45.

89. Folstein, M. F. "Mini-mental state": a practical method for grading the cognitive state of patients for the clinician / M. F. F. Folstein, S. E. Folstein, P. R. Mc Hugh // Journal of Psychiatric Research. - 1975. - Vol. 12, № 3. - P. 189-198.

90. Frisoni, G. B. Mild cognitive impairment with subcortical vascular features

/ G. B. Frisoni [et al] // Journal of Neurology. B.Frisoni [et al.] // Journal of Neurology. - 2002. - Vol. 249, № 10. - P. 1423-1432.

91. Frisoni, G. B. Structural imaging in the clinical diagnosis of Alzheimer's disease: problems and tools / G. B. Frisoni. B. Frisoni // Journal of Neurology, Neurosurgery & Psychiatry. - 2001. - Vol. 70, № 6. - P. 711-718.

92. Gaifutdinov, R.T. Cerebral microangiopathy (small vessel disease) and age-related hypogonadism in men / R.T. Gaifutdinov // Practical Medicine. - 2020. - Vol. 18, №. 6. - P. 176-181.

93. Gasparovic, C. 1H-MR spectroscopy metabolite levels correlate with executive function in vascular cognitive impairment / C. Gasparovic[et al.] // Journal of Neurology, Neurosurgery & Psychiatry. - 2013. - Vol. 84, № 7. - P. 715-721.

94. Gattringer, T. Vascular risk factors, white matter hyperintensities and hippocampal volume in normal elderly individuals / T.Gattringer [et al.] // Dementia and Geriatric Cognitive Disorders. - 2012. - Vol. 33, № 1. - P. 29-34.

95. Gauthier, S. World Alzheimer Report 2021: Journey through the diagnosis of dementia / S. Gauthier [et al. Gauthier [et al.]. - London, England: Alzheimer's Disease International, 2021. - 314 p.

96. Gertje, E. C. Association of Enlarged Perivascular Spaces and Measures of Small Vessel and Alzheimer Disease / E. C. Gertje [et al.] // Neurology. - 2021. - Vol. 96, № 2. - P. e193-e202.

97. Ghosh, S. Mild cognitive impairment: a brief review and suggested clinical algorithm / S. Ghosh, D. Libon, C. Lippa // American Journal of Alzheimer's Disease & Other Dementias. - 2014. - Vol. 29, № 4. - P. 293-302.

98. Giri, M. Genes associated with Alzheimer's disease: an overview and current status / M. Giri, M. Zhang, Y. Lü // Clinical Interventions in Aging. - 2016. - Vol. 11. - P. 665-681.

99. Gómez-Isla, T.Profound loss of layer II entorhinal cortex neurons occurs in very mild Alzheimer's disease / T.Gómez-Isla [et al.] // Journal of Neuroscience. - 1996. - Vol. 16, № 14. - P. 4491-4500.

100. Govindpani, K. Vascular dysfunction in Alzheimer's disease: a biomarker

of disease progression and a potential therapeutic target / K. Govindpani [et al. Govindpani [et al.] // Neural Regeneration Research. - 2020. - Vol. 15, № 6. - Article number: 1030. - URL: https://doi: 10.4103/1673-5374.270306

101. Greenberg, S. M. Cerebral microbleeds: a guide to detection and interpretation / S. M. Greenberg et al. M.Greenberg et al. // Lancet Neurology. - 2009. - Vol. 8, № 2. - P. 165-174.

102. Gridin, V. N. Automated analysis of quantitative characteristics of the hippocampus at magnetic resonance imaging of the brain for the diagnosis of possible Alzheimer's disease (literature review and the results of our own research) / V. N. Gridin, M. I. Trufanov, V. I. Solodovnikov [et al.] // Radiology-practice. - 2017. - № 6. - P. 41-59.

103. Grishina, D. A. Diagnosis and treatment of vascular cognitive impairment / D. A. Grishina, A. B. Lokshina // Medical Council. - 2021. - №. 2. - P. 39-48.

104. Guan, M. Generation of a homozygous ABCA7-knockout human iPSC line using the CRISPR/Cas9 system / M. Guan [et al. Guan [et al.] // Stem Cell Research. - 2023. - Vol. 66. - Article number: 103000. - URL: https://doi:10.1016/j.scr.2018.101378

105. Gulevskaya, T. S. Morphology and pathogenesis of white matter changes in chronic cerebrovascular pathology / T. S. Gulevskaya, P. L. Anufriev, M. M. Tanashyan // Annals of Clinical and Experimental Neurology. - 2022. - Vol. 16, №. 2. - P. 78-88.

106. Gulyaeva, N. V. Does the inability of CA1 area to respond to ischemia with early rapid adenosine release contribute to hippocampal vulnerability? An Editorial Highlight for "Spontaneous, transient adenosine release is not enhanced in the CA1 region of hippocampus during severe ischemia models / N. V. Gulyaeva. V. Gulyaeva // Journal of Neurochemistry. - 2021. - Vol. 159, № 5. - P. 800-803.

107. Hachinski, V. Vascular dementia: a radical redefinition / V. Hachinski // Dementia and Geriatric Cognitive Disorders. Hachinski // Dementia and Geriatric Cognitive Disorders. - 1994. - Vol. 5, № 3-4. - P. 130-132.

108. Hannawi, Y. Association of Vascular Properties with the Brain White Matter Hyperintensity in Middle Aged Population / Y. Hannawi [et al.] // Journal of the American Heart Association. - 2022. - Vol. 11, № 11. - P. 1-14.

109. Hanseeuw, B. J. Mild cognitive impairment: differential atrophy in the hippocampal subfields / B. J. Hanseeuw [et al] // American Journal of Neuroradiology. J. Hanseeuw [et al.] // American Journal of Neuroradiology. - 2011. - Vol. 32, № 9. - P. 1658-1661.

110. Hardy, J. Amyloid deposition as the central event in the aetiology of Alzheimer's disease / J. Hardy. Hardy, D. Allsop // Trends in Pharmacological Sciences. - 1991. - Vol. 12. - P. 383-388.

111. Hari, E. Volumetric changes within hippocampal subfields in Alzheimer's disease continuum / E. Hari [et al.] // Neurological Sciences. - 2022. - Vol. 14. - P. 4175-4183.

112. He, M. Relationships Between Memory Impairments and Hippocampal Structure in Patients With Subcortical Ischemic Vascular Disease / M. He et al. He et al. // Frontiers in Aging Neuroscience. - 2022. - Vol. 14. - Article number: 823535. - URL: https://doi.org/10.3389/fnagi.2022.823535

113. He, P. Structural Alteration of Medial Temporal Lobe Subfield in the Amnestic Mild Cognitive Impairment Stage of Alzheimer's Disease / P. He [et al.] // Neural plasticity. - 2022. - Vol. 2022. - Article ID 8461235. - URL: https://doi.org/10.3389/fnagi.2021.750154

114. Heneka, M. T.Neuroinflammation in Alzheimer's disease / M. T. Heneka [et al.] // Lancet Neurology. - 2015. - Vol. 14, № 4. - P. 388-405.

115. Herholz, K. Evaluation of a calibrated 18F-FDG PET score as a biomarker for progression in Alzheimer's disease and mild cognitive impairment / K. Herholz. Herholz [et al.] // Journal of Nuclear Medicine. - 2011. - Vol. 52, № 8. - P. 1218-1226.

116. Hilal, S. Enlarged perivascular spaces and cognition: a meta-analysis of 5 population-based studies / S. Hilal. Hilal [et al.] // Neurology. - 2018. - Vol. 91, № 9. - P. e832-e842.

117. Hotz, I.Performance of three freely available methods for extracting white matter hyperintensities: FreeSurfer, UBO Detector, and BIANCA / I.Hotz [et al.] //Human Brain Mapping. - 2022. - Vol. 43, № 5. - P. 1481-1500.

118. Huang, J. Diffusion tensor imaging of normal appearing white matter and

its correlation with cognitive functioning in mild cognitive impairment and Alzheimer's disease / J. Huang, A. P. Auchus // Annals of the New York Academy of Sciences. Huang, A. P. Auchus // Annals of the New York Academy of Sciences. - 2007. - Vol. 1097, № 1. - P. 259-264.

119. Huang, Y. Differential associations of visual memory with hippocampal subfields in subjective cognitive decline and amnestic mild cognitive impairment / Y. Huang [et al.] // BMC Geriatrics. - 2022. - Vol. 22, № 1. - Article number: 153. - URL: https://doi:10.1186/s12877-022-02853-7

120. Iadecola, C. Cerebrovascular alterations in Alzheimer's disease: incidental or pathogenic? / C. Iadecola, R. F. Gottesman // Circulation Research. - 2018. - Vol. 123, № 4. - P. 406-408.

121. International Statistical Classification of Diseases and Related Health Problems; 10th revision: ICD-10. / ed. V.K. Ovcharov, M.V. Maksimova [Transl. from English by M. Maksimova, S. Chemyakina, L. Safronova]. - Moscow: Medicine, 1995. - T.1.(1). - 698 c.

122. Izzo, J. The association between hippocampal subfield volumes in mild cognitive impairment and conversion to Alzheimer's disease / J. Izzo. Izzo [et al.] //Brain Research. - 2020. - Vol. 1728. - Article number: 146591.- URL: https://doi: 10.1016/j.brainres.2019.146591

123. Jack, C. R. Tracking pathophysiological processes in Alzheimer's disease: an updated hypothetical model of dynamic biomarkers / C. R. R. Jack [et al.] // Lancet Neurology. - 2013. - Vol. 12, № 2. - P. 207-216.

124. Jack, C. R., Jr. Introduction to the recommendations from the National Institute on Aging Alzheimer's Association workgroups on diagnostic guidelines for Alzheimer's disease / C. R. Jack Jr. [et al.] // Alzheimer's & Dementia. - 2011. - Vol. 7, № 3. - P. 257-262.

125. Jack, C. R., Jr. NIA-AA research framework: toward a biological definition of Alzheimer's disease / C. R., Jr. R. Jack Jr. [et al.] // Alzheimer's & Dementia. - 2018. - Vol. 14, № 4. - P. 535-562.

126. Jansen, W. J. Prevalence of cerebral amyloid pathology in persons without dementia: a meta-analysis / W. J. Jansen [et al. J. Jansen [et al.] // Jama. - 2015. - Vol. 313, № 19. - P. 1924-1938.

127. Jessen, F. Volume reduction of the entorhinal cortex in subjective memory impairment / F. Jessen [et al.] // Neurobiology of Aging. - 2006. - Vol. 27, № 12. - P. 1751-1756.

128. Jiang, J. The association of regional white matter lesions with cognition in a community-based cohort of older individuals / J. Jiang. Jiang [et al.] // NeuroImage: Clinical. - 2018. - Vol. 19. - P. 14-21.

129. Jicha, G. A. Hippocampal sclerosis, argyrophilic grain disease, and primary age-related tauopathy / G. A. A. Jicha, P. T. Nelson // CONTINUUM: Lifelong Learning in Neurology. - 2019. - Vol. 25, № 1. - P. 208-233.

130. Jimenez-Conde J. Hyperlipidemia and reduced white matter hyperintensity volume in patients with ischemic stroke / J. Jimenez-Conde [et al. Jimenez-Conde [et al.] //Stroke. - 2010. - Vol. 41, №3. - P. 437-442.

131. Johansen, M. C. Association of coronary artery atherosclerosis with brain white matter hyperintensity / M. C. Johansen [et al.] // Stroke. - 2021. - Vol. 52, № 8. - P. 2594-2600.

132. Johnson, A. C. Hippocampal Vascular Supply and Its Role in Vascular Cognitive Impairment / A. C. Johnson // Stroke. - 2023. - Vol. 54, № 3. - P. 673-685.

133. Johnson, K. A. Brain imaging in Alzheimer's disease / K. A. A. Johnson [et al.] // Cold Spring Harbor Perspectives in Medicine. - 2012. - Vol. 2, № 4. - Article number: a006213. - URL: https://doi: 10.1101/cshperspect.a006213.

134. Kalashnikova, L. A. Actual problems of brain pathology in cerebral microangiopathy / L. A. Kalashnikova, T. S. Gulevskaya, L. A. Dobrynina // S. S. Korsakov Journal of Neurology and Psychiatry. - 2018. - Vol. 118, № 2. - P. 90-99.

135. Kametani, F. Reconsideration of amyloid hypothesis and tau hypothesis in Alzheimer's disease / F. Kametani, M. Hasegawa // Frontiers in Neuroscience. Kametani, M. Hasegawa // Frontiers in Neuroscience. - 2018. - Vol. 12. - P. 25-36.

136. Kamyshanskaya, I. G. Differential diagnosis of CNS lesions of infectious etiology in neurosurgical practice (Clinical observations) / I. G. Kamyshanskaya, V. M. Cheremisin, M. Yu. Podgornyak [et al] // Russian Neurosurgical Journal named after Professor A. L. Polenov. - 2021. - Vol. 13, № 3. - P. 46-51.

137. Kang, G. Progressive Volume Atrophy in Hippocampal Subfields and the Correlation with Cognition in Alzheimer's Disease and Mild Cognitive Impairment / G. Kang [et al.] // Research Square. - 2021. - URL: https://doi: 0.21203/rs.3.rs-304948/v1.

138. Khan, U. A. Molecular drivers and cortical spread of lateral entorhinal cortex dysfunction in preclinical Alzheimer's disease / U. A. Khan. A. Khan [et al.] // Nature Neuroscience. - 2014. - Vol. 17, № 2. - P. 304-311.

139. Khan, W. Automated hippocampal subfield measures as predictors of conversion from mild cognitive impairment to Alzheimer's disease in two independent cohorts / W. Khan [et al. Khan [et al.] // Brain Topography. - 2015. - Vol. 28, № 5. - P. 746-759.

140. Killiany, R. J. MRI measures of entorhinal cortex vs hippocampus in preclinical AD / R. J. Killiany et al. // Neurology. - 2002. - Vol. 58, № 8. - P. 1188-1196.

141. Kim, G. H. Hippocampal volume and shape in pure subcortical vascular dementia / G. H. Kim [et al. H. Kim [et al.] // Neurobiology of Aging. - 2015. - Vol. 36, № 1. - P. 485-491.

142. Kim, J. S. Role of blood lipid levels and lipid-lowering therapy in stroke patients with different levels of cerebral artery disease: reconsidering recent stroke guidelines / J. S. Kim. S. Kim // Journal of Stroke. - 2021. - Vol. 23, № 2. - P. 149-161.

143. Koberskaya, N. N. Modern concept of cognitive reserve / N. N. Koberskaya, G. R. Tabeeva // Neurology, neuropsychiatry, psychosomatics. - 2019. - Vol. 11, №. 1. - P. 96-102.

144. Koberskaya, N. N. N. Dodement cognitive impairment / N. N. Koberskaya, E. A. Mkhitaryan, A. B. Lokshina, D. A. Grishina // Russian Journal of Geriatric Medicine. - 2022. - № 1. - P. 48-57.

145. Koepsell, T. D. Reversion from mild cognitive impairment to normal or near-normal cognition: risk factors and prognosis / T. D. D. Koepsell, S. E. Monsell //

Neurology. - 2012. - Vol. 79, № 15. - P. 1591-1598.

146. Kondakova, A.K. Possibilities of nuclear medicine in the diagnosis of dementia / A.K. Kondakova, I.A. Znamensky, D.Y. Mosin [et al.] // Bulletin of the Russian State Medical University. - 2016. - № 4. - P. 43-47.

147. Kril, J. J. Patients with vascular dementia due to microvascular pathology have significant hippocampal neuronal loss / J. J. Kril. J. Kril [et al.] // Journal of Neurology, Neurosurgery & Psychiatry. - 2002. - Vol. 72, № 6. - P. 747-751.

148. Kukull, W. A Dementia and Alzheimer disease incidence: a prospective cohort study / W. A Kukull [et al. A Kukull [et al.] // Archives of Neurology. - 2002. - Vol. 59, № 11. - P. 1737-1746.

149. Kurbanova, M. M. Modern methods of diagnostics of cognitive impairment / M. M. Kurbanova, A. A. Galaeva, E. V. Stefanovskaya [et al.] // Russian Family Doctor. - 2020. - Vol. 24, № 1. - P. 35-44.

150. Kwak, K. Differential Role for hippocampal subfields in Alzheimer's disease progression revealed with deep learning / K. Kwak [et al. Kwak [et al.] // Cerebral Cortex. - 2022. - Vol. 32, № 3. - P. 467-478

151. Lambert, J. C. Meta-analysis of 74,046 individuals identifies 11 new susceptibility loci for Alzheimer's disease / J. C. Lambert [et al.] // Nature Genetics. - 2013. - Vol. 45, № 12. - P. 1452-1458.

152. Lee, M. J. Synergistic effects of ischemia and β-amyloid burden on cognitive decline in patients with subcortical vascular mild cognitive impairment / M. J. J. Lee [et al.] // JAMA Psychiatry. - 2014. - Vol. 71, № 4. - P. 412-422.

153. Leritz, E. C. Associations between T1 white matter lesion volume and regional white matter microstructure in aging / E. C. Leritz [et al.] // Human Brain Mapping. - 2014. - Vol. 35, № 3. - P. 1085-1100.

154. Levashkina, I. M. Possibilities of high-field magnetic resonance imaging in the assessment of degenerative changes in the brain in the liquidators of the Chernobyl NPP accident consequences in the remote period / I. M. Levashkina, S. V. Serebryakova // Medico-biological and socio-psychological problems of safety in emergency

situations. - 2016. - №. 4. - P. 98-103.

155. Levin, O. S. Dyscirculatory encephalopathy: anachronism or clinical reality? / O. S. Levin // Modern therapy in psychiatry and neurology. - 2012. - № 3. - P. 40-46.

156. Levin, O. S. The concept of transient cognitive syndrome in the structure of cognitive impairment in elderly persons: approaches to diagnosis and treatment / O. S. Levin, A. Sh. Chimagomedova // Modern therapy in psychiatry and neurology. - 2022. - № 1-2. - P. 25-33.

157. Levin, O.S. Diagnosis and treatment of dementia in clinical practice / O.S. Levin. - Moscow: MEDpress-Inform, 2010. - 255 c.

158. Levin, O.S. Dyscirculatory encephalopathy: modern ideas about the mechanisms of development and treatment / O.S. Levin // Consilium medicum. - 2006. - Vol. 8, № 8. - P. 72-79.

159. Levin, O.S. Moderate cognitive disorder: diagnosis and treatment / O.S. Levin // Effective Pharmacotherapy. - 2012. - №. 5. - P. 14-21.

160. Li X. Hippocampal subfield volumetry in patients with subcortical vascular mild cognitive impairment / X. Li [et al.] // Scientific Reports. - 2016. - Vol. 6, № 1. - URL: https://doi.org/10.3389/fnbeh.2019.00259

161. Li, X. Link between type 2 diabetes and Alzheimer's disease: from epidemiology to mechanism and treatment / X. Li, D. Song, S. X. Leng // Clinical Interventions in Aging. - 2015. - Vol. 10. - P. 549-560.

162. Lin, Q. Incidence and risk factors of leukoaraiosis from 4683 hospitalised patients: a cross-sectional study / Q. Lin [et al.] //Medicine (Baltimore). - 2017. - Vol. 96 (39). - Article number: e7682.- URL: https://doi: 10.1097/MD.0000000000007682.

163. Litvinenko, I. V. Neuroimaging methods of diagnostics of Alzheimer's disease and cerebrovascular diseases accompanied by cognitive impairment / I. V. Litvinenko, A. Yu. Emelin, V. Yu. Lobzin, L. A. Kolmakova // Neurology, Neuropsychiatry, Psychosomatics. - 2019. - No. 11 (Supplement 3). - P. 18-25.

164. Livingston, G. Dementia prevention, intervention, and care: 2020 report of

the Lancet Commission / G. Livingston [et al. Livingston [et al.] // Lancet. - 2020. - Vol. 396. - P. 413-446.

165. Lobzin, V. Yu. A new look at the pathogenesis of Alzheimer's disease: modern ideas about amyloid clearance / V. Yu. Lobzin, K. A. Kolmakova, A. Yu. Emelin // V.M. Bekhterev Review of Psychiatry and Medical Psychology. - 2018. - № 2. - P. 22-28 .

166. Lokshina, A. B. Heterogeneity of the syndrome of mild cognitive impairment (analysis of the work of a specialised outpatient reception) / A. B. Lokshina, V. V. Zakharov, D. A. Grishina [et al] // Neurology, neuropsychiatry, psychosomatics. - 2021. - Vol. 13, № 3. - P. 34-41 .

167. Lokshina, A. B. Modern aspects of diagnosis and treatment of the syndrome of mild cognitive impairment / A. B. Lokshina // Russian Journal of Geriatric Medicine. - 2020. - № 3. - P. 199-204.

168. Long, J. M. Reelin in the years: decline in the number of reelin immunoreactive neurons in layer II of the entorhinal cortex in aged monkeys with memory impairment / J. M. M. Long [et al.] // Neurobiology of Aging. - 2020. - Vol. 87. - P. 132-137.

169. Loreto, F. Visual atrophy rating scales and amyloid PET status in an Alzheimer's disease clinical cohort / F. Loreto [et al.] // Annals of Clinical and Translational Neurology. - 2023. - Vol. 10, № 4. - P. 619-631.

170. Lupanov, I. A. Application of positron emission tomography in early diagnosis of Alzheimer's disease and vascular cognitive impairment / I. A. Lupanov // Bulletin of the Russian Military Medical Academy. - 2014. - № 1 (45). - P. 40-45.

171. Lyu, H. Structural and functional disruptions in subcortical vascular mild cognitive impairment with and without depressive symptoms / H. Lyu [et al.] // Frontiers in Aging Neuroscience. - 2019. - Vol. 11. - Article number: 241. - URL: https://doi.org/10.3389/fnagi.2019.00241

172. Magalhães, T. N. C. Whole-brain DTI parameters associated with tau protein and hippocampal volume in Alzheimer's disease / T. N. N. C. Magalhães [et al.]

// Brain and Behaviour. - 2023. - Vol. 13, No. 2 - Article number: e2863.- URL: https://doi: 10.1002/brb3.2863

173. Magid-Bernstein, J.Cerebral hemorrhage: pathophysiology, treatment, and future directions / J.Magid-Bernstein [et al.] // Circulation Research. - 2022. - Vol. 130, № 8. - P. 1204-1229.

174. Maksimova, M. Yu. Cognitive impairment and dementia of vascular genesis / M. Yu. Maksimova, M. A. Piradov // Russian Medical Journal. - 2017. - Vol. 25, №. 14. - P. 1000-1004.

175. Malashenkova, I. K. Polymorphism of the AroE gene: the impact of the ApoE4 allele on systemic inflammation and its role in the pathogenesis of Alzheimer's disease / I. K. Malashenkova, S. A. Krynskiy, M. V. Mamoshina, N. A. Didkovskiy // Medical Immunology. - 2018. - Vol. 20, № 3. - P. 303-312.

176. Malykhin, N. Differential vulnerability of hippocampal subfields and anteroposterior hippocampal subregions in healthy cognitive aging / N. Malykhin [et al. Malykhin [et al.] // Neurobiology of Aging. - 2017. - Vol. 59. - P. 121-134.

177. Maxwell, S. P. Neuropathology and cholinesterase expression in the brains of octogenarians and older / S. P. Maxwell, M. K. Cash, S. Darvesh // Chemico-Biological Interactions. P. Maxwell, M. K. Cash, S. Darvesh // Chemico-Biological Interactions. - 2022. - Vol. 364. - Article number: 110065.URL: https://doi: 10.1016/j.cbi.2022.110065

178. McDonald, C. R. Regional rates of neocortical atrophy from normal aging to early Alzheimer's disease / C. R. R. McDonald [et al.] // Neurology. - 2009. - Vol. 73, № 6. - P. 457-465.

179. McKhann, G. Clinical diagnosis of Alzheimer's disease: Report of the NINCDS-ADRDA Work Group under the auspices of the Department of Health and Human Services Task Force on Alzheimer's Disease. McKhann [et al.] // Neurology. - 1984. - Vol. 34, № 7. - P. 939-944.

180. Mills, S. Biomarkers of cerebrovascular disease in dementia / S. Mills [et al.] // The British Journal of Radiology. - 2007. - Vol. 80 (special issue 2). - P. 128-145.

181. Mok, V. C. T. Early-onset and delayed-onset poststroke dementia-revisiting the mechanisms / V. C. T. Mok [et al.] // Nature Reviews Neurology. - 2017. - Vol. 13, № 3. - P. 148-159.

182. Morris, M. C. MIND diet associated with reduced incidence of Alzheimer's disease / M. C. Morris [et al.] // Alzheimer's & Dementia. - 2015. - Vol. 11, № 9. - P. 1007-1014.

183. Mosconi, L. Multicenter standardised 18F-FDG PET diagnosis of mild cognitive impairment, Alzheimer's disease, and other dementias / L. Mosconi. Mosconi [et al.] // Journal of Nuclear Medicine. - 2008. - Vol. 49, № 3. - P. 390-398.

184. Mrdjen, D. The basis of cellular and regional vulnerability in Alzheimer's disease / D. Mrdjen [et al.] //Acta Neuropathologica. - 2019. - Vol.138, no. 5. - P. 729-749.

185. Mueller, S. G. Evidence for functional specialisation of hippocampal subfields detected by MR subfield volumetry on high resolution images at 4 T / S. G. Mueller. G. Mueller [et al.] // Neuroimage. - 2011. - Vol. 56, № 3. - P. 851-857

186. Nassif, C. Integrity of Neuronal Size in the Entorhinal Cortex Is a Biological Substrate of Exceptional Cognitive Aging. Nassif [et al.] // Journal of Neuroscience. - 2022. - Vol. 42, № 45. - P. 8587-8594.

187. Neznanov, N. G. Neuroimaging of the hippocampus: role in the diagnosis of Alzheimer's disease at an early stage / N. G. Neznanov, N. I. Ananyeva, N. M. Zalutskaya [et al] // V. M. Bekhterev Review of Psychiatry and Medical Psychology. - 2018. - № 4. - P. 3-11.

188. Niazi, M. Quantitative MRI of perivascular spaces at 3T for early diagnosis of mild cognitive impairment / M. Niazi [et al.] // American Journal of Neuroradiology. - 2018. - Vol. 39, № 9. - P. 1622-1628.

189. Nishio, K. A mouse model characterising features of vascular dementia with hippocampal atrophy / K. Nishio [et al.] // Stroke. - 2010. - Vol. 41, № 6. - P. 1278-1284.

190. Nosheny, R. L. Variables associated with hippocampal atrophy rate in normal aging and mild cognitive impairment / R. L. Nosheny. L. Nosheny [et al.] //

Neurobiology of Aging. - 2015. - Vol. 36, № 1. - P. 273-282.

191. O'Brien, J. T. Vascular cognitive impairment / J. T. T. O'Brien [et al.] // Lancet Neurology. - 2003. - Vol. 2, № 2. - P. 89-98.

192. Odinak, M. M. Modern possibilities of neuroimaging in differential diagnosis of cognitive impairment / M. M. Odinak, A. Yu. Emelin, V. Yu. Lobzin [et al] // Neurology, Neuropsychiatry, Psychosomatics. - 2012. - № S2. - P. 51-55.

193. Oldan, J. D. Complete evaluation of dementia: PET and MRI Correlation and diagnosis for the neuroradiologist / J. D. D. Oldan [et al.] // American Journal of Neuroradiology. - 2021. - Vol. 42, № 6. - P. 998-1007.

194. Olsson, E. White matter lesion assessment in patients with cognitive impairment and healthy controls: reliability comparisons between visual rating, a manual, and an automatic volumetrical MRI method - the gothenburg MCI study / E. Olsson [et al] // Journal of Aging Research. Olsson [et al.] // Journal of Aging Research. - 2013. - Vol. 2013 -Article number: 19847. - URL: https://doi.org/10.1155/2013/198471

195. Oltra-Cucarella, J.Visual memory tests enhance the identification of amnestic MCI cases at greater risk of Alzheimer's disease / J. Oltra-Cucarella [et al.] // International Psychogeriatrics. - 2019. - Vol. 31, № 7. - P. 997-1006.

196. Ono, S. E. Mesial temporal lobe epilepsy: Revisiting the relation of hippocampal volumetry with memory deficits / S. E. E. Ono [et al.] // Epilepsy & Behaviour. - 2019. - Vol. 100. - Article number:106516.- URL: https://doi: 10.1016/j.yebeh.2019.106516

197. Palomero-Gallagher, N. Multimodal mapping and analysis of the cyto-and receptorarchitecture of the human hippocampus / N.Palomero-Gallagher [et al.] // Brain Structure and Function. - 2020. - Vol. 225, № 3. - P. 881-907.

198. Park, H. Y. Diagnostic performance of hippocampal volumetry in Alzheimer's disease or mild cognitive impairment: a meta-analysis / H. Y. Park [et al.] // European Radiology. - 2022. - Vol. 32, № 10. - P. 6979-6991.

199. Petersen, R. C. Mild cognitive impairment as a clinical entity and treatment target / R. C. Petersen, J. C. Morris // Archives of Neurology. - 2005. - Vol. 62, № 7. - P.

1160-1163.

200. Petersen, R. C. Mild cognitive impairment as a diagnostic entity / R. C. Petersen // Journal of Internal Medicine. - 2004. - Vol. 256, № 3. - P. 183-194.

201. Petersen, R. C. Mild cognitive impairment: clinical characterisation and outcome / R. C. Petersen [et al.] // Archives of Neurology. - 1999. - Vol. 56, № 3. - P. 303-308.

202. Petersen, R. C. Practice guideline update summary: Mild cognitive impairment: Report of the Guideline Development, Dissemination, and Implementation Subcommittee of the American Academy of Neurology / R. C. Petersen. C. Petersen [et al.] // Neurology. - 2018. - Vol. 90, № 3. - P. 126-135.

203. Petersen, R. Consensus on mild cognitive impairment: EADC-ADCS / R. Petersen, J. Touchon // Research and Practice in Alzheimer's disease. Petersen, J. Touchon // Research and Practice in Alzheimer's disease. - 2005. - Vol. 10. - P. 38-46.

204. Pin, G Distinct hippocampal subfields atrophy in older people with vascular brain injuries / G. Pin [et al.] // Stroke. - 2021. - Vol. 52, № 5. - P. 1741-1750.

205. Poirier, J. Cerebral lacunae. A proposed new classification / J. Poirier, C. Derouesne // Clinical Neuropathology. - 1984. - Vol. 3, № 6. - P. 266-268.

206. Poirier, J. The concept of cerebral lacunae from 1838 to the present / J. Poirier, C. Derouesne // Revue Neurologique. Poirier, C. Derouesne // Revue Neurologique. - 1985. - Vol. 141, № 1. - P. 3-17.

207. Popuri, K. Using machine learning to quantify structural MRI neurodegeneration patterns of Alzheimer's disease into dementia score: Independent validation on 8,834 images from ADNI, AIBL, OASIS, and MIRIAD databases / K. Popuri. Popuri [et al.] // Human Brain Mapping. - 2020. - Vol. 41, №14. - P. 4127-4147.

208. Pozdnyakov, A. V. Role of functional MRI in mapping of sensory olfactory brain areas in volunteers at different odorant supply / A. V. Pozdnyakov, V. A. Novikov, V. V. Grebenyuk [et al.] // Visualisation in Medicine. - 2020. - Vol. 2, № 1. - P. 40-47.

209. Price, C. C. Subcortical vascular dementia: integrating neuropsychological and neuroradiological data / C. C. C. Price [et al.] // Neurology. - 2005. - Vol. 65, № 3. -

P. 376-382.

210. Prins, N. D. Measuring progression of cerebral white matter lesions on MRI: visual rating and volumetrics / N. D.. D. Prins [et al.] // Neurology. - 2004. - Vol. 62, № 9. - P. 1533-1539.

211. Pronin, I. N Diffusion tensor magnetic resonance imaging and tractography / I. N. Pronin, L. M. Fadeeva, N. E. Zakharova [et al.] // Annals of clinical and experimental neurology. - 2008. - Vol. 2, № 1. - P. 32-40.

212. Qiu, Y. Loss of integrity of corpus callosum white matter hyperintensity penumbra predicts cognitive decline in patients with subcortical vascular mild cognitive impairment / Y.Qiu [et al.] // Frontiers in Aging Neuroscience. - 2021. - Vol. 13. - Article number: 605900.

213. Rao, Y. L. Hippocampus and its involvement in Alzheimer's disease: a review / Y. L. Rao [et al. L. Rao [et al.] // 3 Biotech. - 2022. - Vol. 12, № 2. - Article number: 55

214. Rasmussen, M. K. The glymphatic pathway in neurological disorders / M. K. K. Rasmussen, H. Mestre, M. Nedergaard // Lancet Neurology. - 2018. - Vol. 17, № 11. - P. 1016-1024

215. Riphagen, J. M. Shades of white: diffusion properties of T1-and FLAIR-defined white matter signal abnormalities differ in stages from cognitively normal to dementia / J. M. Riphagen [et al] // Neurobiology of Aging. M. Riphagen [et al.] // Neurobiology of Aging. - 2018. - Vol. 68. - P. 48-58.

216. Rizvi, B. Posterior white matter hyperintensities are associated with reduced medial temporal lobe subregional integrity and long-term memory in older adults / B. Rizvi [et al. Rizvi [et al.] // NeuroImage: Clinical. - 2023. - Vol. 37. - Article number: 103308. - URL: https://doi: 10.1016/j.nicl.2022.103308

217. Rizzi, L. Global epidemiology of dementia: Alzheimer's and vascular types / L. Rizzi, I. Rosset, M. Roriz-Cruz // BioMed Research International. - 2014. - Vol. 2014. - Article ID 908915. - URL: https://doi: 10.1155/2014/908915

218. Roberge, X. Specificity of Entorhinal Atrophy MRI Scale in Predicting Alzheimer's Disease Conversion / X. Roberge. Roberge [et al.] // Canadian Journal of

Neurological Sciences. - 2023. - Vol. 50, № 1. - P. 112-114.

219. Roberts, R. Classification and epidemiology of MCI / R. Roberts, D. S. Knopman // Clinics in Geriatric Medicine. Roberts, D. S. Knopman // Clinics in Geriatric Medicine. - 2013. - Vol. 29, № 4. - P. 753-772.

220. Román, G. C. Vascular dementia: diagnostic criteria for research studies: report of the NINDS-AIREN International Workshop / G. C. Román. C. Román [et al.] // Neurology. - 1993. - Vol. 43, № 2. - P. 250-260.

221. Rostrup, E. The spatial distribution of age-related white matter changes as a function of vascular risk factors - results from the LADIS study. Rostrup [et al.] // Neuroimage. - 2012. - Vol. 60, № 3. - P. 1597-1607.

222. Ryu, J. C. Consequences of metabolic disruption in Alzheimer's disease pathology / J. C. Ryu [et al.] // Neurotherapeutics. - 2019. - Vol. 16, № 3. - P. 600-610.

223. Sachdev, P. Diagnostic criteria for vascular cognitive impairment: a VASCOG statement / P. Sachdev [et al.] // Alzheimer Disease and Associated Disorders. - 2014. - Vol. 28, № 3. - P. 206-218.

224. Sawada, M. Mapping effective connectivity of human amygdala subdivisions with intracranial stimulation / M. Sawada [et al.] // Nature Communications. - 2022. - Vol. 13, № 1. - Article number: 4909. - URL: https://doi: 10.1038/s41467-022-32644-y.

225. Scahill, R. I. Mapping the evolution of regional atrophy in Alzheimer's disease: unbiased analysis of fluid-registered serial MRI / R. I. I. Scahill [et al.] // Proceedings of the National Academy of Sciences. - 2002. - Vol. 99, № 7. - P. 4703-4707.

226. Scarmeas, N. Multimodal dementia prevention - does trial design mask efficacy? / N. Scarmeas. Scarmeas // Nature Reviews Neurology. - 2017. - Vol. 13, № 6. - P. 322-323.

227. Scheltens, P. Atrophy of medial temporal lobes on MRI in" probable" Alzheimer's disease and normal ageing: diagnostic value and neuropsychological correlates / P. Scheltens [et al.] // Journal of Neurology, Neurosurgery & Psychiatry. - 1992. - Vol. 55, № 10. - P. 967-972.

228. Scher, A. I. Hippocampal morphometry in population-based incident Alzheimer's disease and vascular dementia: the HAAS / A. I. I. Scher [et al.] // Journal of Neurology, Neurosurgery & Psychiatry. - 2011. - Vol. 82, № 4. - P. 373-377.

229. Schönheit, B. Spatial and temporal relationships between plaques and tangles in Alzheimer-pathology / B. Schönheit, R. Zarski, T. G. Ohm // Neurobiology of Aging. Schönheit, R. Zarski, T. G. Ohm // Neurobiology of Aging. - 2004. - Vol. 25, № 6. - P. 697-711.

230. Schuff, N. MRI of hippocampal volume loss in early Alzheimer's disease in relation to ApoE genotype and biomarkers / N. Schuff [et al.] // Brain. - 2009. - Vol. 132, № 4. - P. 1067-1077.

231. Schultz, C. Anatomy of the hippocampal formation / C. Schultz, M. Engelhardt // The Hippocampus in Clinical Neuroscience. - 2014. - Vol. 34. - P. 6-17.

232. Shang, Q. Prediction of Early Alzheimer Disease by Hippocampal Volume Changes under Machine Learning Algorithm / Q. Shang [et al.] // Computational and Mathematical Methods in Medicine. - 2022. - Vol. 2022. - Article ID 3144035. - URL: https://doi.org/10.1155/2022/3144035

233. Shing, L. Hippocampal subfield volumes: age, vascular risk, and correlation with associative memory / Y. L. Shing [et al.] // Frontiers in Aging Meuroscience. - 2011. - Vol. 3. - URL: https://doi: 10.3389/fnagi.2011.00002

234. Skrobot, O. A. Progress towards standardised diagnosis of vascular cognitive impairment: Guidelines from the Vascular Impairment of Cognition Classification Consensus Study / O. A. A. Skrobot [et al.] // Alzheimer's & Dementia. - 2018. - Vol. 14, № 3. - P. 280-292.

235. Smith, E. E. Correlations between MRI white matter lesion location and executive function and episodic memory / E. E. E. E. Smith [et al.] // Neurology. - 2011. - Vol. 76, № 17. - P. 1492-1499.

236. Spano, M. Brain PET Imaging: Approach to Cognitive Impairment and Dementia / M. Spano [et al.] // PET Clinics. - 2023. - Vol. 18, № 1. - P. 103-113.

237. Sperling, R. A. Toward defining the preclinical stages of Alzheimer's disease: Recommendations from the National Institute on Aging-Alzheimer's

Association workgroups on diagnostic guidelines for Alzheimer's disease / R. A. A. Sperling [et al.] // Alzheimer's & Dementia. - 2011. - Vol. 7, № 3. - P. 280-292.

238. Stulov, I. K. Method of differential diagnosis of mild cognitive impairment of different genesis using MRI morphometry / I. K. Stulov, N. I. Ananyeva, L. R. Lukina [et al] // Radiation diagnostics and therapy. - 2023. - Vol. 14, № 1S. - P. 40-41.

239. Stulov, I. K. Method of differential diagnosis of mild cognitive impairment of different genesis: cross-sectional study / I. K. Stulov, N. I. Ananyeva, L. R. Lukina [et al] // Radiation diagnostics and therapy. - 2023. - Vol. 14, № 2. - P. 64-73.

240. Stulov, I. K. Morphometry of hippocampal subfields in patients with amnestic type of mild cognitive impairment and subcortical vascular mild cognitive impairment / I. K. Stulov, N. I. Ananyeva, N. M. Zalutskaya, L. V. Lukina // Radiation diagnostics and therapy. - 2022. - Vol. 13, №. 1S. - P. 34-35.

241. Stulov, I. K. Neuroimaging of cerebral small vessel disease in mild cognitive impairment in the elderly / I. K. Stulov, N. A. Gomzyakova, J. D. Plusnina [et al] // Uspekhi gerontologii. - 2023. - Vol. 36, № 1. - P. 89-97.

242. Stulov, I. K. Possibilites of differential diagnostics of mild cognitive impairments of various origins using magnetic resonance morphometry subfields of the hippocampal formation / I. K.. K. Stulov, N. I. Ananyeva, N. A. Gomzyakova [et al.] // Materials of the Foreign International Scientific Conference "Science in the Era of Challenges and Global Changes". - Caracas (Venezuela): HNRI "National development", 2023. - P. 30-33.

243. Stulov, I. K. The role of atrophic changes in the subfields of the hippocampal formation in the reduction of indicators of different types of memory in patients with amnestic type of mild cognitive impairment and subcortical vascular mild cognitive impairment / I. K. Stulov. K. Stulov, N. I. Ananyeva, N. M. Zalutskaya [et al] // Actual issues of pharmacotherapy and psychotherapy of psychiatric disorders: a collection of conference abstracts, St. Petersburg, 21 December 2022 - St. Petersburg. : V.M. Bekhterev NMIC PN, 2022. - P. 63-64.

244. Stulov, I. K. The role of MR-morphometry of hippocampal subfields in the

diagnosis of mild cognitive impairment of different genesis / I. K. Stulov, N. I. Ananyeva, L. V. Lukina, N. M. Zalutskaya // Russian Neurosurgical Journal named after Professor A. L. Polenov. - 2022. - Vol. 14, № 2. - P. 153-159.

245. Sun, P. Mapping the patterns of cortical thickness in single and multiple-domain amnestic mild cognitive impairment patients: a pilot study / P.Sun [et al.] //Aging (Albany NY). - 2019. - Vol. 11, № 22. - P. 10000-10015.

246. Sun, Y. Hippocampal subfield alterations in schizophrenia and major depressive disorder: a systematic review and network meta-analysis of anatomic MRI studies / Y. Sun [et al. Sun [et al.] // Journal of Psychiatry and Neuroscience. - 2023. - Vol. 48, № 1. - P. E34-E49.

247. Sunderland, T. Clock drawing in Alzheimer's disease: a novel measure of dementia severity / T. Sunderland [et al.] // Journal of the American Geriatrics Society. - 1989. - Vol. 37, № 8. - P. 725-729.

248. Świetlik, D. Application of artificial neural networks to identify alzheimer's disease using cerebral perfusion SPECT data / D. Świetlik, J. Białowąs // International Journal of Environmental Research and Public Health. - 2019. - Vol. 16, № 7. - Article number: 1303. - URL: https://doi: 10.3390/ijerph16071303.

249. Tang, Y. P. Genetic studies in Alzheimer's disease / Y. P. Tang, E. S. Gershon // Dialogues in Clinical Neuroscience. P. Tang, E. S. Gershon // Dialogues in Clinical Neuroscience. - 2003. - Vol. 5, № 1. - P. 17-26.

250. Tanzi, R. E. The genetics of Alzheimer's disease / R. E. E. Tanzi // Cold Spring Harbor perspectives in medicine. - 2012. - Vol. 2, № 10. - Article number: a006296. - URL: https://doi: 10.1101/cshperspect.a006296.

251. Tardif, C. L. Regionally specific changes in the hippocampal circuitry accompany progression of cerebrospinal fluid biomarkers in preclinical Alzheimer's disease / C. L. L. Tardif [et al.] // Human Brain Mapping. - 2018 - Vol. 39, № 2. - P. 971-984.

252. ten Brinke, L. F. Aerobic exercise increases hippocampal volume in older women with probable mild cognitive impairment: a 6-month randomised controlled trial

/ L. F. ten Brinke [et al] // British Journal of Sports Medicine. F. ten Brinke [et al.] // British Journal of Sports Medicine. - 2015. - Vol. 49, №4. - P. 248-254.

253. Thyreau, B. Higher-resolution quantification of white matter hypointensities by large-scale transfer learning from 2D images on the JPSC-AD cohort / B. Thyreau [et al.] // Human Brain Mapping. - 2022. - Vol. 43, № 13. - P. 3998-4012.

254. Tran, T. T. Lateral entorhinal cortex dysfunction in amnestic mild cognitive impairment / T. T. T. Tran [et al.] // Neurobiology of Aging. - 2022. - Vol. 112. - P. 151-160.

255. Traschütz, A. The entorhinal cortex atrophy score is diagnostic and prognostic in mild cognitive impairment / A. Traschütz [et al.] // Journal of Alzheimer's Disease. - 2020. - Vol. 75, № 1. - P. 99-108.

256. Tripathi, M. Biomarker-based prediction of progression to dementia: F-18 FDG-PET in amnestic MCI / M. Tripathi [et al] // Neurology India. - 2019. - Vol. 67, № 5. - P. 1310-1317.

257. Trofimova, T. N. Possibilities of magnetic resonance imaging in the study of fetal brain formation / T. N. Trofimova, A. D. Khalikov, M. D. Semenova // Radiation diagnostics and therapy. - 2017. - № 4. - P. 6-15.

258. Trufanov, A. G. Modern possibilities of magnetic resonance imaging in the diagnosis of parkinsonism syndrome / A. G. Trufanov, I. V. Litvinenko, A. A. Yurin [et al] // Russian electronic journal of Radiological diagnostics. - 2018. - Vol. 8, № 1. - P. 52-65.DOI:10.21569/2222-7415-2018-8-1-52-65.

259. Trufanov, G. E. Artificial intelligence technologies in MR-neuroimaging / G. E. Trufanov, A. Y. Efimtsev // Russian Journal of Personalised Medicine. - 2023. - Vol. 3, №. 1. - P. 6-17.

260. Tu, M. C. Comparison of neuropsychiatric symptoms and diffusion tensor imaging correlates among patients with subcortical ischemic vascular disease and Alzheimer's disease / M. C. Tu [et al.] // BMC Neurology. - 2017. - Vol. 17, № 1. - Article number: 144. - URL: https://doi: 10.1186/s12883-017-0911-5.

261. Uetani, H. Prevalence and topography of small hypointense foci suggesting

microbleeds on 3T susceptibility-weighted imaging in various types of dementia / H. Uetani [et al.] // American Journal of Neuroradiology. - 2013. - Vol. 34, № 5. - P. 984-989.

262. Ungvari, Z. Hypertension-induced cognitive impairment: from pathophysiology to public health / Z. Ungvari [et al.] // Nature Reviews Nephrology. - 2021. - Vol. 17, № 10. - P. 639-654.

263. Valotassiou, V. Clinical evaluation of brain perfusion SPECT with Brodmann areas mapping in early diagnosis of Alzheimer's disease / V. Valotassiou. Valotassiou [et al.] // Journal of Alzheimer's Disease. - 2015. - Vol. 47, № 3. - P. 773-785.

264. Valotassiou, V. SPECT and PET imaging in Alzheimer's disease / V. Valotassiou. Valotassiou [et al.] // Annals of Nuclear Medicine. - 2018. - Vol. 32, № 9. - P. 583-593.

265. Van de Pol, L. Hippocampal atrophy in subcortical vascular dementia / L. van de Pol [et al.] // Neurodegenerative Diseases. - 2011. - Vol. 8, № 6. - P. 465-469.

266. Van der Flier, W. M. Vascular cognitive impairment / W. M. van der Flier [et al. M. van der Flier [et al.] // Nature Reviews Disease Primers. - 2018. - Vol. 4. - Article number: 18003.

267. Van Etten, E. J. Influence of regional white matter hyperintensity volume and apolipoprotein E ε4 status on hippocampal volume in healthy older adults / E. J. Etten [et al. J.van Etten [et al.] // Hippocampus. - 2021. - Vol. 31, № 5. - P. 469-480.

268. Van Leemput, K. Automated segmentation of hippocampal subfields from ultra-high resolution in vivo MRI / K.van Leemput [et al.] // Hippocampus. - 2009. - Vol. 19, № 6. - P. 549-557.

269. Van Staalduinen, E. K. Medial Temporal Lobe Anatomy / E. K. van Staalduinen, M. M. Zeineh // Neuroimaging Clinics. K. van Staalduinen, M. M. Zeineh // Neuroimaging Clinics. - 2022. - Vol. 32, № 3. - P. 475-489.

270. Van Straaten, E. C. W. Operational definitions for the NINDS-AIREN criteria for vascular dementia: an interobserver study / E. C. W. van Straaten [et al.] // Stroke. - 2003. - Vol. 34, № 8. - P. 1907-1912

271. Vereshchagin, N. V. Pathology of the brain in atherosclerosis and arterial hypertension / N. V. Vereshchagin, V. A. Morgunov, T. S. Gulevskaya. - Moscow: Medicine, 1977. - 288 c.

272. Verhaaren, B. F. J. High blood pressure and cerebral white matter lesion progression in the general population / B. F. Verhaaren. F. J. Verhaaren [et al.] // Hypertension. - 2013. - Vol. 61, № 6. - P. 1354-1359.

273. Vernooij, M. W. Prevalence and risk factors of cerebral microbleeds: the Rotterdam Scan Study / M. W. Vernooij. W. Vernooij [et al.] // Neurology. - 2008. - Vol. 70, № 14. - P. 1208-1214.

274. Vetreno, R. P. Adolescent binge ethanol-induced loss of basal forebrain cholinergic neurons and neuroimmune activation are prevented by exercise and indomethacin / R. P. Vetreno, F. T. Crews // PloS One. - 2018. - Vol. 13, № 10. - Article number: e0204500. - URL: https: //doi: 10.1371/journal.pone.0204500.

275. Wang, X. Altered whole-brain structural covariance of the hippocampal subfields in subcortical vascular mild cognitive impairment and amnestic mild cognitive impairment patients / X. Wang [et al.] // Frontiers in Neurology. - 2018. - Vol. 9. - Article number: 342. - URL: https://doi.org/10.3389/fneur.2018.00342

276. Wang, Z. Corpus callosum integrity loss predicts cognitive impairment in Leukoaraiosis / Z. Wang [et al.] //Annals of Clinical and Translational Neurology. - 2020. - Vol. 7, № 12. - P. 2409-2420.

277. Ward, A. Mild cognitive impairment: disparity of incidence and prevalence estimates / A.Ward [et al.] // Alzheimer's & Dementia. - 2012. - Vol. 8, № 1. - P. 14-21.

278. Wardlaw, J. M. Neuroimaging standards for research into small vessel disease and its contribution to ageing and neurodegeneration / J. M. Wardlaw. M. Wardlaw [et al.] // Lancet Neurology. - 2013. - Vol. 12, № 8. - P. 822-838.

279. Wechsler, D. A standardised memory scale for clinical use / D. Wechsler // Journal of Psychology. - 1945. - Vol.19, No. 1. - P. 87-95.

280. Wei, K. White matter hypointensities and hyperintensities have equivalent correlations with age and CSF β-amyloid in the nondemented elderly / K. Wei [et al.

Wei [et al.] // Brain and behaviour. - 2019. - Vol. 9, № 12. - Article number: e01457. - URL: https://doi: 10.1002/brb3.1457

281. Whelan, C. D. Heritability and reliability of automatically segmented human hippocampal formation subregions / C. D. D. Whelan [et al.] // Neuroimage. - 2016. - Vol. 128. - P. 125-137.

282. Whitmer R. A. Midlife cardiovascular risk factors and risk of dementia in late life / R. A. A. Whitmer [et al.] // Neurology. - 2005. - Vol. 64, № 2. - P. 277-281.

283. Winblad, B. Mild cognitive impairment-beyond controversies, towards a consensus: report of the International Working Group on Mild Cognitive Impairment. Winblad [et al.] // Journal of Internal Medicine. - 2004. - Vol. 256, № 3. - P. 240-246.

284. Wischik, C. M. Structural characterisation of the core of the paired helical filament of Alzheimer disease / C. M. Wischik [et al. M. Wischik [et al.] // Proceedings of the National Academy of Sciences. - 1988. - Vol. 85, № 13. - P. 4884-4888.

285. Wong, F. C. C. Cerebral small vessel disease influences hippocampal subfield atrophy in mild cognitive impairment / F. C. C. Wong [et al.] // Translational Stroke Research. - 2021. - Vol. 12, № 2. - P. 284-292

286. Worker, A. Test-retest reliability and longitudinal analysis of automated hippocampal subregional volumes in healthy aging and Alzheimer's disease populations / A.Worker [et al.] // Human Brain Mapping. - 2018. - Vol. 39, №. 4. - P. 1743-1754.

287. Wu, J. Multimodal magnetic resonance imaging reveals distinct sensitivity of hippocampal subfields in asymptomatic stage of Alzheimer's disease / J. Wu [et al.] // Frontiers in Aging Neuroscience. - 2022. - Vol. 14. - URL: https://doi.org/10.3389/fnagi.2022.901140.

288. Xiong, W. Genetic architecture of hippocampus subfields volumes in Alzheimer's disease / W. Xiong [et al.] // CNS Neuroscience & Therapeutics. - 2023. - URL: https/doi: 10.1111/cns.14110.

289. Yakhno, N. N. Magnetic resonance morphometry of the hippocampus and neuropsychological indicators in patients with Alzheimer's disease / N. N. Yakhno, N. N. Koberskaya, V. A. Perepelov [et al] // Neurology, Neuropsychiatry, Psychosomatics. - 2019. - Vol. 11, № 4. - P. 28-32.

290. Yakhno, N. N. Volumetric characteristics of the hippocampus according to MR volumetry in patients with Alzheimer's disease / N. N. Yakhno, V. N. Gridin, V. A. Perepelov [et al] // Russian electronic journal of Radiological diagnostics. - 2020. - Vol. 10, № 1. - P. 50-58.- URL: https://doi: 10.21569/2222-7415-2020-10-1-50-58

291. Yassa M. A. High-resolution structural and functional MRI of hippocampal CA3 and dentate gyrus in patients with amnestic mild cognitive impairment / M. A. Yassa [et al.] // Neuroimage. - 2010. - Vol. 51, № 3. - P. 1242-1252

292. Yassine, H. N. Lessons from the multidomain alzheimer preventive trial / H. N. Yassine, L. S. Schneider // Lancet Neurology. - 2017. - Vol. 16, № 8. - P. 585-586.

293. Yeo, J. M. Systematic review of the diagnostic utility of SPECT imaging in dementia / J. M. Yeo [et al.] // European Archives of Psychiatry and Clinical Neuroscience. M. Yeo [et al.] // European Archives of Psychiatry and Clinical Neuroscience. - 2013. - Vol. 263, № 7. - P. 539-552.

294. Zakharov, V. V. Cognitive impairment in cerebrovascular diseases / V. V. Zakharov, N. V. Vakhnina // Effective pharmacotherapy. Neurology and psychiatry. - 2014. - № 1. - P. 14-22.

295. Zakharov, V. V. Combined therapy of Alzheimer's disease / V. V. Zakharov, A. B. Lokshina, N. V. Vakhnina // Neurology, neuropsychiatry, psychosomatics. - 2022. - Vol. 14, №. 3. - P. 74-80.

296. Zakharov, V. V. Syndrome of mild cognitive impairment in old age: diagnosis and treatment / V. V. Zakharov, N. N. Yakhno // Russian Medical Journal. - 2004. - № 10. - P. 573-576.

297. Zammit, A. R. Roles of hippocampal subfields in verbal and visual episodic memory / A. R. Roles of hippocampal subfields in verbal and visual episodic memory. R. Zammit [et al.] // Behavioural Brain Research. - 2017. - Vol. 317. - P. 157-162.

298. Zeineh, M. M. Dynamics of the hippocampus during encoding and retrieval of face-name pairs / M. M. Zeineh [et al.] // Science. - 2003. - Vol. 299, № 5606. - P.577-580.

299. Zeng, Q. Distinct atrophy pattern of hippocampal subfields in patients with progressive and stable mild cognitive impairment: a longitudinal MRI study / Q. Zeng

[et al.] // Journal of Alzheimer's Disease. - 2021. - Vol. 79, № 1. - P. 237-247.

300. Zhao, K. Independent and reproducible hippocampal radiomic biomarkers for multisite Alzheimer's disease: diagnosis, longitudinal progress and biological basis / K. Zhao [et al. Zhao [et al.] // Science Bulletin. - 2020. - Vol. 65, № 13. - P. 1103-1113.

301. Zhao, W. Trajectories of the hippocampal subfields atrophy in the Alzheimer's disease: a structural imaging study / W. Zhao [et al.] // Frontiers in Neuroinformatics. - 2019. - Vol. 13. - URL: https://doi.org/10.3389/fninf.2019.00013

302. Zheng Y. SPECT and PET in Vascular Dementia / Y. Zheng, Z. Zhou // PET and SPECT in Neurology / ed. by R. A. Zheng. A. J. O. Dierckx, A. Otte, E .F. J. de Vries [et al.]. - Berlin; Heidelberg : Springer, 2021. - P. 563-575.

303. Zhou, M. Entorhinal cortex: a good biomarker of mild cognitive impairment and mild Alzheimer's disease / M. Zhou. Zhou [et al.] //Reviews in the Neurosciences. - 2016. - Vol. 27, № 2. - P. 185-195.

304. Zhou, Y. A primary study of diffusion tensor imaging-based histogram analysis in vascular cognitive impairment with no dementia / Y. Zhou [et al.] // Clinical neurology and neurosurgery. - 2011. - Vol. 113, № 2. - P. 92-97.

305. Zhuang, F. J. Prevalence of white matter hyperintensities increases with age / F. J. J. Zhuang [et al.] // Neural Regeneration Research. - 2018. - Vol. 13, № 12. - P. 2141-2146.

306. Zubrikhina, M. O. Machine learning approaches to mild cognitive impairment detection based on structural MRI data and morphometric features / M. O. O. Zubrikhina [et al.] // Cognitive Systems Research. - 2023. - Vol. 78. - P. 87-95.

APPENDIX

PATIENT LIST

Patient №	NAME	№ и/б	Gender	Age	Patient №	NAME	№и/б	Gender	Age
1	G-va L. V.	Amb	f	75	46	I-va N. V.	Amb	f	69
2	Sh-ovV. M.	Amb	m	66	47	S-va T. I.	Amb	f	67
3	K-e M. N.	Amb	f	71	48	Sh-va M. B.	Amb	f	70
4	P-va Z. F.	Amb	f	77	49	K-aya M. M.	Amb	f	67
5	S-ii V. B.	Amb	m	71	50	K-na T. I.	Amb	f	69
6	F-ovaA. A.	Amb	f	85	51	D-ets L. P.	Amb	f	79
7	V-ev D. P.	Amb	m	64	52	R-va G. N.	Amb	f	67
8	V-va A. N.	Amb	f	70	53	M-va N. P.	Amb	f	72
9	O-ov A. B	Amb	m	78	54	S-ov Yu. B.	Amb	m	70
10	L-va E. V.	Amb	f	76	55	Z-in Yu. B.	Amb	f	69
11	S-va I. I.	Amb	f	60	56	Us-k N. I.	Amb	m	67
12	I-na Z. I.	Amb	f	72	57	Ts-lin A. K.	Amb	m	70
13	S-va R. D.	Amb.	f	73	58	Sh-uk Z. N.	Amb	f	79
14	K-va K. M.	Amb	f	62	59	K-na T. M.	Amb	f	70
15	K-v A. P.	Amb	m	62	60	P-va A. B.	Amb	f	77
16	P-aya L. Ф.	Amb	f	77	61	K-va S. C.	Amb	f	75
17	S-ko I. N.	Amb	f	73	62	B-gin V. H.	Amb	m	68
18	Z-an M. G.	Amb	f	82	63	M-naN. M.	Amb	f	80
19	L-va S. F.	Amb	f	68	64	E-va A. L.	Amb	f	87
20	Kh-va E. Y.	Amb	f	74	65	K-nyuk T. I.	Amb	f	65
21	R-va M. A.	Amb.	f	66	66	S-va Z. I.	Amb	f	70
22	Ch-k E. N.	Amb	f	75	67	B-va T. D.	Amb	f	67
23	K-aya M. Ya.	Amb	f	67	68	P-rov B. P.	Amb	m	80

24	E-va T.G.	Amb	f	68	69	T-vich L. A.	Amb	m	71
25	E-va N. I.	Amb	f	82	70	P-kan T. D.	Amb	f	72
26	V-aya L. Г.	Amb	f	65	71	M-va V. N.	Amb	f	79
27	K-v S. M.	Amb	f	78	72	Kut-va G. P.	Amb	f	73
28	Wife P. M.	Amb	m	78	73	K-na H. R.	Amb	f	81
29	O-r V.L.	Amb	m	74	74	Av-kh B. I.	Amb	m	81
30	B-va V. V.	Amb	f	80	75	Kur-tov V. I.	Amb	m	81
31	M-wa L. S.	Amb	f	64	76	L-na T. I.	Amb	f	70
32	U-n E. И.	Amb	f	66	77	P-va L. P.	Amb	f	74
33	P-na L. E.	Amb	f	70	78	S-va N. I.	Amb	f	60
34	Ch-v P. H.	Amb	m	74	79	A-va G. S.	Amb	f	80
35	P-Va L. M.	Amb	f	63	80	P-in V. H.	Amb	m	75
36	S-ko G. A.	Amb	f	85	81	A-ev Y. I.	Amb	m	81
37	Zh-ov N. A.	Amb	m	74	82	R-va L. A.	Amb	f	75
38	Mr O.G.	Amb	f	81	83	E-vic A. R.	Amb	m	76
39	P-va N. A.	Amb	f	76	84	K-ova L. V.	Amb	f	74
40	M-va V.G.	Amb	f	76	85	Sh-na E. H.	Amb	f	69
41	A-nov V. L.	Amb	m	69	86	K-va L. I.	Amb	f	75
42	I-va L. V.	Amb	f	66	87	Sh-na N. N.	Amb	f	69
43	El-ev D. O.	Amb	m	64	88	Ber-ii S. I.	Amb	m	80
44	K-va L. N.	Amb	f	65	89	M-ev E. П.	Amb	m	75
45	B-va N. V.	Amb	f	74	90	Hr-l A. S.	Amb	m	68